EARLY AXONAL TAU PATHOLOGY IN THE HUMAN HIPPOCAMPUS AND THE MOLECULAR CONSEQUENCES OF AT8 TAU PHOSPHORYLATION

By

Kyle Robert Christensen

A DISSERTATION

Submitted to
Michigan State University
in partial fulfillment of the requirements
for the degree of

Neuroscience – Doctor of Philosophy

2018

ABSTRACT

EARLY AXONAL TAU PATHOLOGY IN THE HUMAN HIPPOCAMPUS AND THE MOLECULAR CONSEQUENCES OF AT8 TAU PHOSPHORYLATION

By

Kyle Robert Christensen

Tau is a microtubule-associated protein that is classically thought to play a role in stabilizing microtubules and the pathological accumulation of tau protein is a hallmark of several diseases collectively known as tauopathies, including Alzheimer's disease (AD). Despite the clear implications for tau playing a critical role in tauopathies, many questions regarding its deposition in disease and mechanisms of toxicity remain unanswered. This dissertation was aimed at addressing two key questions in the field. 1) Does tau deposition occur first in the axons of affected neurons before proceeding to the somatodendritic compartment? 2) Does pathological modification of tau cause abnormalities in the ability of tau to modulate protein phosphatase 1 (PP1)?

A long-held hypothesis on the progressive deposition of tau pathology in AD is that pathological tau accumulates first in axons of neurons and then progresses back into the cell bodies to form neurofibrillary tangles, however, studies have not directly analyzed this relationship in human tissue. In the early phases of tau deposition, both AT8 phosphorylation and exposure of the amino terminus of tau occur in tauopathies, and these modifications are linked to mechanisms of synaptic and axonal dysfunction. Here, the hippocampus of 44 well-characterized human samples from cases ranging between non-demented and mild cognitively impaired were examined for AT8 phosphorylation, amino terminus exposure, and amyloid-β (Aβ) pathology in the axons and neuronal cell bodies within strata containing the CA3-Schaffer collateral and dentate granule-mossy fiber pathways. We show that tau pathology first appears in the axonal compartment of affected neurons in the absence of observable tau pathology in the corresponding cell bodies and independent of the presence of Aβ pathologies. Using the

axonal marker, SMI-312, we confirmed that the majority of tau pathology-positive neuropil threads were axonal in origin. These results support the hypothesis that AT8 phosphorylation and PAD exposure are early pathological events and that the deposition of tau pathology occurs first in the axonal compartment prior to observable pathology in the cell bodies of affected neuronal pathways.

The functional implications of AT8 and PAD-exposed tau deposition early in the axons of affected neurons is important because of a recently identified mechanism where these pathogenic forms of tau activate a PP1-dependent signaling pathway and lead to disruption of axonal functions. However, the connection between tau and PP1 was not defined. Here, we performed detailed studies on the interaction between tau and PP1 and subsequent effects on PP1 activity. Wild-type tau interacts with and activates PP1α and γ, but shows little to no interaction with PP1β, and this effect depends primarily on the microtubule binding repeats in tau. Additionally, AT8 tau increased the interactions with and activity of PP1γ, while deletion of PAD in the presence of AT8 reduced this interaction. These results suggest that tau's function likely extends beyond stabilizing microtubules to include regulation of PP1 signaling cascades, and disease-associated tau phosphorylation may alter this function. Collectively, this work suggests forms of pathological tau, such as AT8 phospho-tau, that alter PP1 signaling and disrupt axonal function deposit in the axons of affected hippocampal neurons early during disease pathogenesis and prior to their appearance in the somatodendritic compartment of neurons.

I would like to dedicate this work to my family and friends,
especially my parents, Sonja and Robbe Christensen.
Without your love and support I would have
never made it even half this far

ACKNOWLEDGEMENTS

First, I would like to thank my advisor, Dr. Nicholas Kanaan, for his mentorship, guidance, and support during the completion of this dissertation, and for helping me grow and develop into the adult I am today. I also thank the members of my thesis committee, both past and present – A. J. Robison, Scott Counts, Irving Vega, Michelle Mazei-Robison, Eric Achtyes, Tim Collier, Fredric Manfredsson, and Lena Brundin – for their advice, feedback, and support over the years. Members of the Kanaan lab and Brundin lab also deserve thanks and recognition for their help and companionship in the trenches – Tessa Grabinski, Ben Combs, Andrew Kneynsberg, Chelsea Tiernan, Collin Richards, Chelsey Yob, Mike Kubik, Kris Cox, Analise Sauro-Nagendra, Sarah Keaton, Keerthi Rajamani, Amissa Sei, Jamie Grit, Filip Ventorp, and Oskar Sporre. Special thanks to the Department of Translational Science and Molecular Medicine, especially Caryl Sortwell and Jack Lipton, as well as my friends and colleagues that brightened each day. Finally, I would like to thank my friends and family outside of the lab for constantly hearing me talk about science long after they lost interest and for their love and support throughout the years.

PREFACE

At the time of writing this dissertation, both chapters are in preparation for publication and will be submitted in the near future.

TABLE OF CONTENTS

LIST OF TABLES

LIST OF FIGURES

KEY TO ABBREVIATIONS

3xΔ RVxF	Triple deletion of RVxF binding motif
Aβ	Amyloid-β
AD	Alzheimer's disease
APOE4	Apolipoprotein E4
APP	Amyloid precursor protein
BACE1	β-secretase
CaMKII	Calmodulin-dependent protein kinase II
CERAD	Consortium to Establish a Registry for Alzheimer's Disease
Cdk5	Cyclin-dependent kinase kinase-5
C-term	C-terminus domain of tau
ΔC-term	Tau construct with C-terminus deleted
DG	Dentate gyrus
DMF	Dimethyl fumarate
DS	Down syndrome
EC	Entorhinal cortex
FTDP-17	Frontal temporal dementia with parkinsonism linked to chromosome-17
GSK3	Gycogen synthase kinase
HEK	Human embryonic kidney
HT	HaloTag
IF	Immunofluorescence
IHC	Immunohistochemistry
LTD	Long-term depression
MCC	Mander's colocalization coefficient

MCI	Mild cognitive impairment
MMSE	Mini-Mental State Examination
MTBR	Microtubule binding repeat
ND	Non-demented
NFT	Neurofibrillary tangle
NDMA	*N*-methyl-*D*-aspartate
NLuc	Nano-Luciferase
NOC	Nocodazole
NP	Neuritic plaque
NT	Neuropil thread
N-term	N-terminus domain of tau
ΔN-term	Tau construct with the N-terminus deleted
PAD	Phosphatase activating domain
ΔPAD	PAD deletion
PHF	Paired helical filament
PLA	Proximity Ligation Assay
PNPP	*Para*-nitrophenyl phosphate
psAT8	Pseudophosphorylated AT8 tau
PTM	Post-translational modification
PP1	Protein Phosphatase 1
Ser/Thr	Serine/Threonine
Str. Luc.	Stratum lucidum
Str. Rad.	Stratum radiatum
Sub	Subiculum
WT	Wild type

CHAPTER 1

Overall Introduction

Introduction

Neurodegenerative diseases are debilitating terminal conditions that affect many aspects of life, including cognition, memory, motor function, and emotions. Alzheimer's disease (AD), Parkinson's disease, Huntington's disease, and amyotrophic lateral sclerosis are examples of neurodegenerative diseases (Soto *et al.* 2008). While these conditions differ in clinical symptoms, they share some common themes, such as manifesting late in life, loss of neuronal populations, synaptic dysfunction and loss, and presence of misfolded protein aggregates (Soto 2003). Alzheimer's disease (AD) is the leading cause of dementia and the most common neurodegenerative disorder (Hebert *et al.* 2003, Brookmeyer *et al.* 2007). Currently, an estimated 5.7 million people in the United States over the age of 65 have AD (Alzheimer's 2018), and this is projected to triple by 2050 (Huang *et al.* 2012). This staggering number of AD cases places extraordinary emotional and financial burden on patients, caregivers and society. AD healthcare costs in the United States are estimated at $277 billion in 2018 (Alzheimer's 2018). Developing effective interventions targeting disease progression remains a barrier to progress because of the poor understanding of pathological mechanisms driving the degenerative events in AD. This dissertation investigates the axonopathy that occurs in the early pre-AD stages of tau deposition and a proposed mechanism of axonal dysfunction and neurodegeneration involving tau and protein phosphatase 1 (PP1) signaling. Ultimately, deciphering molecular mechanisms of tau toxicity may facilitate the generation of effective therapies to slow or halt the disease process and alleviate the devastating impact of these diseases.

Tau Protein Biology

Tau is a microtubule-associated protein that was discovered in 1975 while investigators were purifying microtubules, tau co-purified with microtubules and facilitated their assembly and stability *in vitro* (Weingarten *et al.* 1975). Since its discovery, the primary cellular function assigned to tau is to stabilize microtubules; however, numerous studies suggest the functional repertoire of tau is more expansive (discussed further below). Human tau is encoded by the *MAPT* gene on chromosome 17q21 (Neve *et al.* 1986, LoPresti *et al.* 1995). In the central nervous system, adult humans express six isoforms of tau arising from alternative splicing of exons 2, 3, and 10 (Goedert *et al.* 1989, Andreadis *et al.* 1992). Exons 2 and 3 comprise two inserts of 29 amino acid residues each near the N-terminus; tau isoforms containing these inserts are termed 0N, 1N, or 2N. Tau also contains a microtubule binding repeat region consisting of three or four imperfect repeat domains (MTBRs) depending on whether exon 10 (comprising the second MTBR) is present (4R) or absent (3R) (Lee *et al.* 1988). The ratio of 3R to 4R tau is ~1 in the normal brain (Hong *et al.* 1998). Tau is hydrophilic, stable in acidic conditions, and stable at high temperatures (Fellous *et al.* 1977). Overall, tau is basic in charge, but the protein can be subdivided into subregions with highly acidic (N-terminus and proline-rich region) or basic (MTBR and C-terminus) charges. The N-terminus region is composed of the first ~150 amino acids and is referred to as the projection domain because it projects away from microtubules instead of binding to them and overall this region is acidic (Hirokawa *et al.* 1988). The C-terminus region composed of amino acids ~200 – 400 contains the MTBRs and interacts with microtubules, and therefore is called the microtubule assembly domain (Mukrasch *et al.* 2005). This region is more hydrophobic and basic than the projection domain, facilitating tau's interaction with the acidic surface of microtubules (Lee *et al.* 1988, Goedert *et al.* 1989, Mukrasch *et al.* 2009). Finally, the ~40 amino acids closest to the C-terminus contains subregions of both acidic and basic charges, does not interact with microtubules, and can also

project like the N-terminal projection domain. In neurons, tau is involved in maintaining axon integrity and function (Drechsel *et al.* 1992, Rosenberg *et al.* 2008, Wang *et al.* 2008).

Tau typically does not form stable secondary structures in solution typical of globular proteins and contains a high percentage of basic and hydrophilic amino acid residues, implying a highly flexible and mobile chain of amino acids (Schweers *et al.* 1994, Mukrasch *et al.* 2009). However, tau may form temporary secondary and tertiary structures when bound to other proteins (Kadavath *et al.* 2015). Monomeric tau preferentially forms a globally folded conformation known as the “paperclip” conformation, where the C-terminus folds over to come within 23 Å of the MTBR region and the N-terminus folds over the C-terminus within a distance of 24 Å (Jeganathan *et al.* 2006). It is proposed that this paperclip conformation prevents tau from forming aggregates, whereas truncation or certain phosphorylation sites of tau prevents this interaction and could facilitate aggregation (Wang *et al.* 2016).

The function and structure of tau is impacted by post-translational modifications (PTMs) and it is well-established that tau undergoes a number of PTMs during the course of human disease. This includes phosphorylation, acetylation, glycosylation, glycation, truncation, nitration, polyamination, ubiquitination, symoylation, oxidation, and aggregation (Martin *et al.* 2011). Two years after its discovery, tau was recognized as a phosphoprotein (Cleveland *et al.* 1977), and tau is more efficient at facilitating the assembly of microtubules in the dephosphorylated state (Lindwall *et al.* 1984). Tau phosphorylation is developmentally regulated, with fetal tau containing approximately three times the amount of phosphates per molecule than adult tau (Kanemaru *et al.* 1992). There are 85 potential phosphorylation sites in tau, 80 are serines or threonines and five are tyrosines, with 45 of these sites observed experimentally in normal and disease states (Hanger *et al.* 2009). A majority of the phosphorylation sites are located in the amino acids flanking the MTBRs leading to effects on microtubule binding and tau aggregation, and multiple kinases can phosphorylate tau (Wang *et al.* 2016). In addition, phosphorylation within the termini of tau may affect tau behavior. For

example, phosphorylation at tyrosine 18 reduces the affinity of tau for microtubules and facilitates more dynamic microtubule binding (versus static tau-microtubule interactions), which may play a role in facilitating kinesin transport along microtubules (Stern *et al.* 2017).

Alzheimer's Disease

History and Characterization

Alois Alzheimer, the namesake of AD, first described the clinical symptoms of the disease after observing Auguste Deter between 1901 – 1904 in Frankfurt, Germany (Maurer *et al.* 1997). She displayed numerous behaviors, including memory deficits, disorientation, aphasia, paranoia, auditory hallucinations, and difficulties socializing. After her death in 1906, Alzheimer examined her brain after autopsy and found extensive atrophy and loss of cells. Together with the Italian physicians Gaetano Perusini and Francesco Bonfiglio, Alzheimer described plaque deposits throughout the cortex and thick, strongly stained fibrils inside the remaining neurons using a modified Golgi stain (Dahm 2006). This became the first description of amyloid plaques and neurofibrillary tangles, now considered the histopathological hallmarks of AD.

While the specific etiology of AD remains unknown, AD is characterized by pathognomonic pathologies required for a definitive diagnosis. Specifically, AD requires the presence of extracellular amyloid plaques (Terry *et al.* 1964) composed of insoluble aggregates of amyloid-β (Aβ) (Glenner *et al.* 1984, Masters *et al.* 1985, Kowall *et al.* 1991), and intracellular neurofibrillary tangles (NFTs) (Terry *et al.* 1964) composed of abnormally phosphorylated tau (Grundke-Iqbal *et al.* 1986, Kosik *et al.* 1986). Additionally, reduction of brain weight and volume, neurodegeneration which appears to effect specific brain regions such as the entorhinal cortex and CA1 region of the hippocampus (Gomez-Isla *et al.* 1996), and impairment of cognitive function (Terry 1994) are observed in AD cases. Even armed with this knowledge, current treatment options and therapies for AD only help alleviate symptom severity; none are

successful at slowing or halting disease progression (Silva *et al.* 2014). Established criteria and guidelines identify three stages of AD: preclinical AD, mild cognitive impairment (MCI) due to AD, and dementia due to AD (Petersen *et al.* 2001, Petersen 2003). Unfortunately, the progressive nature of AD and significant pre-clinical window of ongoing degenerative changes leads to a likely insurmountable amount of irreversible neuronal loss by the time patients present with symptoms.

Amyloid-β in AD

One hallmark of AD is the accumulation of insoluble extracellular plaques composed of Aβ. Aβ is 42 amino acids in length as is formed by cleavage of the larger amyloid precursor protein (APP) by γ-secretase and presenilins (De Strooper *et al.* 1998). This peptide is the basis of the amyloid hypothesis of AD, which states that misfolding of monomeric Aβ can lead to formation of soluble extracellular oligomers and insoluble amyloid plaques, which disrupt normal synaptic signaling through multiple cellular signaling cascades and can lead to dysfunction and loss of synapses, or degeneration of neuronal populations (Selkoe 2000). Moreover, this hypothesis suggests that Aβ pathology drives the formation and deposition of tau pathology, the other neuropathological hallmark of AD (see below for further details on tau protein).

The majority of AD cases (95%) are sporadic and ~5% or less are familial forms of AD associated with mutations in genes related to APP processing (i.e. APP or presenilins) (Goate *et al.* 1991, Wang *et al.* 2018). The prominent focus on Aβ and APP was supported by the discovery of several point mutations in APP that cause inherited AD, such as the Swedish mutations (KM670/671NL) (Mullan *et al.* 1992), Indiana mutation (V717F) (Murrell *et al.* 1991), Flemish mutation (A692G) (Hendriks *et al.* 1992), and London mutation (V717I) (Goate *et al.* 1991). Additionally, mutations found in the genes encoding for presenilin 1 and presenilin 2 were identified in early onset AD cases that were negative for APP mutations (St George-

Hyslop *et al.* 1992, Levy-Lahad *et al.* 1995, Rogaev *et al.* 1995, Sherrington *et al.* 1995). The presenilins form the catalytic subunit for γ-secretase, the enzyme responsible for the cleavage of the transmembrane unit of APP after they are processed by α- and β-secretase to form Aβ peptides from 39-42 amino acids in length (De Strooper *et al.* 1998, Kimberly *et al.* 2003, Zhang *et al.* 2011). These mutations affect APP processing through α-, β-, and γ-secretases and lead to increased production of Aβ peptide, an increase in the ratio of Aβ 42 to Aβ 40, or both (Zhu *et al.* 2017). Importantly, since Aβ 42 is more prone to aggregation than Aβ 40, mutations in APP that that selectively enhance the production of Aβ 42 may lead to more deposition of amyloid plaques, increased secretion and circulation of Aβ 42, and increased angiopathy (1991, Suzuki *et al.* 1994). APP overexpression in humans is a known risk factor for AD (Bertram *et al.* 2010). In a study of families with autosomal dominant early-onset AD, the APP locus (in chromosome 21) was duplicated (Rovelet-Lecrux *et al.* 2006). Additionally, individuals with Down syndrome (DS) possessing a trisomy of chromosome 21 containing the APP locus develop early onset dementia (Lai *et al.* 1989). Post-mortem analysis of DS brains displayed AD pathology in the form of amyloid plaques and NFTs (Wisniewski *et al.* 1985). Further evidence supporting the idea that APP overexpression promotes AD development is provided through studies analyzing regulatory sequences of APP. Mutations in the APP promoter region that lead to increased activity inversely correlate with age of AD onset and positively correlate with atrophy of cortical and subcortical brain areas and behavioral deficits, including memory impairment, trouble speaking, concentration problems, and confusion (Brouwers *et al.* 2006). Taken together, these data illustrate a genetic abnormality leading to abnormal processing of APP or its overexpression in humans leads to inherited forms of AD.

Aβ aggregation follows a nucleation-elongation mechanism, in which a nucleus of misfolded Aβ oligomers “recruit” other Aβ fragments due to the relatively low critical concentration for Aβ polymerization (Jarrett *et al.* 1993, Harper *et al.* 1997). Additionally, Aβ is associated with a decrease in synaptic strength and aberrant network activity (Palop *et al.*

2010). Pathogenic Aβ modulates glutamatergic synaptic activity by potentially blocking NMDA receptors and causing a shift in intracellular signaling pathway activation towards long-term depression (LTD) (Shankar *et al.* 2007). While the specific mechanism of Aβ on LTD remains to be determined, these findings are consistent with previous studies linking Aβ to impaired long-term potentiation and increased LTD in the hippocampus and parietal cortex (Li *et al.* 2009). Also, Aβ can block NMDA receptors leading to glutamate increases in the synaptic cleft under these conditions, which may contribute to toxicity (Li *et al.* 2009). Elevation of synaptic glutamate initially activates NMDA receptors but is followed by desensitization and internalization of glutamate receptors (Hsieh *et al.* 2006, Li *et al.* 2009). Diffusion of excess glutamate outside the synaptic cleft can lead to stimulation of perisynaptic NMDA receptors and metabotropic glutamate receptors. This causes activation of another signaling pathway to promote LTD development and can lead to loss of synapses and dendritic spines (Hsieh *et al.* 2006). While Aβ toxicity through a glutamate signaling mechanism is heavily studied, numerous other mechanisms are currently being investigated, including altered synaptic transmission, impaired calcium signaling, increased tau phosphorylation, increased plasma membrane permeability, proteasome impairment, disruption of autophagy, production of reactive oxygen species, among several others (Benilova *et al.* 2012, Kayed *et al.* 2013).

Apolipoprotein E4 (APOE4) is another genetic risk factor for late-onset AD (Corder *et al.* 1993). In the CNS, APOE4 production occurs primarily in astrocytes and microglia, but neurons also express APOE4 under pathological conditions (Boschert *et al.* 1999). Since APOE4 can bind lipids after membrane damage, it is thought that the function of APOE4 is to recycle lipids for membrane repair (Mahley 1988). However, APOE4 has an exposed hydrophobic, so-called “molten” core that promotes Aβ-mediated lysosomal degradation by binding phospholipid membranes and disrupting their structural and functional integrity (Ji *et al.* 2002, Morrow *et al.* 2002). Previous research showed significant changes in the levels of difference phospholipids in the hippocampus and neocortex of AD brains, indicating altered interactions and membrane-

mediated functions of receptors, channels, and transporters. (Pettegrew *et al.* 2001). Additionally, increased tau levels and tau redistribution to the somatodendritic compartment in a transgenic mouse model expressing P301S tau and ApoE4 led to increased neuroinflammation and brain atrophy compared to mice expressing P301S and either ApoE2 or ApoE3 (Shi *et al.* 2017). Also, a recent study in human neurons derived from induced pluripotent stem cells expressing APOE4 resulted in higher levels of tau phosphorylation unrelated to the production of Aβ peptides, and this effect was rescued by changing the APOE4 genotype to APOE3 using gene editing (Wang *et al.* 2018). Taken together, these results indicate a synergistic effect of tau pathology and ApoE4 expression in the progression of AD

As a result of investigations into the amyloid cascade hypothesis of AD, several clinical trials targeting amyloid pathology have been conducted and largely produced disappointing results. Bapineuzumab, a humanized anti-Aβ monoclonal antibody drug, did not improve clinical outcomes of patients with mild to moderate AD in a phase 3 trial, as measured through the 11-item cognitive subscale of the AD Assessment Scale and Disability Assessment for Dementia rating scales (Salloway *et al.* 2014). Additionally, immunization of AD patients with Aβ 42 peptide was shown to clear amyloid plaques and improve cognitive function in mice (Schenk *et al.* 1999, Morgan *et al.* 2000). However, immunizing AD patients with Aβ 42 did not result in reduced neurodegeneration, despite the increased clearance of amyloid plaques, in these patients (Holmes *et al.* 2008). The failure of these clinical trials targeting amyloid pathology in AD patients indicates other components of the disease condition influence AD pathogenesis and progression, either independently or in conjunction with amyloid.

Tau Protein in AD

AD pathology contains both 3R and 4R tau isoforms (Goedert *et al.* 1992, Greenberg *et al.* 1992). Tau aggregates into paired helical filaments (PHFs) which then coalesce into NFTs one of the primary forms of pathological tau that accumulates in diseases termed tauopathies

(Kidd 1963, Kosik *et al.* 1986, Bancher *et al.* 1989). Maturation of NFTs follows a pattern of progressive modifications that occur as disease progresses (Binder *et al.* 2005). First, tau undergoes a conformational change from a disordered protein or the paperclip conformation to a “Alz50” conformation, named after the Alz50 antibody that recognizes a discontinuous epitope where the N-terminus of tau interacts with the MTBRs (Carmel *et al.* 1996). Alz50 reactivity appears first in pre-tangle neurons but continues in later stage NFTs (Braak *et al.* 1994). Next, truncation of tau occurs through caspase activity, as shown through reactivity with the Tau-C3 (reacts with tau truncated at D421) and Tau-66 (reacts with a conformation of tau where the proline rich region interacts with the MTBRs) (Ghoshal *et al.* 2001, Guillozet-Bongaarts *et al.* 2005). Tangles positive for Tau-66 and TauC3 indicate middle stage NFTs. Finally, additional cleavage events results in additional shortening of the termini leaving the NFT core remaining, as shown by these late stage tangles no longer reacting with Tau-66 (due to cleavage of the proline-rich region) and gaining reactivity with MN423, which recognizes tau cleaved at E391 (Novak *et al.* 1993, Binder *et al.* 2005).

The temporal relationship between tau phosphorylation and NFT maturation is an important question to understand the development of tau pathology. Across all Braak stages, phosphorylation at the AT8 epitope (Ser199, Ser202, Thr205) (Biernat *et al.* 1992, Goedert *et al.* 1995) was more prevalent than cleaved tau in NFTs (Mondragon-Rodriguez *et al.* 2008). This study also reported AT8 immunoreactivity in neuropil threads and NFTs, while Tau-C3 reactivity was exclusive to NFTs, implying phosphorylation events precede truncation events (Mondragon-Rodriguez *et al.* 2008). These observations support the hypothesis that tau phosphorylation is an early event in the progression of tau pathology, precedes early truncation events associated with NFTs, and precedes caspase processing of tau (Guillozet-Bongaarts *et al.* 2005, Mondragon-Rodriguez *et al.* 2008). Additionally, NFTs are thought to exist in affected neurons in AD patients for over 20 years, and late stage NFTs do not inhibit anterograde axon transport like early stage NFTs (Morsch *et al.* 1999, Morfini *et al.* 2009). It was suggested the

inability of late stage NFTs to inhibit transport could be due to a possible N-terminus proteolytic cleavage event which removes a potential toxic region of the tau protein (Horowitz *et al.* 2004, Morfini *et al.* 2009) Together, these findings suggest tau phosphorylation is likely one of the initial modifications of tau, and sequestering tau undergoing pathological phosphorylation, truncation and/or conformational changes into NFTs protects the neuron from further harm (Binder *et al.* 2005).

The MTBRs promote tau aggregation and form the core of PHFs, while the N-terminus projection region and the C-terminus projection region forms the “fuzzy coat” observed surrounding the core of PHFs (Wischik *et al.* 1988). Using cryo-electron microscopy to investigate the structure of PHFs found that the PHFs are comprised of two interacting C-shaped protofilaments, that the core is comprised of amino acids 306-378 and that the extreme amino terminus (i.e. amino acids 7-9) likely interact with the PHF core (Fitzpatrick *et al.* 2017). Interestingly, an N-terminal antibody, known as TNT1, that identifies species of tau with the N-terminus exposed and that cause toxicity to axonal transport only decorates the terminal ends of tau filaments isolated from AD brains and of those generated *in vitro* with recombinant protein suggesting the epitope (i.e. amino acids 7-12) is not accessible in the majority of tau composing a filament (Kanaan *et al.* 2011, Combs *et al.* 2016). Again, these findings suggest that pre-filamentous species of tau may represent the more toxic forms of tau when compared to tau filaments and/or NFTs.

Numerous lines of evidence support tau’s candidacy as a causative factor in AD. For example, NFT density correlates with cognitive decline (Arriagada *et al.* 1992, Giannakopoulos *et al.* 2003). Another potential mechanism linking tau and toxicity is deficits in axonal transport, proposed to occur by disrupting motor proteins (Kanaan *et al.* 2012, Kanaan *et al.* 2013), competing with cargos for motor protein binding sites (Ittner *et al.* 2009, Morfini *et al.* 2009), or physically blocking motor proteins from traveling along microtubules (Dixit *et al.* 2008). Additionally, FTDP mutations of tau were shown to alter the function of voltage-gated calcium

channels, causing toxicity through a mechanism involving dysregulation of calcium signaling (Furukawa *et al.* 2003) The toxic effects observed with Aβ is reduced when tau is removed or inhibited (Rapoport *et al.* 2002, Vossel *et al.* 2010). Additionally, *in vitro* and *in vivo* models of tauopathies such as neuron cell cultures and transgenic tau knockout mice established tau's role in physiology and disease by showing tau is necessary for Aβ-induced neurotoxicity and may spread between neurons (Roberson *et al.* 2007, Holmes *et al.* 2014). A causal role for tau in neurodegenerative disease is supported by the fact that several genetic tau mutations cause forms of frontal-temporal dementias (FTD) independent of Aβ (Hutton *et al.* 1998). While there are no known tau mutations that cause AD, many of the pathological modifications (such as phosphorylation, truncation or other post-translational modifications) seen in familial and other non-AD tauopathies also occur in AD suggesting some overlap in tau abnormalities and likely tau-mediated toxicity. These findings make tau likely a contributing factor in the pathogenesis of AD and suggest the disease-associated modifications of tau that occur, and/or other cellular components, may work in concert with tau to cause degeneration (Lee *et al.* 2011).

Post-Translational Modifications (PTMs) of Tau in Disease

The prominence of studying tau phosphorylation as a main PTM began when, in the mid 1980's, a set of seminal studies showed that the characteristic tau inclusions of AD were significantly phosphorylated (Grundke-Iqbal *et al.* 1986, Wood *et al.* 1986). In AD, tau possess approximately four times the amount of phosphate per molecule than adult tau (Kopke *et al.* 1993). Tau phosphorylation increases in AD, presumably resulting from an imbalance between tau kinase and phosphatase activities and could be a potentially useful target for therapeutic intervention. There are 85 phosphorylation sites in tau; of those, 28 are phosphorylated only in AD brains, 16 are phosphorylated in both control and AD brains (AT8 belongs in this category), 31 are phosphorylated under normal physiological conditions, and 10 are phosphorylated by an unknown kinase (Martin *et al.* 2013). AT8 phosphorylation is an early and prominent event in the

progression of AD, visible in early stage tangles and neuropil threads (Braak *et al.* 1994). Infusion of physiological concentrations of monomeric pseudophosphorylated AT8 tau into preparations of squid axoplasms inhibited anterograde fast axonal transport through a GSK3-PP1 signaling cascade. This implies AT8 could represent an early and prominent initiator behind a pathological mechanism before it is sequestered into NFTs (Kanaan *et al.* 2011, Kanaan *et al.* 2012).

Tau kinases are broadly categorized into three families: proline-directed protein kinases, non-proline-directed protein kinases, and tyrosine protein kinases. Proline-directed kinases phosphorylate serine or threonine residues immediately followed by a proline residue (S/TP motif) (Pelech 1995). The major tau kinase is the proline-directed Ser/Thr kinase glucose synthase kinase 3 (GSK3). GSK3 is involved in cell division, neuron function, cancer, development, immune signaling, and apoptosis (Hooper *et al.* 2008). GSK3 has two isoforms, GSK3α and GSK3β, encoded by different genes, with these isoforms sharing 85% homology (Shaw *et al.* 1998). GSK3 isoforms are regulated by a phosphorylation event at serine 21 for GSK3α and serine 9 for GSK3β; phosphorylation at these sites inhibits activity. Conversely, dephosphorylation by a serine/threonine kinase, such as PP1, activates GSK3 kinase activity (Stambolic *et al.* 1994, Wang *et al.* 1994). GSK3 kinase activity depends on substrate priming, where the target substrate protein is first phosphorylated four amino acid residues upstream of the GSK3 target residue. This makes tau a prominent target for GSK3 phosphorylation due to the many phosphorylation sites present (Dajani *et al.* 2001). In fact, GSK3 phosphorylates tau at 42 sites, with 29 of those sites also found phosphorylated in AD brains (Hanger *et al.* 2009).

Several lines of evidence point to an interplay between Aβ, tau, and GSK3β-mediated phosphorylation in AD. Aβ peptide administration to cultured primary neurons increases GSK3β activity, tau phosphorylation, and apoptotic cell death (Takashima *et al.* 1996). Injection of Aβ oligomers into the hippocampus of a tau transgenic mouse model (rTg4510) resulted in increased GSK3β activation and tau phosphorylation, even two months after administration,

suggesting a long-lasting effect on tau pathology after Aβ exposure (Selenica *et al.* 2013). Tau knockout mice overexpressing GSK3β showed a reduction of learning and memory deficits in the absence of tau compared to GSK3β overexpressing mice with normal tau levels (Gomez de Barreda *et al.* 2010). In AD patients, GSK3β colocalizes to NFTs and active GSK3β increases in the frontal cortex (Yamaguchi *et al.* 1996, Pei *et al.* 1997, Leroy *et al.* 2007). Other kinases involved in tau phosphorylation in AD include cyclin-dependent kinase-5 (Cdk5), mitogen-activated protein kinases (MAPK) such as p38, ERK, and JNK, protein kinase cAMP-dependent (PKA), Ca^{2+} / calmodulin-dependent protein kinase II (CaMKII), and several others (Martin *et al.* 2013). The role of protein kinases in the pathophysiology of AD continues to be an active area of research, and it remains to be seen which kinases, or a combination of kinases, occur upstream of tau and AD pathology before symptom onset.

Though tau phosphorylation has dominated the literature for disease-associated PTMs of tau, there is an emerging strong interest in understanding how other PTMs affect tau in disease (Martin *et al.* 2011). Acetylation at Lys163, Lys280, Lys281, or Lys369 are inhibitory to degradation, while acetylation at Lys259, Lys290, Lys321, or Lys353 promote degradation (Min *et al.* 2010, Cook *et al.* 2014). Additionally, acetylation of the lysine residues that promote tau degradation (e.g. Lys163, 174, and 180) are reduced in AD individuals and the rTg4510 tau transgenic mouse model, whereas acetylation that is inhibitory (e.g. Lys280) are increased in AD and other tauopathies (Irwin *et al.* 2013, Cook *et al.* 2014). Finally, acetylation at Lys174 occurs in human AD brains, and evidence shows acetylation at this site decreases tau degradation and might be a required modification for tau-mediated toxicity (Min *et al.* 2015).

Glycosylation is the covalent attachment of oligosaccharides to a protein and occurs in two ways, N-glycosylations and O-glycosylation, depending on whether the oligosaccharide is bound to the amine radical of asparagine or the hydroxyl radical of a serine or threonine, respectively. In AD brains, but not normal brains, tau is N-glycosylated which may help maintain and stabilize PHF structure (Wang *et al.* 1996) and promote tau phosphorylation by preventing

phosphatases from acting on tau (Liu *et al.* 2002). O-glycosylation is reduced in AD brains (Liu *et al.* 2004), and may prevent phosphorylation by binding serine and threonine residues and subsequently disrupt tau aggregation (Liu *et al.* 2004, Yuzwa *et al.* 2014). Finally, in AD there is impaired glucose uptake and metabolism, which contributes to GSK3β activation and reduction in tau O-glycosylation, theoretically resulting in an increase in tau phosphorylation and aggregation (Gong *et al.* 2006, Deng *et al.* 2009, Liu *et al.* 2009, Liu *et al.* 2009).

Non-enzymatic modifications of tau, including glycation and isomerization, are present in PHF tau but not monomers and may facilitate aggregation (Yan *et al.* 1995, Watanabe *et al.* 2004). Glycation is a non-enzymatic glycosylation of a lysine residue frequently observed in aging, and these proteins are not degraded or expelled from the cell (Martin *et al.* 2011). Seven of the 12 glycation sites on tau are found in the MTBR (Nacharaju *et al.* 1997, Necula *et al.* 2004, Kuhla *et al.* 2007). Glycated tau also shows increased sensitivity to free radicals and oxidation and may be more stable and prone to oligomerization and aggregation (Yan *et al.* 1994, Necula *et al.* 2004).

Tau truncation occurs in AD brains at three sites in tau, Asp13, Glu391, and Asp421, and occurs in the maturation of NFTs that accumulate in AD brains and correlate with AD progression (Gamblin *et al.* 2003, Horowitz *et al.* 2004, Guillozet-Bongaarts *et al.* 2005, Basurto-Islas *et al.* 2008). Truncation can occur through caspase-3 or calpain and the aggregation of truncated tau is not observed in normal brains (Gamblin *et al.* 2003, Park *et al.* 2005). Cleavage of tau by caspases-3, 6, 7, and 9 contribute to the maturation of NFTs and correspond with early, middle, and late stage histological markers, correlate with cognitive decline, and were used to grade the severity of AD (Fasulo *et al.* 2000, Guo *et al.* 2004, Horowitz *et al.* 2004, Rissman *et al.* 2004, Mondragon-Rodriguez *et al.* 2008, Albrecht *et al.* 2009, Wai *et al.* 2009). Additionally, evidence from these studies support the hypothesis that tau truncation occurs after other post-translational modifications, such as phosphorylation, and is associated with the progression of tau aggregation (Martin *et al.* 2011).

Lastly, tau is a substrate for sumoylation and ubiquitination. Lys340 is the major sumoylation site (Dorval *et al.* 2006), however, whether sumoylation of tau is involved in AD pathogenesis or progression at all is still debated. Sumoylation of tau was reported to not occur in AD brains (Pountney *et al.* 2003), whereas another study found sumoylation of tau in AD brains but not control brains, and that this sumoylation promotes tau phosphorylation and inhibition of tau degradation (Luo *et al.* 2014). Interestingly, SUMO1 reactivity co-localizes with tau aggregates in the presence of amyloid pathology, as shown in APP transgenic mice but not in tau transgenic mice, suggesting amyloid is required for sumoylation of tau (Takahashi *et al.* 2008). Ubiquitination signals for protein degradation by binding one or several ubiquitin molecules in a chain. Under normal conditions, tau is ubiquitinated and degraded by the ubiquitin-proteasome system (Arnaud *et al.* 2009, Liu *et al.* 2009). As PHFs mature and develop, ubiquitination increases, and high levels of ubiquitinated tau proteins are present in PHFs and cerebrospinal fluid of AD patients, suggesting that accumulation of ubiquitinated tau may become a biomarker for AD in the future (Iqbal *et al.* 1991, Iqbal *et al.* 1998). Collectively, the new research avenues investigating tau PTMs hold promise for identifying new therapeutic targets for interventions in tauopathies.

Non-AD Tauopathies

AD is one of several diseases collectively known as tauopathies because they are characterized by neuropathological tau inclusions (Spillantini *et al.* 2013). Frontal temporal dementia with parkinsonism linked to chromosome 17 (FTDP-17), links several mutant forms of tau directly to neurodegeneration; therefore, demonstrating that tau abnormalities are sufficient to cause neurodegenerative disease in humans (Hutton *et al.* 1998). Several FTDP-17 mutations (i.e. A152T, P301L, P301L, R406W) are studied in transgenic rodent models and most of them recapitulate several aspects of human disease, including synaptic and axonal loss, neurodegeneration, tau pathology and behavioral deficits (motor and/or cognitive), further

highlighting the causative role abnormal tau can play in causing disease. (Kneynsberg *et al.* 2017). Other tauopathies include Pick's disease, progressive supranuclear palsy, chronic traumatic encephalopathy, and corticobasal degeneration. These diseases are differentiated by which tau isoform most commonly integrates into pathological inclusions and which cell types are affected. For example, Pick bodies in Pick's disease are mostly composed of 3R tau present in neurons and glia, whereas coiled bodies in progressive supranuclear palsy are mostly composed of 4R tau present in oligodendrocytes (Kovacs 2015). The common characteristic of tau pathology across the tauopathies indicates tau can be modified to undergo biologically relevant changes and facilitate neurodegenerative mechanisms in disease, but whether tau is the initiating factor or a downstream consequence of something else is an active area of research.

Serine/Threonine Protein Phosphatases

Estimates suggest that ~70% of all proteins are regulated by phosphorylation (Olsen *et al.* 2010). The majority of phosphorylation occurs at serine and threonine residues in proteins, with those sites making up 98.2% of sites able to be phosphorylated. Additionally, in the human genome, 420 genes encode Ser/Thr protein kinases, whereas less than 40 genes encode Ser/Thr protein phosphatases (Peti *et al.* 2013). Ser/Thr protein phosphatases are subdivided into multiple families, with the largest family being phosphoprotein phosphatases (PPP), consisting of protein phosphatase 1 (PP1), PP2A, calcineurin (PP3), and several others, with PP1 and PP2A being two of the most abundant enzymes in many cell types (Shi 2009). Additional Ser/Thr phosphatase families include protein phosphatases that are magnesium or manganese dependent (PPM), which includes PP2C (Wenk *et al.* 1992), and dual specificity phosphatases that can dephosphorylate both Ser/Thr residues and tyrosine residues (Patterson *et al.* 2009).

Protein Phosphatase 1

PP1, also knowns as phosphorylase phosphatase, is a highly conserved Ser/Thr phosphatase, abundant in all eukaryotic organisms (Cohen 2002, Gibbons *et al.* 2007). In mammals, three genes encode four PP1 isoforms: *PPP1CA* (PP1α), *PPP1CB* (PP1β), and *PPP1CC* which is alternatively spliced to form PP1γ1 and PP1γ2, with PP1γ1 being more prevalent in the central nervous system (Kitagawa *et al.* 1990, Shima *et al.* 1993, Ouimet *et al.* 1995). These isoforms are greater than 85% similar in their primary structure with the divergences in sequences occurring at the N- and C-termini, leaving the catalytic core highly conserved between the isoforms (Fardilha *et al.* 2010). This implies that the termini of the PP1 isoforms dictate the phosphatase properties; one study provided supporting evidence for this idea by generating a PP1 and PP2B chimera. The first 8 amino acids in PP1 were replaced with the first 12 amino acids of PP2B. Even with the catalytic core and C-terminus unchanged, the synthetic enzyme possessed the properties of PP2B such as less sensitivity to PP1-specific inhibitors like okadaic acid and stimulation by nickel ions and chlorogenic acid (Xie *et al.* 2009).

Within the central nervous system, PP1 mRNA is enriched in the hippocampus while PP1α and γ1 protein were enriched in the striatum (da Cruz e Silva *et al.* 1995). Both neurons and glia express PP1, with PP1 immunoreactivity highly enriched in dendritic spines, implying an important role in post-synaptic signaling (da Cruz e Silva *et al.* 1995, Ouimet *et al.* 1995).

PP1 Structural Biology

PP1 is a globular protein with the catalytic site containing two divalent metal ions essential for facilitating the hydrolysis of phosphate groups from the substrate protein. Recombinant PP1 produced in bacteria contains two manganese ions in the catalytic site, whereas the mammalian native enzyme typically contains iron or zinc (Bollen *et al.* 2010). Radiating out of the intersection of the catalytic site are three grooves proposed to be substrate binding regions: the acidic groove, the hydrophobic groove, and the C-terminal groove

(Goldberg *et al.* 1995, Egloff *et al.* 1997). These grooves were named for the presence of exposed acidic side chains in the acidic groove, exposed hydrophobic sidechains in the hydrophobic groove, and the path of the C-terminal groove passing from the catalytic site to the C-terminus of the protein (Goldberg *et al.* 1995). Most PP1 interacting partners require a specific binding pocket on the surface of PP1. This primary binding motif is the RVxF motif and with the general sequence of [K/R][K/R][V/I][x][F/W], where X is any residue except phenylalanine, isoleucine, methionine, tyrosine, proline, or aspartic acid, however, not all interacting partners conform exactly to this formula (Wakula *et al.* 2003, Meiselbach *et al.* 2006, Hendrickx *et al.* 2009). Other binding domains on the surface of PP1 include the SILK domain present in ~10 interacting partners (Hurley *et al.* 2007), the myosin phosphatase N-terminal element motif present in ~7 interacting partners (Terrak *et al.* 2004, Pinheiro *et al.* 2011), and the elaborate spinophilin docking motif (Ragusa *et al.* 2010). Acidic residues surround the catalytic site of PP1, which is proposed to influence substrate specificity of PP1 relative to other phosphatases (Egloff *et al.* 1997). For example, the β-subunit of phosphorylase kinase is more basic than the α-subunit, and therefore has a higher affinity for PP1's catalytic site. PP1 more readily dephosphorylates the β-subunit, and utilizing this substrate allows investigators to differentiate PP1-dependent dephosphorylation from other phosphatases (Bollen *et al.* 1992).

PP1 Interacts with Regulatory Partners to Determine Localization and Substrate Specificity

There are currently more than 200 known PP1 interacting proteins (Korrodi-Gregorio *et al.* 2014). The broad substrate specificity of PP1 in *in vitro* assays was thought to indicate a regulatory nature in modulating or regulating many kinase signaling cascades, however, several early attempts to isolate PP1 found it co-purifying as a high molecular weight complex, indicating its association with other proteins (Lee *et al.* 1980). Thus, PP1 and interacting partners form numerous combinations of holoenzymes. Proteins that interact with numerous interacting partners are termed "hubs", which is further subdivided into "party" and "date" hubs.

Party hubs interact with many interacting partners at the same time, whereas date hubs interact with one or two partners (Han *et al.* 2004). PP1 is considered a date hub due to the larger number of interacting partners (over 200) but only interacts with one or two in any given moment (Heroes *et al.* 2013). Classically, PP1-interacting partners were identified using yeast two-hybrid screens and microcystin affinity chromatography, with more recent approaches employing *in silico* bioinformatics and prediction algorithms and antibody-based purification methods (Moorhead *et al.* 1994, Flores-Delgado *et al.* 2007, Moorhead *et al.* 2007, Hendrickx *et al.* 2009).

Many PP1 interacting proteins contain specific motifs and domains that act in unison to dictate the topography of the interaction and the functional outcome for PP1, such as modulating its substrate specificity and targeting to specific compartments. Targeting PP1 to cellular compartments or modulating the affinity of the catalytic site for various substrates by physically and electrochemically adjusting the surface of PP1 gives rise to the tight spatial and temporal control of PP1 activity. For example, PP1 interacting partners, such as tau, are known to target PP1 to microtubules (Liao *et al.* 1998), as well as other proteins that target PP1 to the plasma membrane, mitochondria, endoplasmic reticulum, actin, chromatin, and nucleoli (Bollen *et al.* 2010). This targeting function of interacting partners allows for a closer proximity of PP1 and its substrate, however, a local increase of substrate without targeting of PP1 can also increase the rate of dephosphorylation (Zeke *et al.* 2009). Most interacting proteins contain one or more separate PP1 binding motifs that are four to eight amino acid residues long, which together can occupy a large surface of PP1 for its interaction. For example, tau contains three RVxF motifs (Liao *et al.* 1998). If the average docking motif encompasses ~42.5 nm^2 of space, then four docking motifs at the same time will occupy ~85 nm^2 of the surface of PP1, not accounting for non-interacting overlapping residues (Hurley *et al.* 2007). Additionally, PP1 currently has ~30 proposed interaction sites on its surface, much less than the number of known interacting proteins, indicating that binding partners of PP1 share interaction motifs, such as the

RVxF motif. Collectively, the large number of interacting partners and combinations of binding motifs within PP1 and in interacting partners leads to considerable control and modulation of PP1 phosphatase specificity and localization (Bollen 2001).

Phosphatases and Intrinsically Disordered Proteins in Alzheimer's Disease

Broadly speaking, mutations in proteins that result in a misfolded conformation are normally refolded by chaperones or degraded by the proteasome (Glickman *et al.* 2002, Young *et al.* 2004). In neurodegenerative diseases, multiple factors can contribute to this system being unable to keep up with the production of misfolded proteins, such as gene multiplications and a decreased efficiency with aging (Bodner *et al.* 2006). When this system is overwhelmed, aggregation-prone proteins, such as intrinsically disordered proteins, can have an increased likelihood to associate with each other, aggregate, and disrupt normal cellular function, which can lead to neuronal death. Aβ, tau, and αSyn are classified as intrinsically disordered proteins due to the lack of stable secondary and/or tertiary structures and highly flexible nature in solution (Breydo *et al.* 2012). Although intrinsically disordered proteins lack stable secondary and tertiary conformations, they typically change to form stable β-sheet rich secondary structures when they aggregate in disease. Examples of factors that help to facilitate these structural changes in disordered proteins include phosphorylation, acetylation, temperature changes, pH alterations, and increased concentration of monomers (Jarrett *et al.* 1993, Uversky *et al.* 2001, Breydo *et al.* 2012). Several PP1 interacting proteins are intrinsically disordered, such as tau, DARPP-32, inhibitor-2, and spinophilin (Dancheck *et al.* 2008). One reason this may be important is because the disordered nature of the binding partners increases the flexibility of the protein and can facilitate multi-site interactions at several PP1 binding motifs. While a single published paper provided evidence that tau and PP1 might interact and that tau may function to target PP1 to microtubules, many questions regarding the specifics of tau-PP1 interactions and the functional consequences of these interactions remained unclear.

PP1 in Alzheimer's Disease

Tau is a known substrate and interacting partner of PP1, and interest in the role PP1 plays in tau physiology and AD pathology naturally followed (Liao *et al.* 1998). In preparations generated from post-mortem human tissue, PP1 dephosphorylated Thr212, Thr217, Ser262, Ser396, and Ser422, but was unable to dephosphorylated Thr181, Ser199, Ser202, Thr205, Ser214, and Ser404 (Liu *et al.* 2005, Rahman *et al.* 2005). Additionally, several lines of evidence point to PP1 and its binding proteins as important components in the pathogenesis of AD. Okadaic acid, an inhibitor of PP1 and PP2A, reduced Aβ peptide production and promoted secretion of soluble APP when used at a concentration that inhibits both enzymes; this result was capitulated in hippocampal slices from APPswe/PS1 transgenic mice. (Buxbaum *et al.* 1993). In AD, PP1 may play a role in synaptic plasticity by dephosphorylating NMDA and AMPA glutamate receptors to regulate their trafficking to the synapse. Alternatively, it was suggested that PP1's regulatory role in AD may be at the transcription factor level by modulating CREB or the kinase level by regulating GSK3 or CaMKII (Braithwaite *et al.* 2012).

Another proposed mechanism of PP1 involvement in AD is through regulating expression of β-secretase (BACE1) (O'Connor *et al.* 2008). BACE1 is the rate-limiting enzyme in Aβ peptide formation and is upregulated in AD (Yang *et al.* 2003, Zhao *et al.* 2007). This regulation is achieved through the translational initiator eIF2α, which when phosphorylated, typically results in an inhibition of translation. However, some mRNAs are preferentially upregulated under this condition, with BACE1 being one such gene, potentially resulting in increased BACE1 protein production (Braithwaite *et al.* 2012). PP1 dephosphorylates eIF2α when in complex with the PP1 interacting protein GADD34 (Brush *et al.* 2003, Marciniak *et al.* 2006). In primary neuron experiments, salubrinal, a small molecule inhibitor of PP1 when in complex with GADD34, increased phosphorylation of eIF2α and subsequently BACE1 proteins levels increased with exacerbated Aβ peptide production and blocking eIF2α had the opposite effect (Boyce *et al.* 2005).

PP2A In Alzheimer's Disease

PP2A has received more research attention in the etiology of AD than PP1, as most dephosphorylation of tau (~71%) occurs through the action of this enzyme (Sontag *et al.* 1996, Liu *et al.* 2005). While the phosphatase activity of PP2A on tau is important to the normal physiology of the proteins, PP2A also can modulate tau's trafficking, targeting, localization, and scaffolding function (Taleski *et al.* 2018). PP2A, similar to PP1, relies on several interacting partners to govern substrate specificity and targeting (Sents *et al.* 2013). PP2A exists as a heterotrimeric holoenzyme consisting of a scaffolding "A" subunit, a catalytic "C" subunit, and a regulatory "B" interacting partner subunit (Hoffman *et al.* 2017). The isoform possessing the strongest affinity for tau and highest level of dephosphorylation of tau is the Bα subunit (PP2A/Bα) (Xu *et al.* 2008). PP2A/Bα binds to the MTBRs of tau to promote tau dephosphorylation. Additionally, there is a preference for 4R tau and PP2A can only bind tau in the absence of tau-tubulin binding (Sontag *et al.* 1996, Sontag *et al.* 1999).

In AD, PP2A is downregulated, less active, and its substrate specificity and localization are dysfunctional (Gong *et al.* 1993, Sontag *et al.* 2004, Sontag *et al.* 2004). Interestingly, methylation of PP2A is largely decreased in AD, which results in reduced PP2A/Bα, as the Bα subunit preferentially binds to the methylated form of the PP2A catalytic subunit, possibly underlying some of the PP2A dysfunction observed in AD. (Bryant *et al.* 1999, Sontag *et al.* 2004, Zhou *et al.* 2008). Reduced PP2A activity could be a driving force behind tau phosphorylation and development of NFTs (Iqbal *et al.* 2005). Several models of AD investigating the role of PP2A exist, but care must be taken to ensure cell viability, as PP2A activity is essential for survival (Gotz *et al.* 1998). Inhibiting endogenous PP2A with specific inhibitors or overexpressing a dominant-negative form of the protein in these models shows increased tau phosphorylation, Aβ deposition, NFTs, and neurodegeneration (Arendt *et al.* 1995, Arendt *et al.* 1998). Taken together, dysfunction of Ser/Thr protein phosphatases is a

common characteristic of AD brains, and several lines of evidence support their central role in maintaining normal phosphorylation levels before onset of symptoms.

Tau as a Signaling Regulator in Neurodegeneration

Axon Degeneration and Dysfunction in Tauopathies

Axons undergoing degeneration typically follow a well characterized pattern, such as development of axonal swellings called spheroids and thinning of the axon between spheroids to resemble an image of beads on a string (Raff *et al.* 2002). Eventually, this thinning results in axon fragmentation and degeneration characteristic of tauopathies (Zhou *et al.* 1998). In AD, inclusions of tau within neurites, called neuropil threads, are thought to appear before the formation of NFTs in the cell body (Kowall *et al.* 1987, Ghoshal *et al.* 2002), although clear evidence from human tissue directly supporting this hypothesis is lacking. Additionally, these changes, as well as synaptic changes and degeneration, are early and prominent pathological events in AD (DeKosky *et al.* 1990, Masliah *et al.* 1991, Bell *et al.* 2006, Vana *et al.* 2011). Patients with AD exhibit pronounced white matter atrophy, indicating loss of axons, whereas patients with mild cognitive impairment display demyelination of axons in the perforant pathway and cortical regions (Stoub *et al.* 2006, Huang *et al.* 2007). Finally, loss of axons in more severe AD cases correlates with cognitive decline, as does the presence of NFTs (Bozzali *et al.* 2002, Giannakopoulos *et al.* 2003)..

Pathological Forms of Tau Inhibit Axon Transport

Several studies have investigated pathological forms of tau and the effects on axonal transport. Tau aggregates were infused into squid axoplasms at a physiological concentration where they were shown to reduce anterograde fast axonal transport (LaPointe *et al.* 2009). This effect was dependent on the extreme N-terminus of tau (amino acids 2-18), as deleting this region eliminated the toxic effect and infusion of a peptide comprised of this motif recapitulated

the same effects as the tau filaments (LaPointe *et al.* 2009, Kanaan *et al.* 2011). These studies also showed this deficit was dependent on a signaling through PP1 and GSK3β, as co-infusion with the GSK3β inhibitors ING-135 or CREBpp, and the PP1 inhibitor inhibitor-2 (I-2) rescued this deficit (LaPointe *et al.* 2009, Kanaan *et al.* 2011). Following up this study, deeper investigation and characterization into this N-terminal motif with additional pathological forms of tau was performed. Specifically, AT8 tau in its monomeric state was infused into squid axoplasms and this resulted in reduced fast anterograde axonal transport similar in fashion to tau filaments (Kanaan *et al.* 2011). Further studies also showed that this mechanism of tau toxicity to transport was engaged by all six human tau isoforms when aggregated as well as modifications at other phosphosites in tau (i.e. monomeric phospho-Ser422 tau protein) (Cox *et al.* 2016, Tiernan *et al.* 2016) Therefore, this region in tau corresponding to amino acids 2-18 was termed the phosphatase activating domain (PAD) (Kanaan *et al.* 2011). These studies also highlighted several key aspects of this potential mechanism of tau toxicity. Specifically, the ability of tau to impair axonal transport had no dependence on microtubule binding, did not require aggregation, and that specific modifications alter tau structure in ways that aberrantly activate the PP1-GSK3 pathway. However, they did not fully explore the relationship between tau and PP1, the first step in this proposed cascade of tau-induced axonal dysfunction.

Tau is Proposed to Signal Axon Dysfunction Through a PP1-GSK3β Cascade

There is growing evidence that tau's functional repertoire is much larger than just stabilizing microtubules and may include cell signaling functions, among others(LaPointe *et al.* 2009, Souter *et al.* 2010, Kanaan *et al.* 2011, Kanaan *et al.* 2012). Moreover, there is evidence that abnormalities in the non-microtubule stabilizing functions of tau may underlie the mechanisms of tau-induced toxicity in disease. Several disease-related modifications of tau, including the AT8 phosphoepitope, alter its conformation causing abnormal exposure of PAD (Jeganathan *et al.* 2008, Kanaan *et al.* 2011). Previous work showed that psAT8 tau extends

the N-terminus out of the “paperclip” conformation (Jeganathan *et al.* 2008), which exposes PAD. Monoclonal antibodies specific for the exposed N-terminus of tau (TNT1 and TNT2) confirms the finding that this region is exposed when tau is phosphorylated at the AT8 epitope and that PAD exposure occurs early during pathological tau deposition and in several human tauopathies (Kanaan *et al.* 2011, Combs *et al.* 2016, Combs *et al.* 2017). PAD exposure triggers activation of PP1, which subsequently dephosphorylates glycogen synthase kinase-3β (GSK3β) at Ser9 (Zhang *et al.* 2003). The resulting activated GSK3β phosphorylates kinesin light chains causing cargoes to dissociate from the motor complex, leading to impaired anterograde fast axonal transport (Morfini *et al.* 2002, Morfini *et al.* 2004, Morfini *et al.* 2007, Kanaan *et al.* 2011, Kanaan *et al.* 2012). Importantly, PAD was both necessary and sufficient to reduce transport (Kanaan *et al.* 2011). Interestingly, ablation of tau prevents amyloid-β-induced GSK3β activation, further suggesting a role for tau in GSK3β-mediated neuronal dysfunction (Moorhead *et al.* 2007). While this recent evidence has suggested a potential signaling mechanism of tau in AD, there remains a gap in our knowledge involving the specifics of how tau activates the PP1/GSK3β cascade leading to axon degeneration. Specifically, whether tau directly binds to and activates PP1 and how disease-associated modifications known to cause axonal toxicity, such as AT8 tau, affect this mechanism was not clearly defined in prior work.

Dissertation Objective

The goal of this dissertation was to further investigate if PAD exposure is an early pathological event in the development of tau protein deposition in humans as well as elucidate and characterize the capacity for tau to regulate PP1 activation and subsequent dysfunction in axons. Only one previous publication investigated the interaction between tau and PP1, and did not differentiate between PP1 isoforms, domains of tau, or pathological modifications (Liao *et al.* 1998). I investigated if AT8 phosphorylation and PAD exposure appear in axonal compartments of the hippocampus using ND and MCI post-mortem human brain cases to systematically

determine where in a neuron pathology appears first in the human condition. Furthermore, I established that tau interacts with PP1 in an isoform-dependent manner, and this interaction depends on the MTBRs, not the N- or C-termini. Additionally, I investigated whether AT8 phosphorylation and the presence of the PAD domain change tau's interaction with PP1 and whether these modifications impact PP1 phosphatase activity. Further characterizing this proposed tau signaling cascade behind the etiology of axonal degeneration in AD could lead to the development of new therapeutic interventions for the treatment of AD. The specific aims for my dissertation are as follows:

Specific Aim 1: Determine if AT8- and PAD exposed tau appear in the axonal compartment of affected neurons before the somatodendritic compartment in human tissue. Specific Aim 1 is addressed in chapter 2 using a cohort of post-mortem human cases ranging from non-demented controls to mild cognitive impairment to capture a brain environment before the development of AD. The hippocampal formation from these cases were processed for immunohistochemistry to visualize AT8 phosphorylated tau, PAD exposed tau, and amyloid plaques. The extent of tau pathology was estimated specifically in the mossy fiber and Schaffer collateral pathways, as the terminal fields and corresponding originating cell bodies are extensively characterized and relatively discretely contained within specific strata of the hippocampus. I hypothesized that tau inclusions containing AT8 phosphorylation and PAD exposure deposit early and appear first in the axons of affected neurons before the cell bodies.

Specific Aim 2: Characterize the interaction between tau and PP1 and the effect of AT8 phosphorylation on PP1 phosphatase activity. Specific Aim 2 is addressed in chapter 3 using *in vitro* protein interaction assays and a phosphatase activity assay. The interaction between tau and PP1 was investigated for each PP1 isoform and several modifications of tau, including AT8 phosphorylation and dependence on the PAD region. Tau's influence on PP1 phosphatase

activity was investigated using *para*-nitrophenyl phosphatase as a substrate for recombinant PP1 in solution with several recombinant tau proteins. I hypothesized that tau and PP1 directly interact, AT8 pseudophosphorylation increases this interaction, and deletion of the PAD region reduces this interaction. Additionally, I hypothesized that the resulting changes in tau-PP1 interactions results in changes of PP1 phosphatase activity.

CHAPTER 2

Pathogenic Tau Modifications Occur in Axons Before the Somatodendritic Compartment in Mossy Fiber and Schaffer Collateral Pathways

Abstract

Tau is a microtubule-associated protein that is classically thought to play a role in stabilizing microtubules and the pathological accumulation of tau protein is a hallmark of several diseases collectively known as tauopathies (including AD). A long-held hypothesis on the progressive deposition of tau pathology in AD is that pathological tau accumulates first in axons of neurons and then progresses back into the cell bodies to form neurofibrillary tangles, however, studies have not directly analyzed this relationship in human tissue. In the early phases of tau deposition, both AT8 phosphorylation and exposure of the amino terminus of tau occur in tauopathies, and these modifications are linked to mechanisms of synaptic and axonal dysfunction. Here, we examined the localization of tau pathology using well-characterized post-mortem human tissue samples in the hippocampus of 44 cases ranging between non-demented and mild cognitively impaired to capture a time in which intrahippocampal pathways show a range in the extent of tau deposition. The tissue sections were analyzed for AT8 (AT8 antibody), amino terminus exposure (TNT2 antibody), and amyloid-β plaque (MOAB2 antibody) pathology in the axons and neuronal cell bodies in hippocampal strata containing the CA3-Schaffer collateral and dentate granule-mossy fiber pathways. We show that tau pathology first appears in the axonal compartment of affected neurons in the absence of observable tau pathology in the corresponding cell bodies. Additionally, deposition of tau in these intrahippocampal pathways was independent of the presence of Aβ plaques. Using an axonal marker (i.e. SMI312 antibody) we confirmed that the majority of tau pathology positive neuropil threads were indeed axonal in origin. Taken together, these results support the hypothesis that AT8 phosphorylation and PAD exposure are early pathological events and that the deposition of tau pathology occurs first in the axonal compartment prior to observable pathology in the somata of affected neuronal

pathways. These findings highlight the importance on targeting tau deposition, ideally in the initial phases of its deposition in axons.

Introduction

Tau is a microtubule- associated protein involved in regulating axon integrity and function (Drechsel *et al.* 1992, Wang *et al.* 2008). Notably, tau aggregation and deposition is a hallmark of Alzheimer's disease (AD) as well as numerous other tauopathies (Glenner *et al.* 1984, Masters *et al.* 1985, Kosik *et al.* 1986, Braak *et al.* 1991, Hebert *et al.* 2013). Pathological modifications and aggregation of tau associate with cognitive decline (DeKosky *et al.* 1990, Ghoshal *et al.* 2002, Giannakopoulos *et al.* 2003). The deposition of amyloid-β (Aβ) in plaques represents the other hallmark pathology and likely contributes to neurotoxicity in AD (Masters *et al.* 1985, Kowall *et al.* 1991). Alterations in synapse morphology, synapse loss, and axon degeneration occur early in the progression of AD (DeKosky *et al.* 1990, Masliah *et al.* 1991, Bell *et al.* 2006, Vana *et al.* 2011). This has led to the hypothesis of a "dying-back" pattern of degeneration, where axon degeneration precedes loss of cell bodies (Kanaan *et al.* 2013). The hypothesis that tau pathology begins in the axonal compartment and appears in the somatodendritic compartment afterwards is often suggested, however, a direct analysis of axon enriched layers in the hippocampal formation, has not previously been conducted (Kowall *et al.* 1987, Ghoshal *et al.* 2002) . Moreover, the amyloid cascade hypothesis suggests that Aβ pathology precedes and induces the accumulation of tau pathology presumably starting in axonal target regions of neurons affected by tau (Selkoe 1991, Hardy *et al.* 1992, Hardy *et al.* 2002). Animal models of tauopathy also support the contention that tau deposition occurs in the synaptic and axonal compartments prior to the somatodendritic compartment (Andorfer *et al.* 2003, de Calignon *et al.* 2012). Observations in human tissue describing the appearance of extensive neuropil threads (NTs) before detection of neurofibrillary tangles (NFTs) in neuronal cell bodies within a given neuroanatomical region support this hypothesis (Su *et al.* 1997,

Ghoshal *et al.* 2002, Vana *et al.* 2011) but none of these studies assessed the terminal fields and somata of specific pathways in the earliest stages of tau deposition precluding a clear determination of whether axonal pathology precedes cell body pathology in cells.

The hippocampal formation comprises the entorhinal cortex (EC), dentate gyrus (DG), hippocampus proper (subdivided into CA1, CA2, and CA3, and hilus), subiculum, presubiculum, and parasubiculum (Amaral *et al.* 1989, Andersen *et al.* 2006). The EC is typically considered the start of the circuit because it receives most of the neocortical input into the hippocampal formation (Adey *et al.* 1952, Andersen *et al.* 2006). EC efferents project through the angular bundle and perforant path to terminate on DG granule cells in the molecular layer. The DG granule cells do not project back to the EC, but instead project to CA3 pyramidal cells through the mossy fiber pathway and terminate in the CA3 stratum lucidum layer (Str. Luc). Next, CA3 pyramidal cells project to CA1 pyramidal cells through the Schaffer collateral pathway and terminate in the CA1 stratum radiatum layer (Str. Rad.). A majority of the CA1 pyramidal cell projections terminate in the subiculum, however, some also project back to the EC. Finally, most subiculum projections pass back through the angular bundle to the EC to complete the circuit, with other projections connecting to additional subcortical areas (Amaral *et al.* 1989, Andersen *et al.* 2006). The well-defined intrahippocampal circuitry and relatively distinct strata provide an ideal structure to analyze the compartmental progressive deposition of pathological tau within discrete neuronal pathways in post-mortem human tissue.

Tau pathology in the form of neurofibrillary tangles (NFTs), neuropil threads (NTs) and neuritic plaques (NPs) follows a regional progression in severity, that was described by Braak and Braak in the early 1990's (i.e. Braak staging) and now represents the most common method for describing the post-mortem staging of AD tau pathology (Braak *et al.* 1991, Braak *et al.* 1994). Braak staging was originally developed based on silver staining of tau pathology and later adapted to AT8+ pathology (Braak *et al.* 1994). Deposition of tau inclusions begins in the trans entorhinal and EC at Braak stages I-II, but these stages are not associated with cognitive

decline(Giannakopoulos *et al.* 2003, Markesbery *et al.* 2006). The limbic stages (Braak III-IV) display spread of tau pathology further into the hippocampal formation, including CA1 and the subiculum. Cognitive decline occurs at these stages and patients may display criteria for mild cognitive impairment (MCI), a prodromal stage of AD progression (Bancher *et al.* 1993). MCI is considered an intermediate stage before AD (Gamblin *et al.* 2003, Mufson *et al.* 2016, Tiernan *et al.* 2016). These observations support the notion of a preclinical AD stage (Mufson *et al.* 2016). Finally, the isocortical stages (Braak V-VI) displays extensive tau pathology throughout the hippocampal formation and subdivisions of the cerebral cortex. Additionally, these late stages correspond with the pathological criteria for AD diagnosis(Braak *et al.* 1995). Deposition of Aβ is required for AD diagnosis and is typically accompanied by other pathological staging criteria, such as the Consortium to Establish a Registry for Alzheimer's Disease (CERAD) scores (Hyman *et al.* 2012, Boluda *et al.* 2014).

During the course of tau deposition in disease the tau proteins undergo fairly well-characterized changes including both the morphology of and the post-translational modifications to the tau proteins within the pathology (Bancher *et al.* 1993, Binder *et al.* 2005, Guillozet-Bongaarts *et al.* 2005, Mondragon-Rodriguez *et al.* 2008, Combs *et al.* 2016). Importantly, there are specific changes that occur during the earliest detectable deposition of tau inclusions in human brains and these are often referred to as pretangle markers for their ability to recognize tau pathology prior to its maturation and coalescence into compact tau inclusions (Bancher *et al.* 1993, Braak *et al.* 1994, Braak *et al.* 1995, Braak *et al.* 2006, Combs *et al.* 2016).. For example, AT8, a triple phosphoepitope including phospho-S199/S202/T205, appears early in diffuse granular pretangle inclusions in neurons (Biernat *et al.* 1992, Goedert *et al.* 1995). Additionally, conformational display of an N-terminal region known as the phosphatase-activating domain (PAD), a change recognized by the TNT2 antibody, occurs in pretangle neurons in AD and several tauopathies (Combs *et al.* 2016, Combs *et al.* 2017). Importantly, both AT8 and exposure of PAD are linked to a specific mechanism of tau toxicity involving impaired axonal

function (i.e. axonal transport inhibition) (LaPointe *et al.* 2009, Kanaan *et al.* 2011, Kanaan *et al.* 2012). Though these markers are modifications of tau that appear in the earliest detectable tau inclusions, it remained unclear whether these pathogenic forms of tau first appeared in axons before progressing to the neuronal cell bodies.

The current study addresses the hypothesis that tau pathology first deposits in the axonal compartment of neurons prior to its appearance in the somata. Using post-mortem human hippocampal sections from ND controls and MCI cases, the extent of axonal and somatodendritic tau pathology (AT8 phosphorylated and PAD exposed), as well as Aβ pathology in the CA3-Schaffer collateral and DG-mossy fiber pathways was measured with stereological methods. We found AT8 phosphorylation and PAD exposure occurs in the axon compartment of affected neurons even in the absence of observable cell body pathology. Additionally, these tau pathological modifications were observed in the absence of amyloid pathology. Our results support the hypothesis that tau pathology begins in the axonal compartment and is observed independently of Aβ plaque deposition.

Materials and Methods

Human Brain Tissues

Formalin-fixed temporal lobe free-floating sections (40 μm) from ND (n = 31) and MCI (n = 13) cases were obtained de-identified from Banner Sun Health Research Institute and Body Donation Program (Sun City, AZ) (Beach *et al.* 2015). Table 2.1 summarizes the clinical, demographic, and neuropathology of the cases. A schematic of relevant hippocampal connections is shown in Figure 2.1. The mossy fiber and Schaffer collateral pathways are illustrated in red.

Tissue Immunohistochemistry (IHC)

Temporal lobe sections were immunohistochemically stained to visualize the pattern of AT8 phosphorylation, PAD exposure, and amyloid pathology using the monoclonal AT8 (Thermo MN1020), TNT2 (Combs *et al.* 2016), and MOAB2 (Youmans *et al.* 2012) antibodies, respectively, using previously published methods (Kanaan *et al.* 2011, Kanaan *et al.* 2012, Combs *et al.* 2016). Primary antibodies were diluted in tris-buffered saline (TBS; 150 mM NaCl, 50 mM Tris, pH 7.4) containing 2% goat serum and 0.1% Triton X-100 at 1:16,000 for AT8, 1:400,000 for TNT2, 1:4,000 for MOAB2. Immunoreactivity was detected using biotinylated goat-anti-mouse IgG (H+L) secondary antibody (Jackson ImmunoResearch Laboratories 115-065-166) diluted in TBS+2% goat serum + 0.1% Triton X-100, VectaStain Elite ABC-HRP Kit (Vector Laboratories PK-6100), and 3,3'-diaminobenzidine supplemented with 0.25% ammonium nickel (II) sulfate hexahydrate (Sigma A1827). All sections were counterstained with cresyl violet before being mounted on microscope slides and coverslipped with Cytoseal 60 (Thermo Scientific, #8310-16). Tissue sections from each case were processed simultaneously for each antibody to eliminate inter-run staining variability. Primary antibody delete controls were run using the same protocol with the exception that the primary antibody was omitted. As expected, the primary delete produced no staining (Figure 2.2).

Stereological Axon Measurements and Total Neuron Enumeration

The unbiased stereological spaceballs probe was used to estimate the total length of axon fibers stained with AT8 and TNT2 in the Str. Luc. Layer of CA3 (i.e. mossy fibers) and Str. Rad. Layer of CA1 (i.e. Schaffer collaterals). The Str. Luc. was defined using fiduciary neuroanatomical landmarks, including the CA3 pyramidal cell layer dorsally, Str. Rad. of CA3 ventrally, the CA2 medially, and hillus laterally. The CA3 pyramidal layer was defined using fiduciary neuroanatomical landmarks, including the Str. Luc. dorsally, stratum oriens ventrally, CA2 medially, and hillus laterally. The Str. Rad. was defined using fiduciary neuroanatomical

landmarks, including the CA1 pyramidal cell layer dorsally, stratum lacunosum-moleculare ventrally, subiculum medially, and CA2 laterally. The DG granule cell layer was defined using fiduciary neuroanatomical landmarks, including the hillus dorsally and the molecular layer ventrally, and is clearly defined by cresyl violet staining. If specific subregions were not reliably identifiable within the sections, the case was not used for analyses requiring that region. A hemisphere probe with a radius of 8 µm was used to sample sites throughout each region. Tissue thicknesses ranged from ~11-14 µm across all cases and regions analyzed. A 4x objective was used to outline each contour and a 60x oil immersion objective (numerical aperture = 1.35) was used for making the stereological measurements. Fiber staining density was calculated by dividing the estimated total axon length by the volume of the region of analysis, and fiber density was used for comparisons. Somata staining was quantified in the CA3 pyramidal cell layer (i.e. Schaffer collateral pathway) and DG layer (i.e. mossy fiber pathway) by total enumeration within the regions of interest using at 10x magnification. Total cell numbers were used for comparisons. Brightfield images were acquired on a Nikon Eclipse 90i microscope equipped with a Nikon DS-Ri1 camera and processed using NIS-Elements software.

Triple Label Immunofluorescence (IF)

Temporal lobe sections from a subset of the 44 cases (n = 12 cases with high and low tau pathology) were triple labeled with TNT2 (mouse IgG1, 1:8000), SMI-312 (mouse IgG1, 1:5000, Covance SMI-312R), and biotinylated AT8 (mouse IgG1-biotin, 1:800, Thermo Scientific MN1020B) using methods similar to those previously published (Kanaan *et al.* 2016, Tiernan *et al.* 2016). Each primary antibody incubation period was overnight at 4°C. SMI-312 and TNT2 immunoreactivity was detected using AlexFluor 488- and 647-conjugated goat-anti-mouse IgG (H+L) Fab fragments (Jackson ImmunoResearch Laboratories 115-547-003 and 115-607-003), and AT8 immunoreactivity was detected using AlexaFluor 568-conjugated streptavidin

(ThermoScientific Pierce S11226). Sections were blocked with unconjugated goat-anti-mouse IgG (H+L) Fab fragments (Jackson ImmunoResearch Laboratories 115-007-003) to prevent cross-labeling of the secondary antibodies between each primary and subsequent secondary antibody incubations. Control sections included omission of each individual primary and omission of all three primary antibodies. As expected, the individual primary delete sections did not produce cross-reaction of signals in the deleted antibody channel and the full primary delete produced no signal (Figure 2.10). Sections were mounted on microscope slides and autofluoresence of the tissue was blocked by treating with 2% Sudan Black B before coverslipping with VectaShield Hard Set mounting medium (Vector Laboratories H-1000). All IF images were obtained using a Nikon A1+ scanning confocal microscope system. Z-stacks were acquired in 0.5 µm steps and images for figures were generated with a maximum intensity projection using NIS-Elements software. Colocalization of fluorescent markers was analyzed by calculating the Manders Colocalization Coefficient in ImageJ (Manders *et al.* 1993).

Statistical Analyses

All data were analyzed using Prism v7.0 software (GraphPad). Stereological estimate outcomes were analyzed for normality using the D'Agostino and Pearson normality test. All data sets were not normally distributed, and subsequently, non-parametric statistical analyses were performed. All correlation comparisons were performed using the Spearman rank correlation. Demographic variables were compared between clinical diagnostic groups using Mann-Whitney, Fisher's exact, or the Chi-squared test. Statistical significance was set at $p \leq 0.05$.

Results

Subject Demographics

Demographic, clinical, and neuropathological results for the 44 cases used in this study are summarized in Table 2.1. Notably, no significant differences were observed between the ND

and MCI groups for age ($p = 0.13$), sex ($p > 0.99$), postmortem interval (PMI, $p = 0.84$), Mini-Mental State Examination (MMSE, $p = 0.34$), Braak stage ($p = 0.85$), or CERAD score ($p > 0.99$).

AT8 and TNT2 Fiber Density Correlates with Age and Braak Staging

Table 2.2 summarizes the Spearman correlations between AT8+ and TNT2+ fiber and cell tau pathology and several demographic and neuropathology scores. AT8 and TNT2 fiber densities showed a significant positive correlation with age, Braak stage, and total tangles in both the Schaffer collateral and mossy fiber pathways. The only significant correlation with total plaques was a positive correlation with TNT2 fiber density in the Schaffer collateral pathway. AT8+ cell number in the CA3 region positively correlated with age, Braak stage and total tangles, while AT8+ DG cell number correlated with Braak stage, MMSE, and total tangles. TNT2+ cell numbers in the CA3 pyramidal cell layer showed a significant positive correlation with total tangles. Finally, no statistical differences in axonal tau pathology staining (with both AT8 and TNT2) were observed between diagnosis states (Figures 2.3 A-B, 2.4A-B), sex (Figures 2.3 C-D, 2.4 C-D), or CERAD (Figures 2.3 E-F, 2.4 E-F) scores.

Axonal AT8 Tau Pathology Occurs in the Absence of Cell Body Pathology in the Mossy Fiber and Schaffer Collateral Pathways

We measured the amount of AT8+ immunoreactivity in the mossy fiber pathway (Figure 2.5) and the Schaffer collateral pathway (Figure 2.6). All cases displayed AT8+ neuropil threads in the Str. Luc., however, AT8+ staining in the corresponding cell bodies of the DG was less common (Figure 2.5A). Specifically, 16.7% of cases (7 of 42) displayed no observable AT8+ staining in the DG cell bodies, but all of these cases showed AT8+ staining in the Str. Luc., the target region of the mossy fiber projections of the DG (Table 2.3). Axonal AT8 fiber density significantly correlated with the number of AT8+ cell bodies (Spearman $r = 0.640$, $p < 0.0001$,

Figure 2.5B). In cases lacking AT8+ cell bodies in the DG, the observable mossy fiber pathology ranged from sparse to moderate (Figures 2.5 C-D). Similarly, all cases displayed AT8+ neuropil threads within the Str. Rad., however, AT8+ cell bodies within the CA3 pyramidal layer was less common (Figure 2.6A). No observable AT8+ staining was found in the CA3 pyramidal layer of 12.8% of cases (5 of 39), but all of them showed AT8+ staining in the Str. Rad., the target region of the CA3 Shaffer collateral projections (Table 2.4). Axonal AT8 staining correlated strongly with the number of AT8+ cell bodies (Spearman r = 0.648, $p \leq 0.0001$, Figure 2.6B). Importantly, in the absence of observable cell body pathology, the terminal regions of these pathways contained a range of tau pathology from (Figure 2.6C-D), and cases with cell body staining were never without fiber staining. Together, these findings support the hypothesis that AT8 tau pathology occurs in axons before the somatodendritic compartment within these intrahippocampal pathways.

Axonal PAD Exposed Tau Pathology Occurs Without Cell Body Pathology in the Mossy Fiber and Schaffer Collateral Pathways

Next, we analyzed the amount of TNT2+ immunoreactivity in the mossy fiber pathway (Figure 2.7) and the Schaffer collateral pathway (Figure 2.8) as a measure of PAD-exposed tau, an early pathological event in tauopathies (Combs *et al.* 2016). The majority of cases displayed TNT2+ staining in Str. Luc. (Figure 2.7A), but of the cases that contain TNT+ axonal pathology 17.1% of cases (7 of 41) displayed no observable TNT2+ DG cells (Table 2.5). Axonal TNT2 staining in the mossy fiber pathway correlated with the number of TNT2+ DG cell bodies (Spearman r = 0.702, $p \leq 0.0001$, Figure 2.7B). Several cases contained axonal staining without observable reactive cell bodies (11.4%), although not every case contained TNT2+ staining in the Str. Luc. All but one case displayed TNT2 staining in the Str. Rad. (Figure 2.8A). Specifically, 12.8% of cases (5 of 39) displayed TNT2+ staining in the Str. Rad., but no

observable TNT2+ staining in the CA3 pyramidal layer (Table 2.6). Axonal TNT2 staining in the Schaffer collaterals correlated strongly with the number of TNT2+ CA3 cell bodies (Spearman r = 0.719, $p \leq 0.0001$, Figure 2.8B). Importantly, axonal pathology was found even in the absence of observable cell body pathological staining in both pathways and cases with cell body staining were never without fiber staining. Again, in the absence of observable cell body pathology fiber pathology in the terminal regions ranged from relatively low to high (Figure 2.8C-D), and cases with cell body staining were never without fiber staining. Together, these results further support the hypothesis that PAD exposed tau pathology occurs in axons before the somatodendritic compartment of affected neurons.

Early AT8 and TNT2 Pathology in the Stratum Lucidum and Stratum Radiatum is Axonal

To confirm that the AT8+ and TNT2+ staining observed in the Str. Luc. and Str. Rad. occurs in axons, we used triple-label immunofluorescence staining for AT8, TNT2, and the SMI-312, an axonal-specific marker (Figure 2.9). In the Schaffer collaterals, AT8 (MCC = 0.85) and TNT2 (MCC = 0.97) staining display a high degree of colocalization with SMI-312. These values correspond to 85% of AT8+ staining and 97% of TNT2+ staining in the axon enriched layer Str. Rad. of CA1. Similarly, in the mossy fibers, AT8 (MCC = 0.84) and TNT2 (MCC = 0.95) staining display a high degree of colocalization with SMI-312. These values corresponding to at least 84% of AT8+ and 95% of TNT2+ staining in the axon enriched layers of the hippocampus occurring in the axonal compartment of those neurons.

Early Axonal AT8 and TNT2 Tau Pathology is Independent of Amyloid-β Pathology

Finally, we stained for Aβ pathology in the CA3-Shaffer collateral and DG-mossy fiber pathway regions using the MOAB2 antibody (Youmans *et al.* 2012) and counted plaques using total enumeration (Figure 2.11A). The majority of cases did not contain Aβ plaques, and none contained intraneuronal staining with MOAB2 within the regions analyzed. Specifically, 84.2%

contained zero plaques in the Str. Luc. and 59% contained zero plaques in the DG, while 55.8% had zero plaques in the Str. Rad. and 78.9% contained zero plaques in the CA3 pyramidal cell layer (Table 2.7). Interestingly, in the Schaffer collateral pathway, neither AT8 phosphorylation nor PAD exposed tau correlated with the presence of Aβ plaques (Spearman r = -0.182, p = 0.242 for AT8, Figure 8C, and r = 0.026, p = 0.867 for TNT2, Figure 2.11 B-C). The extent of both AT8+ and TNT2+ tau pathology in some cases was remarkably robust in regions devoid of observable Aβ plaques (Figure 2.11 D-F). Taken together, these results indicate that AT8 phosphorylation and PAD exposure occur independently of the presence of Aβ pathology in the Schaffer collateral and mossy fiber pathways.

Discussion

The hypothesis that pathological tau progression starts at the axons and axon terminals and moves back to the somatodendritic compartment has been proposed for server decades (Bancher *et al.* 1989, Braak *et al.* 1991), but to our knowledge, no evidence from relatively discrete neuronal pathways was available previously. The present study characterizes the localization of mossy fiber and Schaffer collateral pathway tau pathology in a cohort of ND and MCI human cases. Our focus on relatively discrete neuronal pathways within in the hippocampus provides an opportunity to dissect the spatial changes that occur in the axonal and cell body compartments of neurons with some degree of specificity. Moreover, the use of Braak I-III cases with a range of pathology load was instrumental in uncovering the first detectable deposition of tau inclusions in cell bodies the hippocampal pathways analyzed, which is reflected in the lack of pathology and sparseness of pathology in several cases. Two early pathological markers in tauopathies, AT8 phosphorylation (Biernat *et al.* 1992, Braak *et al.* 1994, Goedert *et al.* 1995) and PAD exposure (TNT2) (Combs *et al.* 2016, Combs *et al.* 2017), appeared in the axonal compartment of these pathways, even in cases where no cell body pathology was observed. Additionally, there was a strong correlation between axonal

pathological staining and the number of stained cell bodies. It is noteworthy that other hippocampal formation pathways such as the CA1 projections and EC-perforant pathway were not usable for the purposes of this study because both cell body and axonal pathology already existed in all cases. Taken together, these results support the hypothesis that tau pathology is first observed in the axonal compartment and subsequently progresses into the somatodendritic compartment.

The strong colocalization of the AT8 and TNT2 pathological tau markers with the axon-specific antibody SMI-312 further supports our conclusion that we evaluated predominantly axonal pathology. Notably, these correlated observations occurred before any diagnosis of dementia. While this likely indicates that these pathological changes occur early in disease progression, in post-mortem human tissue studies we cannot rule out the possibility that the tau deposition here is independent of a progressive condition that would have definitively converted to AD. Indeed, cohorts of MCI patients from previous studies clearly indicate that some patients do not ultimately convert to AD (Mufson *et al.* 2016). In addition, no significant differences were observed in tau staining between several clinical exam scores (MMSE, CERAD, diagnosis), suggesting cognitive deficits are a downstream consequence of these initial pathological changes.

In AD, synaptic loss and axon dysfunction are well-established early events in the progression of disease pathogenesis in AD and other tauopathies (DeKosky *et al.* 1990, Bell *et al.* 2006). Previously, the N-terminal PAD domain of tau (i.e. amino acids 2-18) was identified as a biologically active motif that when aberrantly exposed inhibits anterograde fast axonal transport in squid axoplasm(LaPointe *et al.* 2009, Kanaan *et al.* 2011). Additionally, the underlying molecular pathway of the axonal dysfunction was PAD-mediated activation of a PP1-GSK3β signaling cascade (Morfini *et al.* 2002, Morfini *et al.* 2004, Kanaan *et al.* 2012, Kanaan *et al.* 2013). Our observation that AT8 phosphorylation, which structurally exposes PAD (Jeganathan *et al.* 2008), and PAD exposed tau appear first in the axonal compartment of

affected neurons before the observation of clinical symptoms further supports the hypothesis that the Tau-PP1-GSK3β signaling cascade may represent a relevant mechanism of neurodegeneration early in tauopathies (Morfini *et al.* 2009, Kanaan *et al.* 2013). Additionally, PAD exposure is a common occurrence across a range of tauopathies beyond AD, such as frontal temporal dementia (Combs *et al.* 2017). Several pathological modifications of tau can contribute to PAD exposure, including phosphorylation (Jeganathan *et al.* 2008, Tiernan *et al.* 2016), oligomerization, and aggregation (Cox *et al.* 2016, Kanaan *et al.* 2016) Therefore, our observations that pathological modifications of tau previously shown to cause axonal dysfunction suggests that this may be one of the early tau-based mechanisms of degeneration in AD.

Our data now provide human tissue-based evidence supporting the hypothesis that tau deposition can occur in axons prior to the somata, but the nature of human tissue studies does not clarify whether the axonal tau pathologies are mobile and traverse retrogradely to the somata or are generated locally in each compartment. Originally, tau was thought to be an axonal protein (Binder *et al.* 1985), however, after the production of tau-specific antibodies, tau was found to be present throughout the neuron with an enrichment in axons (Binder *et al.* 1986, Mandell *et al.* 1995). Under disease conditions, redistribution of tau from enrichment in the axon to the somatodendritic compartment is thought to be an important early event in pathogenesis. Additionally, phosphorylation of tau at residues known to alter tau's conformation in disease are localized to the somatodendritic compartment, including AT8 (Braak *et al.* 1995, Kimura *et al.* 1996, Jeganathan *et al.* 2008). Recently, investigation into the axon initial segment identified TRIM46 as a protein involved in maintaining a parallel array of microtubules in the axon hillock and preventing tau from diffusing into the somatodendritic compartment (van Beuningen *et al.* 2015). Additionally, TRIM46 is an essential component of the developing axon and maintaining neuronal polarity (Huang *et al.* 2018). Our lab previously showed that redistribution of tau beyond the axon initial segment into the somatodendritic compartment depends on the MTBRs

of tau (Kneynsberg 2018, unpublished data). Interestingly, another study found that treating cultured neurons with nocodazole to disrupt microtubules resulted in increased diffusion of axonal tau into the somatodendritic compartment, suggesting a role for tau binding to microtubules as an important event in maintaining an enrichment of axonal tau (Li *et al.* 2011). Future studies investigating axon initial segment proteins and their potential dysfunction in tauopathies, and subsequent redistribution of tau and loss of axon polarity, may lead to a novel mechanism of AD pathogenesis.

Notably, we observed AT8- and TNT2+ tau pathology independent of MOAB2+ Aβ pathology. The amyloid cascade hypothesis suggests that amyloid pathology occurs first in AD, and that tau pathology is a downstream consequence of Aβ pathology (Hardy *et al.* 1992). We observed evidence to the contrary; AT8 and TNT2 tau pathology occurred in the hippocampus in the absence of Aβ pathology. Our data clearly indicate that overt Aβ pathology is not present despite the presence of pathological tau accumulation in the axon that can be quite robust in some cases, thereby demonstrating a disconnection between Aβ plaque deposits and the emergence of tau inclusions. This is consistent with the known spatiotemporal distribution of amyloid pathology (i.e. occurs first in neocortical regions) and tau pathology (i.e. occurs much later in neocortical areas) (Braak *et al.* 1991, Braak *et al.* 1994, Thal *et al.* 2002). The containment of the axonal compartment and cell bodies within discrete hippocampal strata provides a clear demonstration that amyloid pathology in the terminal regions of tau-affected neurons does not occur. Our findings align with previous findings by Braak and colleagues (1994) that very little to no Aβ pathology was present despite the presence of AT8 tau pathology within the transentorhinal/entorhinal cortical regions of Braak stage 0-III cases (Braak *et al.* 1994). Amyloid plaques are thought to precipitate via a sequential process of going from monomeric proteins, to oligomeric species and then fibrillar forms (Murphy *et al.* 2010). The MOAB-2 antibody is a pan-Aβ specific antibody that reacts with monomeric, oligomeric and

fibrillar forms of Aβ (Youmans *et al.* 2012), suggesting that the tau pathologies observed in these pathways were not associated with pre-fibrillar or fibrillar forms of Aβ pathology. Additional studies assessing the time course of the spatiotemporal distribution of various Aβ and tau species may further clarify the relationship between these two hallmark AD pathologies. However, the data presented here directly challenge the proposition that aggregated Aβ triggers tau pathology in the Schaffer collateral and mossy fiber pathways within the hippocampus

Overall, this study provides strong evidence that two early tau pathological markers, AT8 phosphorylation and PAD exposure, can appear first in axons followed by deposition of cell body pathology. To our knowledge, this is the first study to systematically investigate two well-defined pathways within the hippocampus to differentiate between axon enriched strata and the corresponding cell bodies. Furthermore, visualizing these pathologically relevant modifications of tau in ND and MCI human tissue cases provides valuable insight into early tau pathology in the human condition before the onset of AD. Importantly, both AT8 and PAD exposed forms of tau are linked to mechanisms of toxicity in axonal functions such as axonal transport. Coupling these results with the lack of observable Aβ pathology suggests amyloid is not causing the early tau changes in these hippocampal pathways. This raises questions of whether the amyloid cascade is a viable hypothesis to explain the complex nature of AD etiology, but perhaps later in the disease process, tau and Aβ pathologies work together to enhance ongoing cell dysfunction and degeneration once the pathologies overlap or interact. Nonetheless, our findings suggest that early axonal tau pathologies may trigger degenerative events in the hippocampal circuitry prior to overt cognitive decline, and more longitudinally focused future studies specifically on connecting the earliest forms of tau pathology in axons and clinical decline are needed.

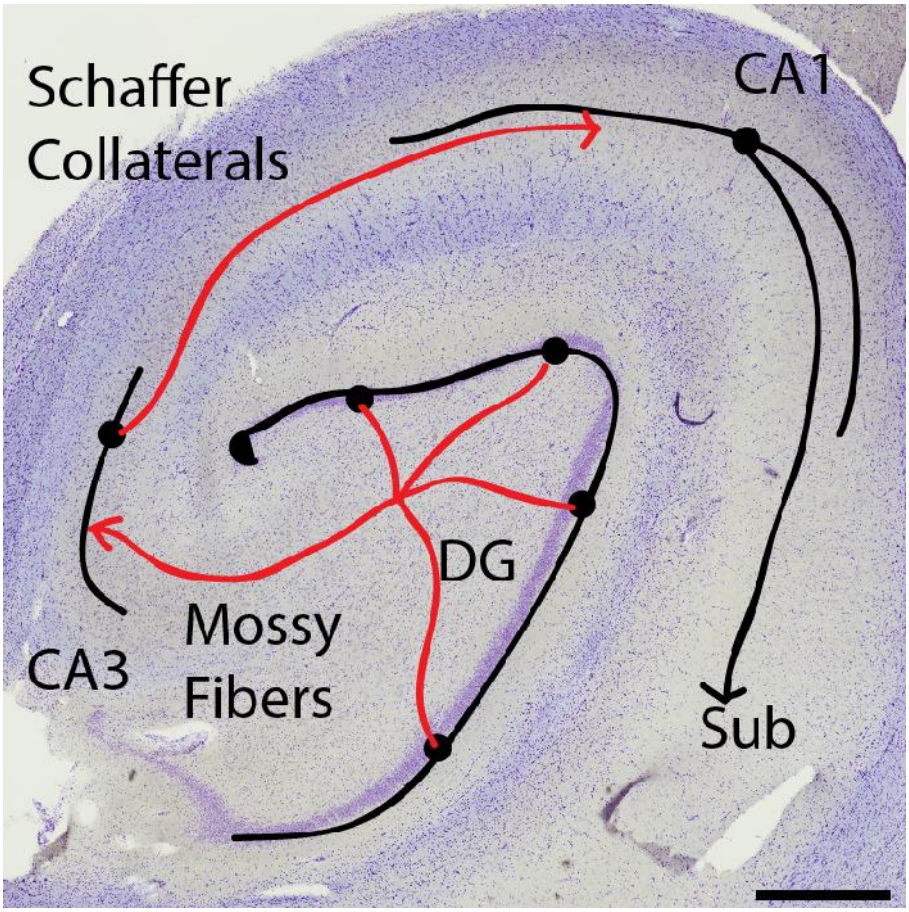

Figure 2.1 Schematic of hippocampal connections. Projections arising in the EC pass through the angular bundle to terminate on several regions, including the DG via the perforant path (not shown). DG granule cell neurons form the mossy fiber pathway and project to the CA3 pyramidal cells, where they terminate in the Str. Luc. CA3 pyramidal cells forms the Schaffer collateral pathway and project to CA1 pyramidal cells, where they terminate in the Str. Rad. CA1 pyramidal cells terminate in the subiculum and the EC. Finally, to complete the circuit subiculum neurons project to the pre- and para-subiculum as well as the EC to complete the loop (not shown). The two pathways investigated in this study are shown in red. Scale bar = 1 mm.

Table 2.1 Demographic, Clinical, and Neuropathological Characteristics by Diagnosis

	Clinical diagnosis			Comparison by diagnosis group
	ND (N=31)	MCI (N=13)	Total (N=44)	(*P* value)
Age at death (years)				
Mean ± SD	83.1 ± 6.1	86.2 ± 5.4	84.0 ± 6.0	0.13*
(Range)	(69-97)	(74-95)	(69-97)	
No. (%) Males	19 (61.3%)	8 (61.5%)	27 (61.4%)	>0.99‡
Postmortem Interval (hours)				
Mean ± SD	2.7 ± 0.6	2.7 ± 0.5	2.7 ± 0.6	0.84*
(Range)	(1.5-4.8)	(1.8-3.5)	(1.5-4.8)	
MMSE				
Mean ± SD	28.5 ± 1.3	27.4 ± 2.4	28.2 ± 1.7	0.34*
(Range)	(26-30)	(23-30)	(23-30)	
No Score (N)	8	4	12	
Braak Stage				
I	5	3	8	0.85§
II	7	3	10	
III	19	7	26	
CERAD Diagnosis (likelihood of AD)				
Not AD	15	6	21	
Possible AD	15	6	21	>0.99‡
No Score (N)	1	1	2	

ND, non-demented; MCI, mild cognitive impairment; MMSE, Mini-Mental State Examination; CERAD, Consortium to Establish a Registry for Alzheimer's disease; AD, Alzheimer's disease.

*p ≤ 0.05 Mann-Whitney test; ‡ p ≤ 0.05 Fisher's exact test; §p ≤ 0.05 Chi-square test

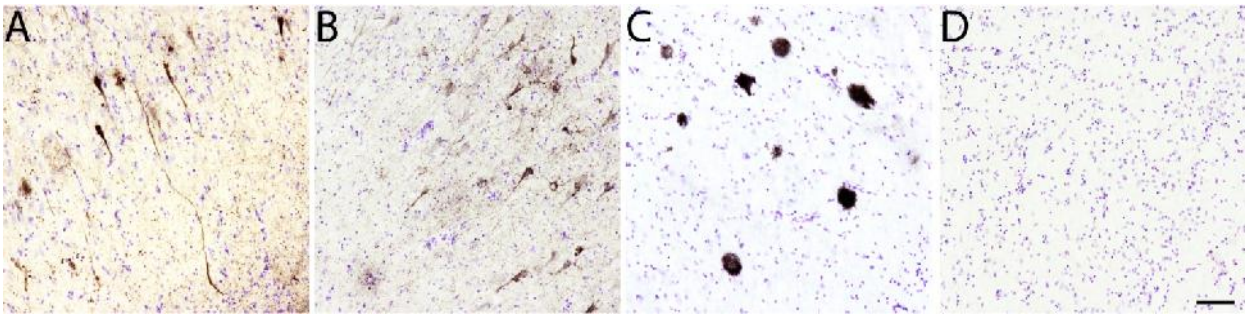

Figure 2.2 Primary delete control experiment of antibodies used in IHC experiments. The same case was used for each staining and images were obtained in the same cortical gyrus. (A) AT8-labeled, (B) TNT2-labeled, and (C) MOAB2-labeled sections show positive immunoreactivity with each antibody. (D) Section stained with all components used in the IHC technique except the primary antibody resulted in no development of IHC signal, indicating the signals obtained in sections containing primary antibody is not due to non-specific reactivity or background signal from the tissue. Scale bar in (D) is 100 µm and applies to all panels.

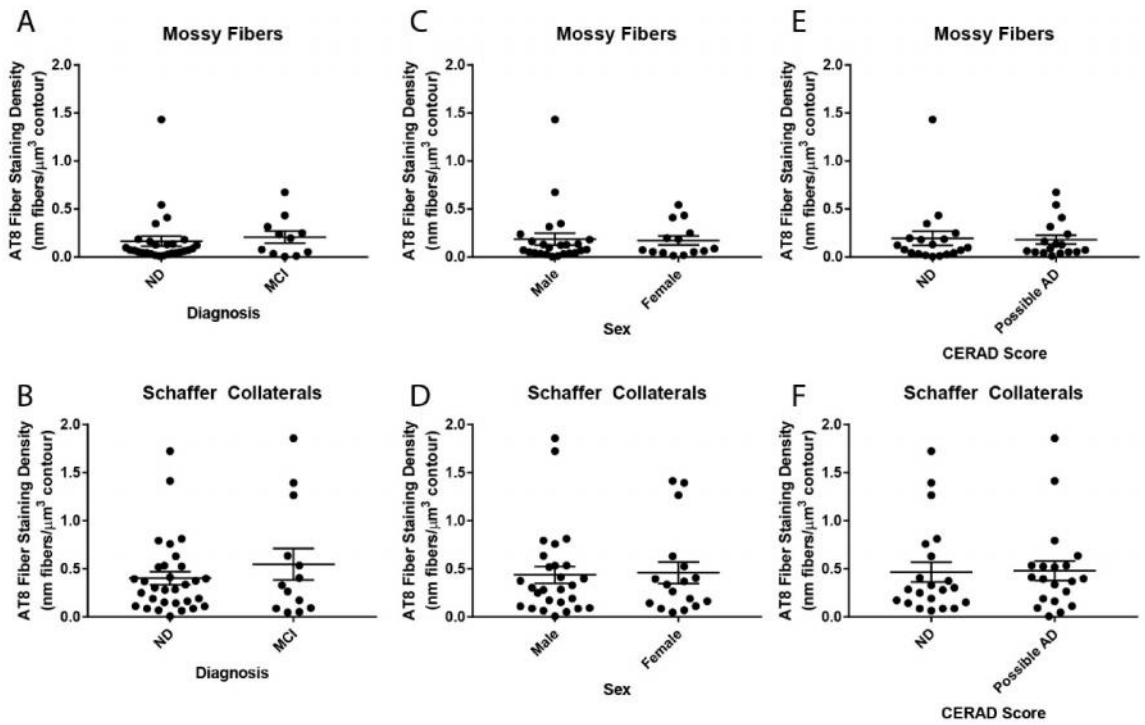

Figure 2.3 AT8 phosphorylation does not change with clinical diagnosis, gender, cognition, or CERAD score in the axonal compartment of the mossy fiber and Schaffer collateral pathways. (A-B). No significant differences in the axonal AT8 staining were observed between diagnosis groups in neither the Str. Luc. (A; mossy fiber pathway; Mann-Whitney test, $p = 0.4311$) nor the Str. Rad. (B; DG fiber pathway; $p = 0.7977$). (C-D). No significant differences were observed between gender in neither the Str. Luc. (C; Mann-Whitney test, $p = 0.5982$) or nor the Str. Rad. (D; $p = 0.9710$). (E-F). No significant differences were observed between CERAD scores in neither the Str. Luc. (E; Mann-Whitney test, $p = 0.6111$) or nor the Str. Rad. (F; $p = 0.5568$).

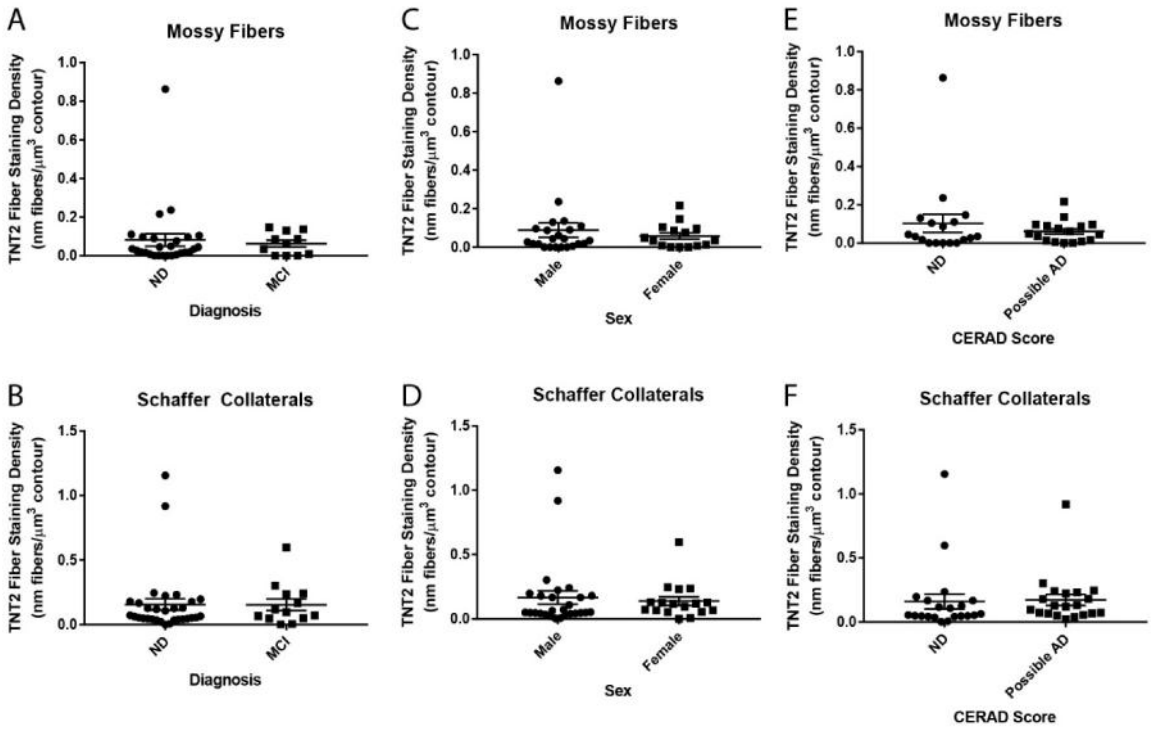

Figure 2.4 PAD exposure does not change with clinical diagnosis, gender, cognition, or CERAD score in the axonal compartment of the mossy fiber and Schaffer collateral pathways. (A-B). No significant differences in the axonal TNT2 staining were observed between diagnosis groups in neither the Str. Luc. (A; mossy fiber pathway; Mann-Whitney test, p = 0.8296) nor the Str. Rad. (B; DG fiber pathway; p = 0.5239). (C-D). No significant differences were observed between gender in neither the Str. Luc. (C; Mann-Whitney test, p = 0.9352) or nor the Str. Rad. (D; p = 0.3255). (E-F). No significant differences were observed between CERAD scores in neither the Str. Luc. (E; Mann-Whitney test, p = 0.9088) or nor the Str. Rad. (F; p = 0.0871).

Table 2.2 Spearman correlations between demographic, cognitive, or neuropathological measures and tau markers in both the axonal and somatodendritic compartments

Region	Tau Marker	PMI	Age	MMSE	Braak Stage	Total Plaques	Total Tangles	Infarcts
Schaeffer Collaterals	**AT8**	r=0.013 p=0.933	r=0.521***** p=0.0003	r=-0.004 p=0.981	r=0.524***** p=0.0003	r=0.109 p=0.481	r=0.533***** p=0.0002	r=0.185 p=0.235
	TNT2	r=0.132 p=0.392	r=0.305***** p=0.044	r=0.007 p=0.968	r=0.497***** p=0.0006	r=0.331***** p=0.028	r=0.522***** p=0.0003	r=0.093 p=0.555
Mossy Fibers	**AT8**	r=0.011 p=.946	r=0.446***** p=0.004	r=-0.294 p=0.129	r=0.337***** p=0.036	r=0.205 p=0.211	r=0.418***** p=0.008	r=0.166 p=0.319
	TNT2	r=0.053 p=0.747	r=0.477***** p=0.002	r=0.017 p=0.930	r=0.484***** p=0.002	r=0.156 p=0.344	r=0.580 p=0.0001	r=0.199 p=0.230
CA3 Pyramidal Cells	**AT8**	r=0.024 p=0.884	r=0.344***** p=0.032	r=-0.014 p=0.943	r=0.462***** p=0.003	r=0.241 p=0.139	r=0.441***** p=0.005	r=0.078 p=0.640
	TNT2	r=0.070 p=0.672	r=0.227 p=0.165	r=-0.309 p=0.110	r=0.213 p=0.193	r=0.062 p=0.979	r=0.322***** p=0.046	r=0.142 p=0.393
Dentate Gyrus Granule Cells	**AT8**	r=0.164 p=0.305	r=0.299 p=0.058	r=-0.206 p=0.0274	r=0.472***** p=0.002	r=0.069 p=0.670	r=0.504***** p=0.0008	r=0.160 p=0.323
	TNT2	r=0.204 p=0.207	r=0.255 p=0.113	r=-0.041 p=0.833	r=0.280 p=0.080	r=0.004 p=0.702	r=0.239 p=0.137	r=0.132 p=0.422

PMI – post-mortem interval; MMSE – mini mental state exam; CA – cornu ammonis; Braak stages ranged from 1-3. * indicates a significant correlation ($p \leq 0.05$).

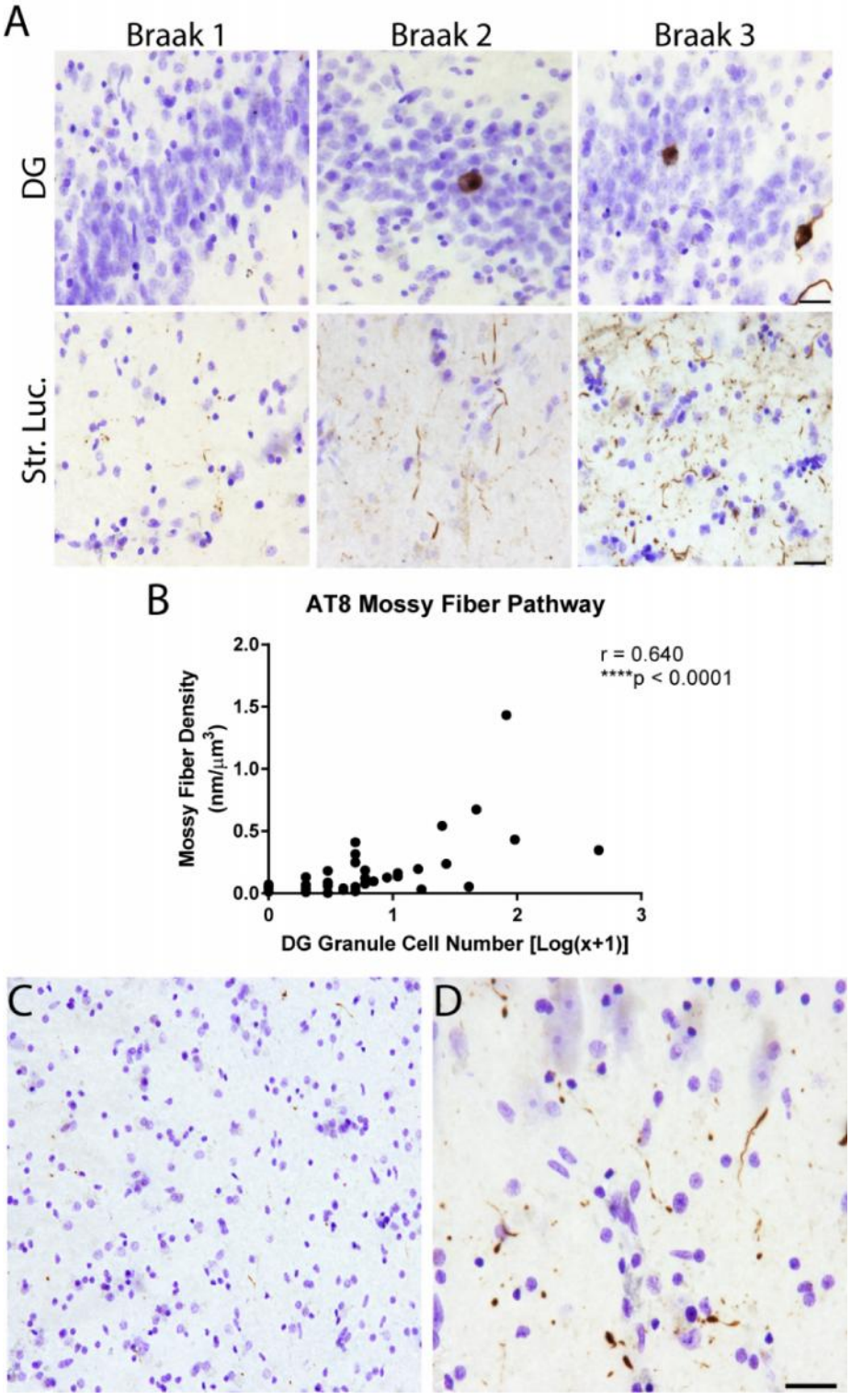

Figure 2.5 Axonal AT8 phosphorylation in the mossy fiber pathway occurs in the absence of DG cell body pathology. (A) AT8 staining in the dentate gyrus granule cell layer (DG) and their corresponding mossy fiber terminal fields in the stratum lucidum of CA3 (Str. Luc.) across

Figure 2.5 (cont'd)

Braak stages. All sections were counter stained with cresyl violet. The increase in cell body staining and neuropil thread staining positively correlates with Braak staging (see Table 2). Scale bars are 25 µm. Quantification of cell body staining using total enumeration indicates the low number of positive cells in these cases. 71.4% of cases (30 of 42) displayed five or fewer cells stained in the DG, with 16.7% (7 of 42) showing no observable cell body pathology (see Table 3). By comparison, 100% of cases displayed axonal AT8 staining in the Str. Luc. (B). Spearman correlation analysis of AT8+ axonal density and cell body number in the mossy fiber pathway. Data points are plotted as each individual case. A strong, positive correlation (r = 0.640, $p \leq 0.0001$) indicates an increase in axonal pathology as cell body pathology increases. (C-D). Representative images from cases with sparse (C) and dense (D) AT8+ mossy fiber axons in cases lacking cell body pathology demonstrate the extent of axonal pathology that can occur prior to observable somatodendritic pathology. Scale bars are 50 µm.

Table 2.3 Distribution of cases with different levels of AT8 pathology in the dentate gyrus granule cells.

DG Granule Cells	Number of Cases	Percent of Cases	Average Fiber Density (nm / μm^3 contour)
0	7	16.7	0.043
1	5	11.9	0.056
2	5	11.9	0.084
3	4	9.5	0.034
4	5	11.9	0.209
5	4	9.5	0.129
≥6*	12	28.6	0.344

DG – dentate granule; *full range was from 6-453 cells.

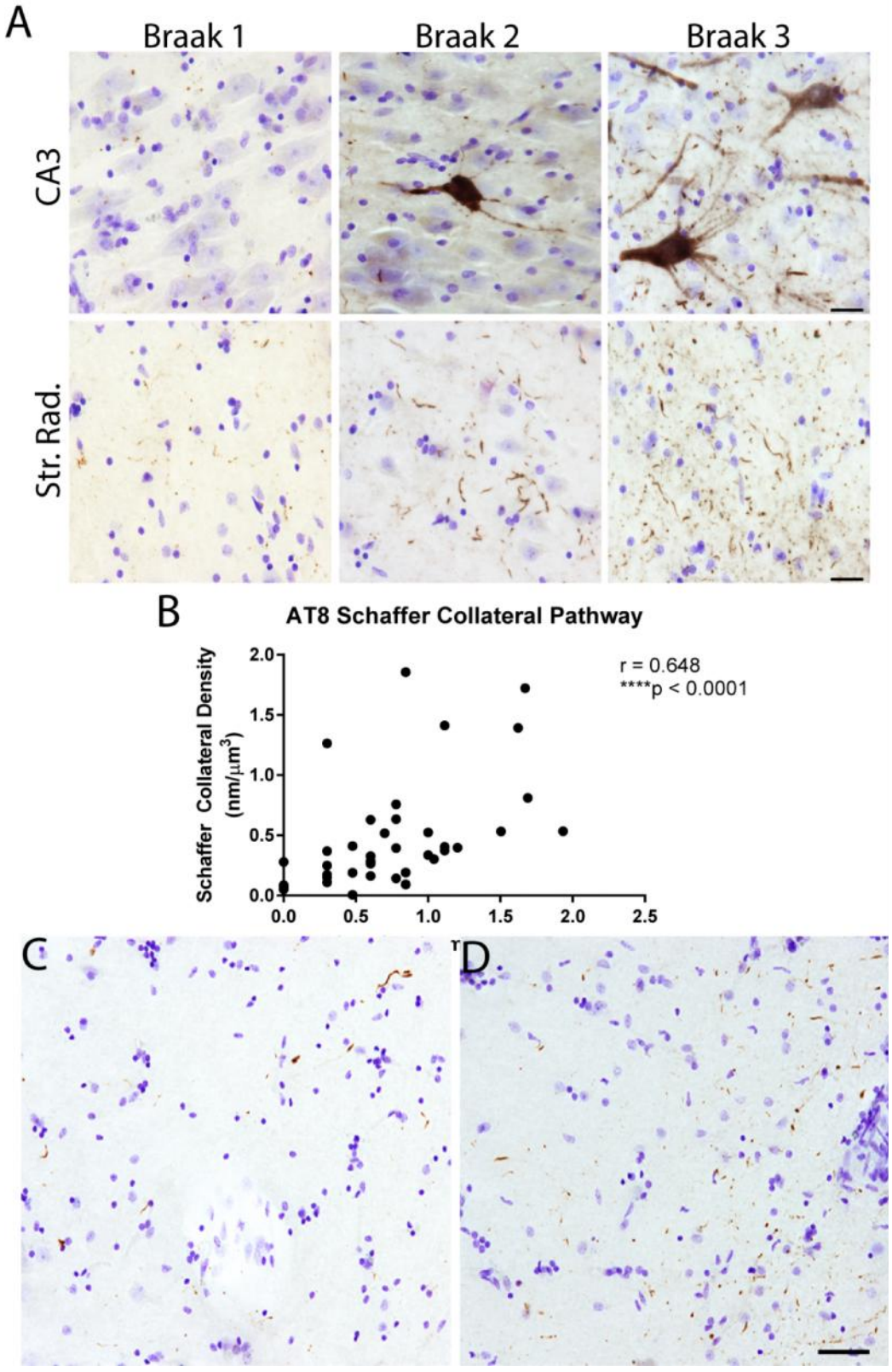

Figure 2.6 Axonal AT8 phosphorylation in the Schaffer collateral pathway occurs in the absence of CA3 cell body pathology. (A). AT8 staining in the pyramidal cell layer of CA3 and

Figure 2.6 (cont'd)

their corresponding Schaffer collateral terminal fields in the stratum radiatum of CA1 (Str. Rad.) across Braak stages. All sections were counter stained with cresyl violet. The increase in cell body staining and neuropil thread staining positively correlates with Braak staging (see Table 2). Scale bars are 25 µm. Quantification of cell body staining using total enumeration indicates the low number of cells stained in these cases. 61.5% of cases (24 of 39) displayed five or fewer cells stained in the CA3 pyramidal cell layer, with 12.8% (5 of 39) showing no observable cell body pathology (see Table 4). By comparison, 100% of cases displayed axonal AT8 staining in the Str. Rad. (B). Spearman correlation analysis of AT8+ axonal density and cell body number in the Schaffer collateral pathway. Data points are plotted as mean ±SD. A strong, positive correlation ($r = 0.648$, $p \leq 0.0001$) indicates an increase in axonal pathology as cell body pathology increases. (C-D). Representative images from cases with sparse (C) and dense (D) AT8+ Schaffer collateral axons in cases lacking cell body pathology demonstrate the extent of axonal pathology that can occur prior to observable somatodendritic pathology. Scale bars are 50 µm.

Table 2.4 Distribution of cases with different levels of AT8 pathology in CA3 pyramidal cells

CA3 Pyramidal Cells	Number of Cases	Percent of Cases	Average Fiber Density (nm / μm^3 contour)
0	5	12.8	0.114
1	6	15.4	0.386
2	3	7.7	0.202
3	5	12.8	0.333
4	1	2.6	0.518
5	4	10.3	0.482
≥6*	15	38.5	0.726

CA – cornu ammonis; *full range was from 6-85

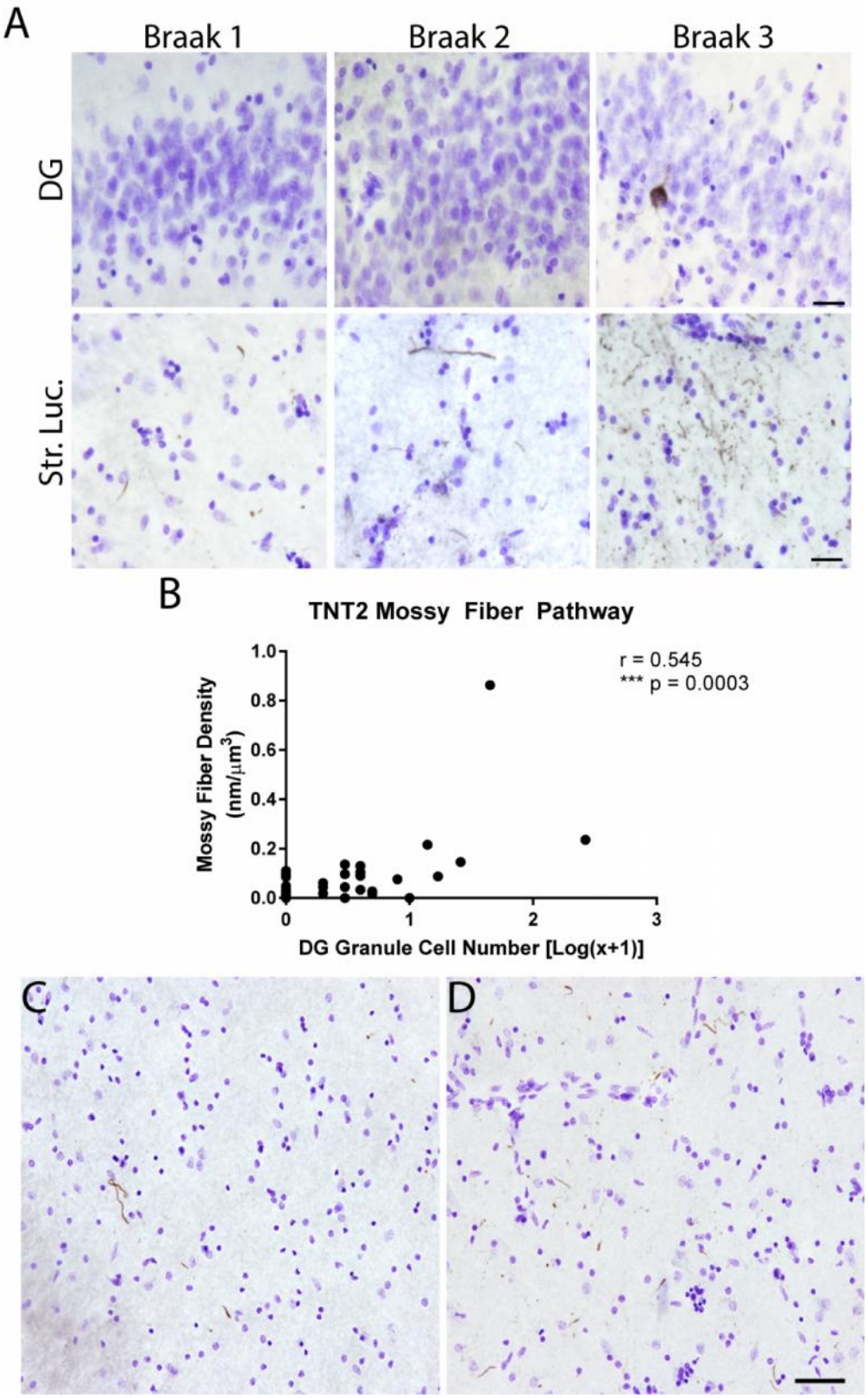

Figure 2.7 Axonal PAD exposure in the mossy fiber pathway occurs in the absence of CA3 cell body pathology. (A) TNT2 staining in the dentate gyrus granule cell layer (DG) and

Figure 2.7 (cont'd)

their corresponding mossy fiber terminal fields in the stratum lucidum of CA3 (Str. Luc.) across Braak stages. All sections were counter stained with cresyl violet. The increase in cell body staining and neuropil thread staining positively correlates with Braak staging (see Table 2.5). Scale bars are 25 μm. Quantification of cell body staining using total enumeration indicates the low number of positive cells in these cases. 82.1% of cases (32 of 39) displayed five or fewer cells stained in the DG, with 43.6% (17 of 39) showing no observable cell body pathology (see Table 3). A subset of cases without cell body staining still contained axonal TNT2 staining (see Table 2.5). (B). Spearman correlation analysis of TNT2+ axonal density and cell body number in the mossy fiber pathway. Data points are plotted as mean ±SD. A strong, positive correlation (r = 0.545, p = 0.0003) indicates an increase in axonal pathology as cell body pathology increases. (C-D). Representative images from cases with sparse (C) and dense (D) TNT2+ mossy fiber axons in cases lacking cell body pathology demonstrate the extent of axonal pathology that can occur prior to observable somatodendritic pathology. Scale bars are 50 μm.

Table 2.5 Distribution of cases with different levels of TNT2 pathology in DG granule cells.

DG Granule Cells	Number of Cases	Percent of Cases	Average Fiber Density (nm / μm^3 contour)
0	17	43.6	0.027
1	4	10.3	0.035
2	4	10.3	0.070
3	5	12.8	0.079
4	2	5.1	0.022
5	0	0	
≥6*	7	17.9	0.232

DG – dentate gyrus; *full range was from 6-265 cells

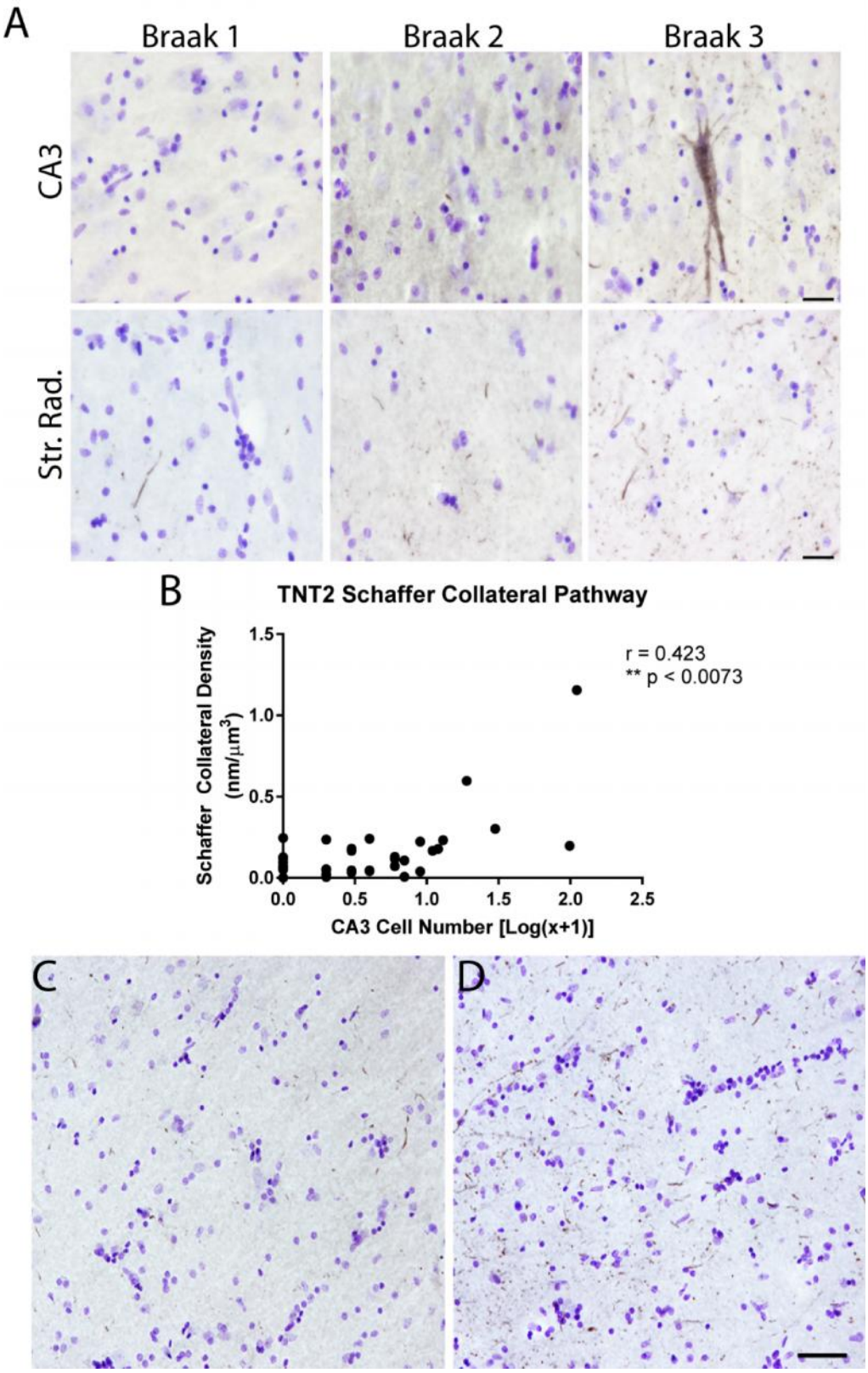

Figure 2.8 Axonal PAD exposure in the Schaffer collateral pathway occurs in the absence of CA3 cell body pathology. (A) TNT2 staining in the pyramidal cell layer of CA3 pyramidal

Figure 2.8 (cont'd)

cell layer and their corresponding mossy fiber terminal fields in the stratum radiatum (Str. Rad.) across Braak stages. All sections were counter stained with cresyl violet. The increase in cell body staining and neuropil thread staining positively correlates with Braak staging (see Table 2.6). Scale bars are 25 µm. Quantification of cell body staining using total enumeration indicates the low number of positive cells in these cases. 71.8% of cases (28 of 39) displayed five or fewer cells stained in the CA3 pyramidal cell layer, with 25.6% (10 of 39) showing no observable cell body pathology (see Table 2.6). A subset of cases without cell body staining still contained axonal TNT2 staining (see Table 2.6). (B). Spearman correlation analysis of TNT2+ axonal density and cell body number in the mossy fiber pathway. Data points are plotted as mean ±SD. A moderate, positive correlation ($r = 0.423$, $p = 0.0073$) indicates an increase in axonal pathology as cell body pathology increases. (C-D). Representative images from cases with sparse (C) and dense (D) TNT2+ Schaffer collateral axons in cases lacking cell body pathology demonstrate the extent of axonal pathology that can occur prior to observable somatodendritic pathology. Scale bars are 50 µm.

Table 2.6 Distribution of cases with different levels of TNT2 pathology in CA3 pyramidal cells

CA3 Pyramidal Cells	Number of Cases	Percent of Cases	Average Fiber Density (nm / μm^3 contour)
0	10	25.6	0.083
1	6	15.4	0.069
2	4	10.3	0.107
3	4	10.3	0.092
4	0	0	
5	4	10.3	0.111
≥6*	11	28.2	0.291

CA – cornu ammonis; *full upper range was from 6-110 cells

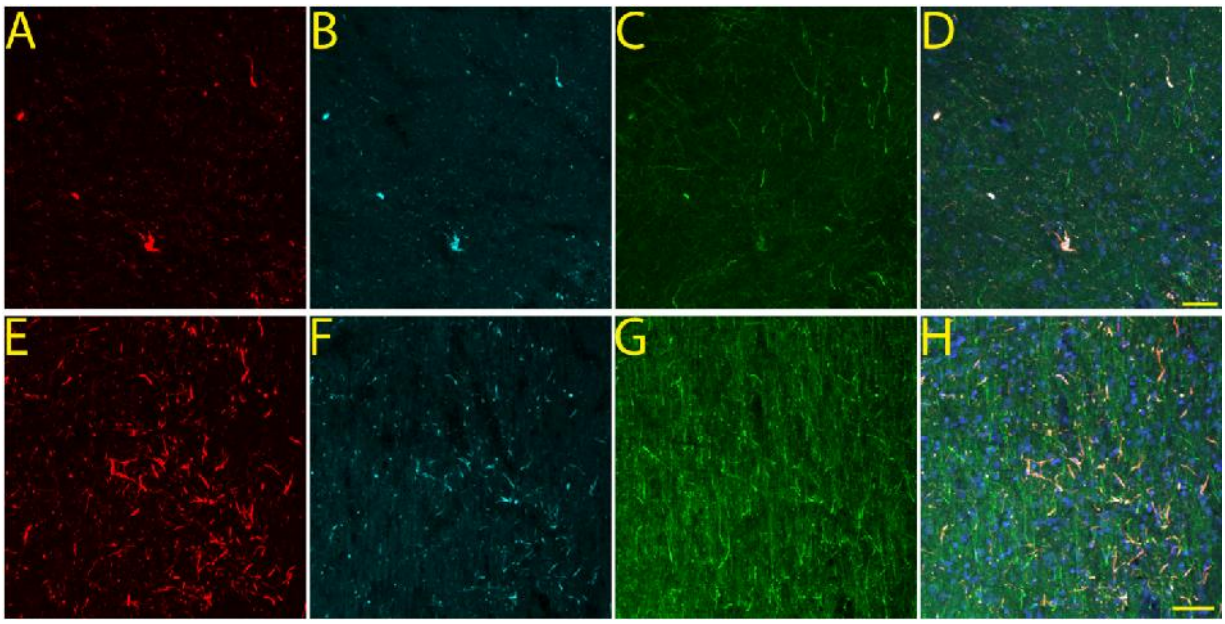

Figure 2.9 Tau pathology occurs in axons as indicated by colocalization with SMI-312. (A-D). Representative images of AT8 (A), TNT2 (B), and SMI-312 (C) staining (and merged image in D includes DAPI nuclear counter stain) in the Str. Rad. (DG-mossy fiber pathway) of a Braak stage III case. Note the high degree of colocalization with these pathological markers and SMI-312. The Mander's coefficient of colocalization between AT8 and SMI-312 (0.85) or TNT2 and SMI-312 (0.97) confirms the majority of observed tau immunoreactivity is within the axons. (E-H). Representative images of AT8 (E), TNT2 (F), and SMI-312 (G) staining (and merged image in H includes DAPI nuclear counter stain) in the Str. Luc. (CA3-Shaffer collateral pathway) of a Braak stage III case. Note the high degree of colocalization with these pathological markers and SMI-312. The Mander's coefficient of colocalization between AT8 and SMI-312 (0.82) or TNT2 and SMI-312 (0.94) confirms the majority of observed tau immunoreactivity is within the axons. Scale bar are 50 μm.

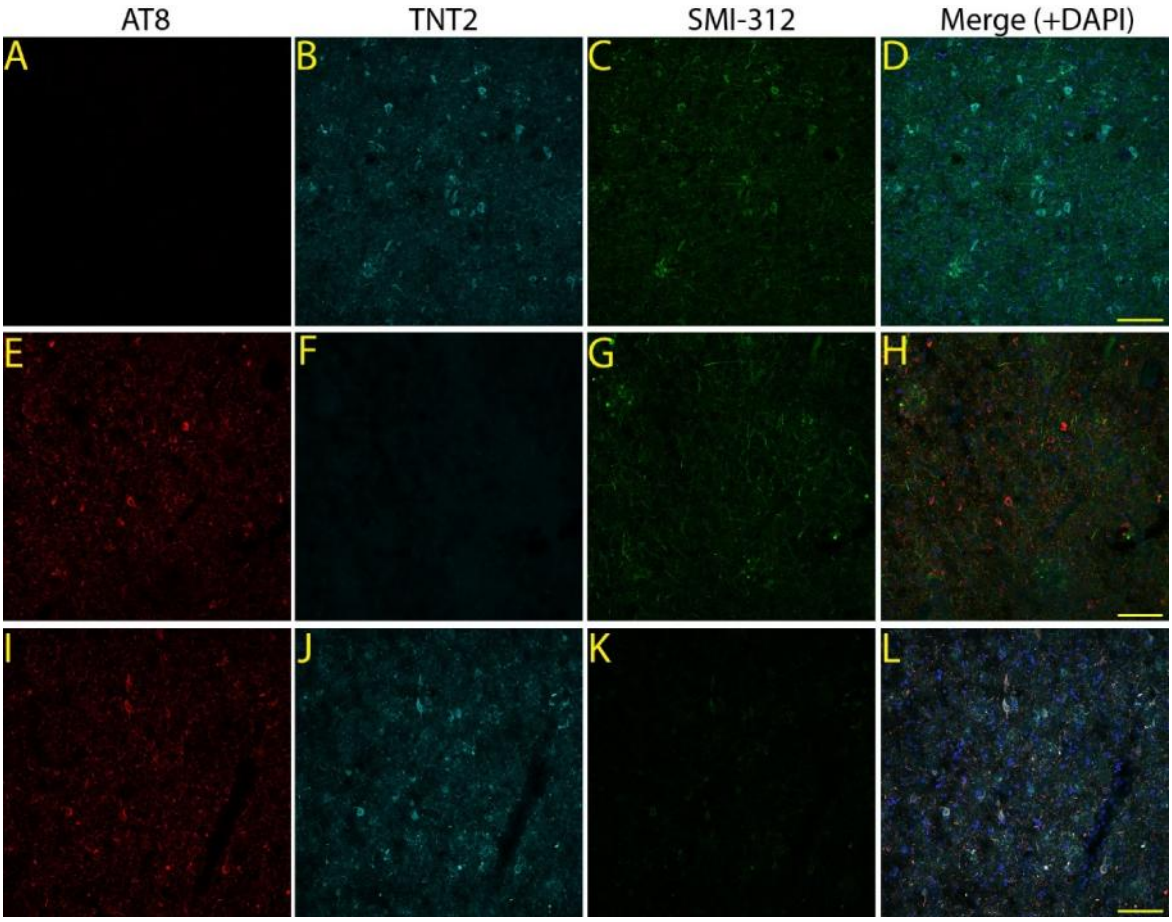

Figure 2.10 Primary delete control experiment of antibodies used in IF experiments. The same case was used for each staining and all images were obtained in the same cortical gyrus. (A-D) Representative images of a section lacking the AT8 primary antibody showing no immunoreactivity (A), whereas including TNT2 (B) and SMI-312 (C) resulting in development of immunoreactive signal as expected. The merged image is shown in (D). (E-H). Representative images of a section showing positive AT8 immunoreactivity when the AT8 antibody is included (E), no TNT2 immunoreactivity upon omission on the TNT2 antibody (F), and development of SMI-312 signal when the SMI-312 antibody is included (G), as expected. The merged image is shown in (H). (I-L). Representative images of a section showing positive immunoreactivity when the AT8 (I) and TNT2 (J) antibodies are included, and no SMI-312 immunoreactivity upon omission on the SMI-312 antibody (K), as expected. The merged image is shown in (L). AT8-labeled, TNT2-labeled, and SMI-312-labeled sections show positive immunoreactivity with each

Figure 2.10 (cont'd)

antibody. Omission of each antibody resulted in a lack of IF signal, indicating the signals obtained in sections containing primary antibody is not due to non-specific reactivity or signal from the tissue. Scale bars are 50 μm and apply to all panels.

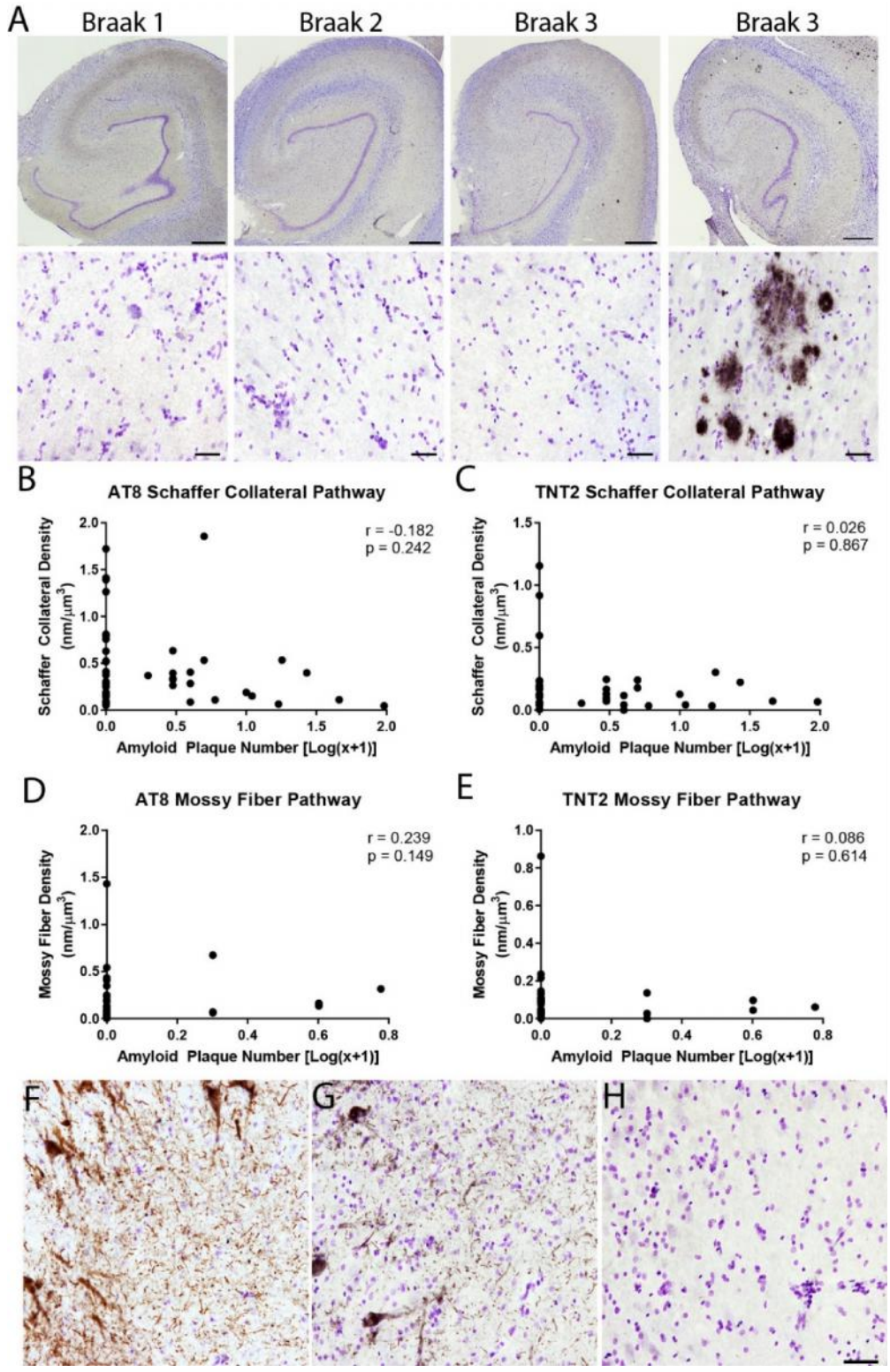

Figure 2.11 Tau pathology is observed in the absence of amyloid-β pathologies. (A). Representative hippocampi across Braak stages stained with MOAB2. Note the rarity of

Figure 2.11 (cont'd)

MOAB2+ plaques in the hippocampus and in the Schaffer collateral terminal region of the Str. Rad. (similar lack of Aβ pathology occurred in the mossy fiber terminal region of the Str. Luc). A representative image of the relatively rare cases containing a significant amyloid load in the hippocampus is shown to confirm the effective labeling of Aβ plaques with MOAB2 antibody. In the mossy fiber pathway, 84.2% of cases contained zero plaques in the Str. Luc. and 59% of cases contained zero plaques in the DG (see Table 2.7). In, the Schaffer collateral pathway, 55.8% of cases contained zero plaques in the Str. Rad. and 78.9% of cases contained zero plaques in the CA3 pyramidal cell layer (see Table 2.7). Scale bars are 1 mm in upper images and 50 μm in lower images. (B-C). No significant correlation was observed in the Schaffer collateral pathway between the presence of Aβ plaques and AT8+ staining (B, Spearman r = -0.182, $p = 0.242$) or TNT2+ staining (C, Spearman r = 0.026, $p = 0.867$). (D-E). No significant correlation was observed in the mossy fiber pathway between the presence of Aβ plaques and AT8+ staining (D, Spearman r = 0.239, $p = 0.149$) or TNT2+ staining (E, Spearman r = 0.086, $p = 0.614$). F-H. Representative images of AT8 (F), TNT2 (G), and MOAB2 (H) staining in the same location within the CA3 region from the same case illustrates the robust tau pathology possible in the absence of detectable Aβ pathology. It is noteworthy that no cases contained intraneuronal MOAB2 signal in the regions analyzed. Scale bar is 50 μm and applies to panels F, G, and H.

Table 2.7 Distribution of cases with different levels of Aβ pathology in the mossy fiber and Schaffer collateral pathway regions.

Aβ Plaques	% Cases (N) (Str. Rad.)	% Cases (N) (CA3 Layer)	% Cases (N) (Str. Luc.)	% Cases (N) (DG Layer)
0	55.8 (24)	78.9 (30)	84.2 (32)	59.0 (23)
1	2.3 (1)	7.9 (3)	7.9 (3)	7.7 (3)
2	11.6 (5)	5.3 (2)	0 (0)	12.8 (5)
3	7.0 (3)	2.6 (1)	5.3 (2)	10.3 (4)
4	4.7 (2)	2.6 (1)	0 (0)	2.6 (1)
≥5*	18.6 (8)	2.6 (1)	2.6 (1)	7.7 (3)

Aβ - amyloid-β; Str.Rad. – Stratum radiatum; CA – cornu ammonis; Str. Luc. – stratum lucidum; DG – dentate granule; *full range was from 5-13 plaques.

CHAPTER 3

The AT8 Tau Phosphoepitope Modulates Tau-Protein Phosphatase 1 Interactions and Phosphatase Activity

Abstract

The functional repertoire of the tau protein continues to evolve, and one relatively understudied potential biological function is signaling regulation, which has implications in tau-mediated dysfunction and degeneration in disease such as AD. Recently, our group identified a mechanism through which the pathology-associated AT8 phosphoepitope of tau leads to deficits in fast axonal transport through a signaling pathway dependent on protein phosphatase 1 (PP1) and glycogen synthase kinase-3β (GSK3β). Amino acids 2-18 of tau, termed the phosphatase-activating domain (PAD), are necessary and sufficient to activate this pathway and cause transport deficits. In prior studies, tau toxicity was PP1-dependent, but the connection between tau and PP1 was not well defined. Here, we studied the interaction between tau and PP1 and subsequent effects on PP1 activity. Wild-type tau interacts with PP1α and γ, but shows little to no interaction with PP1β, and this interaction depends primarily on the microtubule binding repeats in tau. Additionally, pseudophosphorylation of tau at AT8 (psAT8) increased interactions with PP1γ, and deletion of PAD in the presence of psAT8 reduced this interaction. Finally, wild-type tau increased PP1 phosphatase activity in the *para*-nitrophenyl phosphate assay, and psAT8 tau further increased activity. Results from this study indicate that pathological modifications of tau observed in AD increase interaction and activity of PP1γ. This provides evidence that tau's function likely extends beyond stabilizing microtubules to include regulation of PP1 signaling cascades, and disease-associated tau phosphorylation may alter this function.

Introduction

Tau is a microtubule-associated protein and traditionally it is characterized as a microtubule stabilizing protein. Indeed, several *in vitro* studies confirm the ability of tau to increase microtubule stability and cell-based studies clearly indicate an association with microtubules. However, multiple lines of evidence support alternative or additional functions of the tau protein. For example, tau not only associates with the plasma membrane and ribosomes, but also is present within the nuclei and dendrites of cells. In rat cortical neurons, tau exhibits a dynamic interaction with the plasma membrane, and is phosphorylation dependent. Inhibiting Casein kinase 1 or GSK3β increased localization of tau to the membrane, whereas mimicking phosphorylation at several residues in the N-terminus region or proline-rich region of tau, including AT8, enriched tau in the cytosol (Pooler *et al.* 2012). Tau also associates with ribosomes in AD brains but not control brains (Brady *et al.* 1995). This implies a mechanism related to protein synthesis, but the functional significance of this association remains to be determined (Bukar Maina *et al.* 2016). Nuclear tau exists in different isoforms, and some cells show a diffuse pattern of tau in the nucleus while others show tau localized to the nucleolus (Loomis *et al.* 1990, Wang *et al.* 1993, Liu *et al.* 2013, Lu *et al.* 2014) Moreover, tau appears to regulate localization and potentially the activity of multiple signaling molecules. For example, tau can signal for the activation of Src family kinases by acting as a scaffold. Tau interacts with the tyrosine kinase Fyn and PSD-95, an important scaffolding protein at the post-synaptic density, to modulate and signal for Fyn kinase to localize to dendritic spines (Ittner *et al.* 2010, Morris *et al.* 2011) Thus, tau's functional repertoire appears much larger than just stabilizing microtubules and may include cell signaling functions, including regulation of protein phosphatase 1 (PP1).

PP1 is a member of the serine/threonine protein phosphatase family, one of the most highly conserved protein families with ubiquitous expression in eukaryotes (Cohen 2002). Existing as a holoenzyme complex between its catalytic subunit (PP1c) and a regulatory protein, PP1 is involved in several cellular functions including cytoskeletal reorganization, membrane

channel regulation, axonal transport and many others (Cohen 2002, Morfini *et al.* 2009). There are over 200 PP1c regulator proteins, allowing for the broad context of its functions (Ceulemans *et al.* 2004, Fardilha *et al.* 2010). Three genes encode PP1c: *PPP1CA* (PP1α), *PPP1CB* (PP1β), and *PPP1CC* (PP1γ). Alternative splicing of *PPP1CC* produces two isoforms, $PP1\gamma_1$ and $PP1\gamma_2$, with $PP1\gamma_1$ being more prevalent in the central nervous system (CNS) (Kitagawa *et al.* 1990, Shima *et al.* 1993, Ouimet *et al.* 1995). Variations between the isoforms exist in the N- and C-termini, while the catalytic core is highly conserved between isoforms (Peti *et al.* 2013, Korrodi-Gregorio *et al.* 2014). Most regulatory proteins interact with PP1c through the RVxF binding motif (Egloff *et al.* 1997, Wakula *et al.* 2003), of which tau has three, including one in the PAD region (amino acids 5-8, 343-346, and 375-378 of full-length human tau) (Liao *et al.* 1998). Additionally, a single prior publication demonstrated that tau interacts with PP1 through a blot overlay assay, and tau targets PP1 to microtubules by using a microtubule co-sedimentation assay where PP1 pelleted with microtubules in the presence of tau, where PP1 was unable to co-sediment by itself (Liao *et al.* 1998). Whether tau directly binds PP1 isoforms and how disease-related modifications such as AT8 affect the relationship between tau and PP1 was unclear.

One important aspect of the regulatory functions of tau in the context of PP1 is the involvement in maintaining axonal functions such as axonal transport and the role of this mechanism in tau-mediated toxicity (Drechsel *et al.* 1992, Wang *et al.* 2008). Our group discovered that amino acids 2-18 in the amino terminus of tau can activate PP1; this region of tau was termed the phosphatase-activating domain (PAD) (Kanaan *et al.* 2013), and PAD exposure leads to activation of a signaling pathway involving PP1 and GSK3 that impairs axonal transport in squid axoplasm. These findings were recently supported by Vossel and colleagues that showed tau-mediated activation of GSK3β was required for amyloid-β toxicity in neurons (Vossel *et al.* 2015). Indeed, AD and other tauopathies are characterized by the dysfunction and aggregation of abnormally modified forms of tau protein that are associated with synapse loss

(DeKosky *et al.* 1990, Masliah *et al.* 1991) and axon degeneration (Bell *et al.* 2006, Vana *et al.* 2011), which correlate with cognitive decline during disease progression (Braak *et al.* 1991, Arriagada *et al.* 1992, Giannakopoulos *et al.* 2003, Braak *et al.* 2006). Several disease-related modifications of tau, including the phosphoepitopes and oligomerization, alter tau conformation causing abnormal exposure of PAD (Jeganathan *et al.* 2008, Kanaan *et al.* 2011). The AT8 phosphoepitope of tau (phospho-Ser199/Ser202/Thr205) is an early and prominent modification associated with AD pathology (Braak *et al.* 2006, Kanaan *et al.* 2011). Phosphomimicking the AT8 modification with pseudophosphorylation (psAT8) causes disrupts the “paperclip” conformation where the N-terminus folds over to interact with the C-terminus (Jeganathan *et al.* 2008) and inhibits anterograde fast axonal transport in squid axoplasms (Kanaan *et al.* 2011). PAD exposure leads to impaired anterograde axonal transport in a PP1-dependent manner (Morfini *et al.* 2002, Morfini *et al.* 2004, Morfini *et al.* 2007, Kanaan *et al.* 2011, Kanaan *et al.* 2012), but whether pathological forms of tau engage this pathway by directly interacting with PP1 was not determined. Interestingly, utilizing a PAD-specific antibody (TNT1), increased PAD exposure was observed in pre-tangle neurons in post-mortem human sporadic AD tissue, further suggesting that PAD exposure is an early event in the progression of AD pathology (Kanaan *et al.* 2012).

We tested the hypothesis that tau directly interacts with and activates PP1, and the AT8 tau modification will increase these effects. We found that tau interacts with and activates PP1α and PP1γ and modifying tau through AT8 pseudophosphorylation or deletion of the PAD region increases or decreases these effects, respectively. These findings suggest that one function of tau is modulation of PP1 and that the disease-associated AT8 phosphoepitope of tau may lead to altered PP1 regulation.

Materials and Methods

Tau and PP1 Constructs

Tau proteins are designated by the longest human tau isoform in the CNS (hT40 or 2N4R, possessing 441 amino acids). This tau isoform contains both N-terminal exons and four microtubule binding repeat regions (MTBRs) and here we will refer to this as wild-type tau (WT tau). Tau domain constructs corresponding to the different regions in the tau protein were generated to assess how the specific regions of tau interact with PP1 (Figure 3.1). The N-terminus domain (N-term) contains amino acids 1-224, the MTBR domain contains the four MTBRs and is composed of amino acids 225-380, and the C-terminus domain (C-term) contains amino acids 381-441. Additionally, constructs with containing the N-terminus and MTBR (ΔC-term) or the MTBR and C-terminus (ΔN-term) were used. Point mutations in WT tau were performed to mutate S199, S202, and T205 to glutamic acid to mimic phosphorylation at the AT8 epitope (psAT8). The PAD (amino acids 2-18) was deleted from these constructs to assess the role of PAD in modulating PP1 interactions and activity (ΔPAD WT and ΔPAD psAT8). Finally, a construct where all three RVxF motifs at amino acids 5-8, 343-346, and 375-378 are deleted was produced to investigate the role of this canonical binding motif in the interactions between tau and PP1γ (Figure 3.14)

HaloTag Pulldown Assays

Human embryonic kidney (HEK) 293T (ATCC CRL-3216) cells were transfected with Tau and PP1 constructs under control of a pCMV promoter. Tau protein was fused to NanoLuciferase (NLuc) tag and PP1 was fused to HaloTag (HT, Promega HaloTag System G6051)(Machleidt *et al.* 2015). HEK 293T cells were grown in DMEM (Thermo 11995-065) supplemented with 5% FBS and 1% penicillin/streptomycin (Thermo 15140-122) in a humidified incubator at 37° and 5% CO_2. Cell were plated in a 12-well plate at 300,000 cells/well in 1 mL DMEM (supplemented with 5% FBS and 1% penicillin/streptomycin) one day prior to

transfection. Cells were co-transfected with an equal amount of pCMV tau-NLuc fusion construct and pCMV HT-PP1 isoform fusion constructs using Lipofectamine 2000 (Invitrogen 52887) according to the manufacturer's instructions and incubated overnight. The next day, cells were collected in lysis buffer (50 mM Tris-HCl, 150 mM NaCl, 1% Triton X-100, 10 µg/mL pepstatin, 10 µg/mL leupeptin, 10 µg/mL bestatin, 10 µg/mL aprotinin, 1 mM PMSF, pH 7.5) and dounce homogenized. For the experiments using nocodazole, 2 µg/mL was added to the cell culture media for 15 minutes (to disrupt labile microtubule domains) or 60 minutes (to disrupt more stabled microtubule domains) prior to lysing. Homogenates were centrifuged at 14,000 x g for 5 minutes at 4° C to pellet debris, and the supernatant was transferred to a new tube. Lysates were diluted in TBS to bring the Triton X-100 to 0.3%. 12.5 µl of lysate was removed as the "Input" fraction. 50 µl HaloLink resin (Promega G1915) was equilibrated in Halo Wash Buffer (50 mM Tris-HCl, 150 mM NaCl, 0.05% NP-40, pH 7.5) by washing three times in 500 µl wash buffer. Resin was centrifuged at 800 x g for 2 minutes at room temperature after each wash to settle resin and allow for aspiration of the supernatant. After removing the last wash buffer, 450 µl lysate was added to resin and incubated for one hour at room temperature with end-over-end mixing. Resin was pelleted via centrifugation, and the supernatant saved as the "flow-through" fraction. The resin was washed four times with Halo Wash Buffer, and bound proteins were eluted by incubating in 50 µl 2x Laemmli Sample Buffer (40 mM Tris pH 6.8, 3.3% SDS, 10.7% glycerol, 2.5% β-mercaptoethanol, 0.004% bromophenol blue) for 30 minutes at 30°C and 1000 RPM shaking. Resin was pelleted via centrifugation, and the resulting supernatant was saved as the "Elution" fraction for Western blot analysis.

NanoBRET Assays

HEK 293T cells were plated in a 12-well plate at a density of 400,000 cells/well in 1 ml plating volume. Six hours later, cells were co-transfected with a pCMV tau-NLuc fusion

construct (donor) and a pCMV HT-PP1 construct (acceptor) with Lipofectamine 2000. For the donor saturation assay, cells were transfected with 10 ng donor DNA and a range of acceptor DNA from 0 ng to 1000 ng to obtain a ratio of donor DNA to acceptor DNA (DNA Ratio, from 0 – 100) with a serial dilution factor of 3. Single ratio NanoBRET assays were performed at a 1:30 DNA ratio (10 ng donor DNA and 300 ng acceptor DNA). An empty, non-coding pTRE3G plasmid was used as a carrier DNA to standardize transfection amounts. After transfection, cells were incubated overnight. The next day cells were replated in triplicate into a white-wall, clear-bottom 96-well plate with a 618nm fluorescent ligand that covalently binds to HT or DMSO as a control according to the manufacturer's instructions (Promega NanoBRET Nano-Glo Detection System N1661) (Machleidt *et al.* 2015). Replated cells were incubated overnight. The next day, the cell culture media was removed and replaced with 100 μl fresh media to remove unbound 618 nm ligand before Nano-Glo substrate was added to each well according to the manufacturer's instructions. Donor luminescence and acceptor fluorescence was measured on a BioTek Synergy H1 microplate reader using a 460/40 nm bandpass filter and a 610 nm longpass filter respectively. NanoBRET ratios were calculated by dividing the acceptor signal by the donor signal and subtracting the ratios from the no-ligand DMSO controls.

Western Blotting and Dot Blotting

Input, flow-through, and elution fraction samples were denatured at 98°C for 5 minutes before being loaded onto a 4-20% Tris-HCl Criterion gel (BioRad 3450034) and proteins separated by SDS-PAGE. Proteins were transferred to a nitrocellulose membrane and probed with HaloTag (1:1000, mouse monoclonal IgG1, Promega G9211) to label PP1 proteins or HaloTag alone, and either NanoLuciferase (1:5000, rabbit polyclonal, Promega) or R1 (1:100,000, rabbit polyclonal pan-tau antibody)(Berry *et al.* 2004) antibodies for the tau domains or full-length and ΔPAD tau proteins, respectively. Antibodies were diluted in 2% non-fat dry milk in TBS and blots were incubated overnight at 4°C. The next day, blots were incubated for 1

hour at room temperature with IRDye 800CW goat-anti-rabbit IgG (H+L) (1:20,000, LiCor Biosciences 925-32211) and IRDye 680LT goat-anti-mouse IgG (H+L) (1:20,000, LiCor Biosciences 926-68020). Blots were imaged using a LiCor Odyssey system. Band signal intensities were quantified using ImageStudio software, with the tau band intensities normalized to efficiency of HaloTag affinity pulldown (i.e. difference between HaloTag signal in the input and flow-through samples).

Recombinant tau proteins were analyzed using western blots and dot blots as described (Kanaan *et al.* 2011). Briefly, 500 ng of WT tau and psAT8 recombinant proteins were used per spot or gel lane. Both blots were probed for R1 (as above) and TNT1 (1:200,000) to detect PAD exposed tau (Kanaan *et al.* 2011). The signal from TNT1 (PAD exposed tau) (Kanaan *et al.* 2011, Kanaan *et al.* 2012, Combs *et al.* 2016, Cox *et al.* 2016) was normalized to R1 signal (total tau).

Proximity Ligation Assay

Primary neurons from E18 rat hippocampus were plated at 30,000 cells/well in 8-well chamber slides coated with poly-D-lysine and cultured for 9 days as described previously (Grabinski *et al.* 2016) before being fixed for 20 minutes at room temperature with warm 4% paraformaldehyde in cytoskeletal buffer (10 mM MES, 138 mM KCl, 3 mM $MgCl_2$, 4 mM EGTA, pH 6.1). Fixed cells were rinsed three times in TBS for 5 minutes each before blocking with DuoLink blocking solution (Sigma DUO82007) for 1 hour at room temperature. Cells were incubated with Tau7 (mouse monoclonal IgG1 pan-tau antibody, 1:5,000) (Horowitz *et al.* 2006), PP1α (1:250, rabbit polyclonal, Invitrogen PA5-28218), PP1β (1:250, rabbit polyclonal, Invitrogen PA5-28225), and PP1γ (1:250, rabbit polyclonal, Invitrogen PA5-21671) antibodies diluted in 2% donkey serum in TBS overnight at 4°C. The next day, cells were washed in TBS, incubated with DuoLink In Situ PLA Probes Anti-Mouse PLUS (Sigma DUO82001) and Anti-Rabbit MINUS (Sigma DUO82005), and PLA signal developed in the green channel using

Duolink In Situ Detection Reagents Green according to the manufacturer's instructions (Sigma DUO92014). After amplification of PLA signal, cells were washed four times for 5 minutes with TBS and re-blocked with 5% goat serum + 2% BSA + 0.2% Triton X-100 for 1 hour at room temperature. Next, cells were incubated in 5H1 β-tubulin antibody (mouse monoclonal IgM, 1:2000)(Thurston *et al.* 1997) diluted in 2% goat serum in TBS overnight at 4°C. The next day, cells were washed in TBS and incubated in AlexaFluor goat anti-mouse IgM 647 (Thermo A-21238) for one hour at room temperature. DAPI was included in the first wash. Images were acquired using a Nikon A1+ laser scanning confocal microscope system with the Nikon Elements AR software.

Recombinant Protein Production

All tau and PP1 constructs were expressed in *Escherichia coli* using the pT7c backbone and fused to a 6x histidine tag for purification and use in the PNPP assay. The histidine tag was present on the C-terminus for each tau construct and on the N-terminus for each PP1 construct. Inclusion of the His-tag on the C-terminus of PP1 resulted in reduced activity (Figure 3.16) Recombinant proteins were purified on an Akta Pure 25L fast protein liquid chromatography machine (GE Healthcare 29018224) by immobilized metal affinity chromatography using a HiTrap TALON Crude column (GE Healthcare 28953767) as described previously(Combs *et al.* 2017). Tau protein purifications were followed by size exclusion chromatography over an S500 column (GE Healthcare 28-9356-06) and anion exchange chromatography over a HiTrap Q HP column (GE Healthcare 17-1154-01)(Combs *et al.* 2017). DTT was added to a final concentration of 1 mM before aliquoting the purified tau proteins and storing at -80°C. PP1 protein purifications were followed by a buffer exchange step using a HiTrap Desalting column (GE Healthcare 17-1408-01) into PP1 Final Storage Buffer (10 mM Tris, 300 mM NaCl, 1 mM $MnCl_2$, 1 mM EGTA, pH 7.0)(Watanabe *et al.* 2003). DTT was added to a final concentration of 2.5 mM before aliquoting the purified PP1 protein and storing at -80°C. Protein concentrations

were determined using the SDS-Lowry assay method as described (Cox *et al.* 2016). The specific activities for each PP1 enzyme was determined to be ~2.0 µmol/min/µg for PP1α and ~5.4 µmol/min/µg for PP1γ, consistent with previous published reports producing PP1 with this method (Watanabe *et al.* 2003).

Para-Nitrophenyl Phosphate (PNPP) Phosphatase Activity Assay

Recombinant tau and PP1 proteins were mixed in equal molar ratios in PP1 buffer (150 mM NaCl, 20 mM MOPS, 0.1 mM $MnCl_2$, 1.0 mM $MgCl_2$, 10% glycerol, pH 7.5) to a final volume of 50 µl and incubated at 30°C for 1 hour. For experiments utilizing tau antibodies to confirm the increase in phosphatase activity was specific to tau and not any protein, tau solutions were mixed with two times the concentration of tau antibody for 1 hour at 16°C prior to mixing with PP1. For experiments digesting tau with trypsin, trypsin (Gibco 15400) was added to a concentration of 500 µg/ml and incubated at 50°C for 30 minutes. Trypsin was subsequently deactivated by heating the solution at 95°C for 10 minutes and allowing to cool prior to addition to PP1 solution. The entire volume of protein solution was transferred to a clear 96-well plate. PNPP substrate (Fisher Scientific BP2534-10) was freshly dissolved in PP1 buffer and 50 µl was added to each well containing the protein solution. Absorbance was measured in 5 minute intervals on a Molecular Devices SpectraMax Plus 384 spectrophotometer at 405 nm at 37°C for three hours. The final reaction conditions for each PP1 isoform were determined by tittering each PP1 protein preparation individually where the enzyme alone reacted with PNPP substrate to obtain ~50% absorbance after three hours. Absorbance values were converted to the amount of product produced (in µmol) using the Beer-Lambert law equation:

$$Abs = \varepsilon \, L \, c$$

In this equation, ε = 18,000 mol·cm^{-1} (McAvoy *et al.* 2010), *L* = 0.29 cm, and *Abs* is the measured absorbance. The resulting curve of product produced over time was fit to a Michaelis-Menten equation model to obtain V_{max} and $t_{1/2}$, as a measure of the maximum product produced and the reaction rate, respectively.

Statistical Analysis

All data and statistical analyses were performed using GraphPad Prism 7.0 software. All data were found to be normally distributed using the Shapiro-Wilk test. Pulldown and NanoBRET assay results to determine which PP1 isoform WT tau interacts with were analyzed by paired t-test. Experiments investigating which domain of tau interacts with PP1, the effect of AT8 pseudophosphorylation, and the effect of PAD deletion were analyzed by repeated-measures one-way ANOVA with *post hoc* comparisons made using the Holm-Sidak test. Comparisons between V_{max} and $t_{1/2}$ in the PNPP assay and the amount of phosphate produced in the malachite green assay were analyzed by repeated-measures one-way ANOVA with *post hoc* comparisons made using the Holm-Sidak test. Significance was set at $p \leq 0.05$ for all tests.

Results

Tau Specifically Interacts with PP1α and PP1γ

We previously described a mechanism by which pathological forms of tau activated a PP1-dependent mechanism of axonal transport inhibition in the squid axoplasm model (LaPointe *et al.* 2009, Kanaan *et al.* 2011, Kanaan *et al.* 2013). To further expand on these findings, we tested whether WT tau interacts with PP1 isoforms using pulldown assays in HEK 293T cells. Tau eluted with PP1α and PP1γ, but little to no pulldown of tau occurred with PP1β (Figure 3.2A-C). HaloTag protein alone was used as a negative control and, as expected, no tau was detected in the pulldown sample (Fig. 3.2A-C). The tau-PP1 interaction was further investigated in living HEK 293T cells using the NanoBRET assay. Donor saturation assays

produced hyperbolic curves that saturate at a low DNA ratio further supporting an in-cell interaction between tau and the PP1 α and γ isoforms, while a weaker and more linear curve was observed with PP1β indicating little to no interaction (Figure 3.2 D-I). This pattern of interaction was observed for all recombinant tau proteins tested in the donor saturation assay (Figure 3.13). Single DNA ratio experiments (i.e. 30 PP1 acceptor:1 tau donor) show that WT tau significantly increases NanoBRET signal with PP1α and γ, but not PP1β when compared to their respective HaloTag only controls (Figure 3.2 D-I). Finally, PLA was performed on E18 primary hippocampal neuron cultures to show that tau and PP1 associate in neurons. Puncatate PLA fluorescent signal was observed throughout the neuron, including the somatodendritic and axonal compartments (Figure 3.2J-N), indicating that endogenous tau and PP1 normally associate in neurons. As expected, when either primary antibody was omitted, no PLA signal developed (Figure 3.3). Taken together, these results demonstrate that tau preferentially interacts with PP1α and γ through a direct interaction.

The MTBR Domain of Tau is Necessary and Sufficient for Interacting with PP1

Next, we investigated which domain of tau is responsible for the interaction with PP1. Due to the little to no interaction observed between Tau and PP1β we focused on PP1α and γ in subsequent assays. Tau was divided into five domains (Figure 3.1) and each construct was co-transfected with PP1α or PP1γ in HEK 293T cells and used for HaloTag pulldown and NanoBRET assays. Only domains containing the MTBRs (MTBR, ΔC-term, ΔN-term) significantly increased interaction with PP1α and γ relative to HT only controls (Figure 3.4 A-C, Figure 3.5 A-C). Constructs containing the MTBRs also significantly increased PP1α and γ phosphatase activity in the PNPP assay similar to WT tau (Figure 3.4D and 3.5D, Table 3.1 and 3.2). These findings suggest the MTBRs of tau are necessary and sufficient to interact with both PP1α and PP1γ, whereas the N- and C-termini are not sufficient for the interaction.

AT8 Pseudophosphorylation Modulates Tau's Interaction with PP1

Phosphorylation at the AT8 epitope causes extension of the N-terminus of tau (Jeganathan *et al.* 2008); therefore, we hypothesized that AT8 phosphorylation would expose the PAD region and promote and interaction between tau and PP1. Confirmation that psAT8 tau displays an extended PAD region was obtained through dot blots and western blots using TNT1 and R1 (Figure 3.7A). Under the non-denaturing conditions of a dot blot, TNT1 reactivity is observed with psAT8 tau but not WT tau, indicating PAD is exposed in psAT8 tau. Additionally, in the denaturing conditions of a western blot, TNT1 reactivity is observed with both WT tau and psAT8, indicating psAT8 tau has PAD extended and not removed. Additionally, each recombinant protein was visualized through SDS-PAGE and subsequent staining with Coomassie Brilliant Blue to confirm the proper size and expected purity of the preparations (Figure 3.12). Additionally, recombinant WT tau, psAT8 tau, Δ2-18 WT tau, and Δ2-18 psAT8 tau were visualized on western blots to confirm deletion of PAD (Figure 3.12). HEK 293T cells were co-transfected with WT tau or psAT8 tau with each PP1 isoform and the interactions determined through the HaloTag pulldown and NanoBRET assays. While psAT8 tau did not display a significant increase in interaction with PP1α relative to hT40 in the affinity pulldown assay (Figure 3.6). a significant increase in interaction was observed with PP1γ (Figure 3.7).

The PAD Facilitates the Interaction Between Tau and PP1

The PAD region, amino acids 2-18, inhibits anterograde fast axonal transport through a PP1-dependent mechanism, and pathological forms of tau, such as psAT8, that expose PAD inhibit axon transport through this pathway(Morfini *et al.* 2004, LaPointe *et al.* 2009, Kanaan *et al.* 2011, Kanaan *et al.* 2012). We investigated the role of the PAD in tau-PP1 interaction, and the pulldown assays indicate that all of the tau constructs interact with PP1α and PP1γ (Figure 3.8A-C and Figure 3.9A-C). Deleting PAD from WT tau did not significantly change the interaction with PP1α or γ (Figure 3.8B and Figure 3.9B). However, deleting PAD from psAT8

tau significantly reduced the interaction with PP1α and γ (Figure 3.8C and Figure 3.9C). Taken together, these results show the PAD region is an important motif in facilitating the interaction with PP1γ when the AT8 phosphoepitope (as indicated by pseudophosphorylation) is present.

Tau Increases PP1 Activity In Vitro

To determine whether these differences in tau-PP1 interactions have functional effects, we investigated tau's ability to influence PP1 phosphatase activity in the PNPP assay. Addition of WT tau to PP1α and γ resulted in a significant increase in V_{max} and $t_{1/2}$ when compared to PP1 alone (Figure 3.10A and Figure 3.11A, Table 3.3 and Table 3.4). While addition of psAT8 tau protein to PP1α did not result in a further increase in phosphatase activity relative to WT tau (Figure 3.10 and Table 3.3), the psAT8 tau protein showed a significant increase in V_{max} and a lower $t_{1/2}$ when compared to PP1γ incubated with WT tau (Figure 3.11 and Table 3.4). Unexpectedly, deleting PAD from WT tau resulted in a significant increase in V_{max} and a lower $t_{1/2}$ compared to PP1γ with full-length WT tau (Figure 3.11 and Table 3.4). Interestingly, deleting PAD from psAT8 did not significantly change PP1γ activity relative to incubation with full-length psAT8 (Figure 3.11 and Table 3.3). Additionally, deleting PAD from either WT Tau or psAT8 Tau constructs did not modify the V_{max} and $t_{1/2}$ of PP1α when compared to incubation of PP1α with full-length WT or psAT8 tau proteins (Figure 3.10 and Table 3.3). To confirm this increase in activity was due to the presence of tau and not an effect of any protein, digesting WT tau with trypsin, followed by inactivation of trypsin and then addition to the solution containing PP1α did not change PP1α phosphatase activity compared to the enzyme by itself (Figure 3.17). Additionally, the presence of tau antibodies, Tau2 or R1, in the reaction solution did not increase PP1α phosphatase activity and even blocked the increase in activity from WT tau. (Figure 3.17). These results indicate that the increase in phosphatase activity is specific to the presence of tau protein.

The RVxF Motif Facilitates Tau's Interaction with PP1

The RVxF motif is a canonical PP1 binding motif present in a majority of PP1 interacting partners (Wakula *et al.* 2003, Hendrickx *et al.* 2009). We investigated the role of this binding motif in tau-PP1γ interactions using the pulldown assay. Deletion of all three RVxF motifs from WT tau resulted in a ~50% decrease in interaction with PP1γ but did not completely abolish it (Figure 3.14). These results indicate that the interaction between WT tau and PP1γ does not depend on the RVxF motif, but instead possibly plays an role in stabilizing the interaction.

Disruption of Microtubules with Nocodazole Did Not Reduce Tau-PP1 Interactions

Nocodazole disrupts microtubules by binding to β-tubulin and interfering with polymerization (Florian *et al.* 2016). Addition of nocodazole for either 15 minutes or 60 minutes prior to the pulldown assay was used to investigate whether tau's interaction with PP1 depends on the presence of microtubules. Disruption of either the labile domains or more stable domains of microtubules did not result in a significant decrease in the interaction between WT tau and PP1γ (Figure 3.15). These results indicate that the interaction between WT tau and PP1γ does not depend on the presence of assembled microtubules.

Discussion

Tau-Mediated Regulation of PP1

Tau is a known substrate for PP1 dephosphorylation, however, recent evidence indicates tau possesses other targeting and signaling functions (Liao *et al.* 1998, LaPointe *et al.* 2009, Kanaan *et al.* 2011). An interaction between PP1 and tau *in vitro* was previously described using recombinant protein blot overlay assays and microtubule targeting assays in Sf9 insect cells(Liao *et al.* 1998). Additionally, tau can target PP1 to microtubules, presumably to promote phosphatase activity at that location (Liao *et al.* 1998). The differential subcellular localization of each PP1 isoform has previously been reported, and all three major neuronal

PP1 isoforms are expressed by neurons. (Strack *et al.* 1999, Bordelon *et al.* 2005). Interestingly, PP1β and PP1γ localize to distinct regions, with PP1β more prevalent in the cell body and PP1γ more prevalent in dendritic spines and synaptic terminals (Ouimet *et al.* 1995, Strack *et al.* 1999). Additionally, subcellular fractionation experiments indicate PP1β is closely associated with microtubules, however, the proposed hypothesis is PP1β first interacts with a cell body-enriched interacting partner, which then targets PP1β to microtubules (Strack *et al.* 1999). According to our results, this interacting partner is a different protein than tau. We confirm that tau and PP1 are in close association within neuronal cell bodies and processes using the PLA in rat primary hippocampal neurons. Using a combination of pulldown and in-cell protein-protein interaction assays we show that WT tau directly interacts with PP1α and PP1γ. Interestingly, our studies suggest there is little to no interaction between WT tau and the PP1β isoform. To our knowledge, this is the first study specifically investigating the interaction with tau and PP1 in an isoform-dependent manner and utilizing biochemical approaches to mimic tau modifications commonly observed in AD.

The majority of PP1 interacting partners bind the RVxF motif in PP1 isoforms, however, there are several other docking sites on PP1. Tau contains three putative PP1 binding motifs, one in the extreme N-terminus (aa 5-8) and the other two are located in the MTBR (aa 343-346 and 375-378). Prior studies suggested that the PAD, which contains the N-terminal RVxF motif, was critical to the PP1-dependnet toxic effects of pathological forms of tau on axonal transport (LaPointe *et al.* 2009, Kanaan *et al.* 2011). Here, we show that the interaction between WT tau and PP1 depends on the MTBR domain in tau, while the termini do not appear to be sufficient or required for an interaction with PP1 or modulation of PP1 activity in the assays used here. Additionally, deletion of the three RVxF motifs reduced the interaction between tau and PP1γ by ~50%, indicating the interaction is not dependent on this motif but may act in a mole stabilizing role. Disruption of labile domains or more stable domains of microtubules with nocodazole did not reduce the interaction between WT tau and PP1γ, indicating this interaction is not

dependent on intact microtubules. The apparent discordance between prior studies and the current studies may be due to the use of isolated squid axoplasms. In these functional assays of axon autonomous mechanism, WT tau does not cause abnormal transport even at supraphysiological levels. Thus, endogenous regulatory mechanism may be effective in squid axoplasm that prohibit aberrant activation of the PP1 pathway by WT Tau. Collectively, the findings with WT tau and tau domains support the suggestion that tau has the ability to modulate PP1 signaling pathways.

Implications of the Tau-PP1 Interaction in Tauopathies

In tauopathies, tau undergoes several post-translational modifications and aggregation into oligomers and filaments. The mechanisms underlying toxicity from pathological forms of tau is actively investigated by several groups and a number of potential mechanisms are identified. One distinctive feature of tauopathies is the presence of a “dying-back” pattern of degeneration where synaptic and axonal degeneration precedes overt cell body loss. Among the potential molecular mechanisms driving axonal toxicity in neurons affected by tauopathies involves PP1 activation. Specifically, tau modifications that occur in disease, such as specific phosphoepitopes and oligomerization, alter the structure of tau in such a way that exposes PAD, a biological active motif in the N-terminus of tau. PAD exposure leads to PP1-mediated activation of GSK3β via dephosphorylation of Ser9, resulting in GSK3β phosphorylating kinesin light chains and disrupting anterograde transport of cargoes down the axon to the synapse(Morfini *et al.* 2002, Morfini *et al.* 2004, Morfini *et al.* 2007, LaPointe *et al.* 2009, Kanaan *et al.* 2011, Kanaan *et al.* 2012). Though these studies clearly demonstrate that tau-induced toxicity is PP1-dependent, they did not determine whether the connection between pathological tau and PP1 was through a direct interaction.

AT8 tau is a prominent pretangle modification in AD and other tauopathies that appears as pathological tau first begins to deposit in affected neurons, implying it may act at the early

stages of tau-mediated pathogenesis (Bancher *et al.* 1993, Kanaan *et al.* 2016). Previous structural studies showed that the psAT8 modification disrupts tau conformation by extending the amino terminus (containing PAD) out of the folded "paperclip" conformation (Jeganathan *et al.* 2008). We further support the finding that psAT8 aberrantly exposes PAD using non-denaturing dot blots of recombinant psAT8. Not only does psAT8 expose PAD, but this modification causes toxicity to axonal transport as a monomeric protein in isolated squid axoplasm (Kanaan *et al.* 2011). We have expanded on these findings by characterizing the interaction between tau and PP1 and the resulting effect on PP1 activation through a combination of protein-protein interaction assays and phosphatase activity assays.

Pseudophosphorylation at the AT8 significantly increased the interaction with PP1γ and deletion of PAD significantly reduced the interaction with PP1γ and PP1α. Interestingly, deletion of PAD did not alter the interaction with WT tau suggesting the role for PAD may be more prominent in abnormally modified forms of tau. These results support the previously proposed model of tau-PP1 interactions where aberrant exposure of the PAD domain is involved in facilitating the interaction between tau and PP1 (Kanaan *et al.* 2013). These changes in tau-PP1γ interactions may also have functional signaling consequences. WT tau increased PP1γ and PP1α phosphatase activity in the PNPP assay, but AT8 tau significantly increased phosphatase activity further than WT tau only with PP1γ. These results establish the link between AT8 tau and PP1 in the molecular mechanism responsible for impairing axon transport in the squid axoplasm model (Kanaan *et al.* 2013).

Pathological tau-mediated interaction and subsequent activation of PP1, as shown in this report, could lead to an accelerated feed-forward loop in disease where AT8 tau activates the PP1-GSK3β signaling cascade resulting in GSK3β phosphorylating more tau at the AT8 epitope. Over time, this pathway may become unbalanced, where an accumulation of AT8 tau prevents the neurons from transporting cargoes down the axon normally, leading to the

degeneration observed in AD. Since the correlation between tau phosphorylation, development of neurofibrillary tangles, and cognitive decline has previously been reported (Bancher *et al.* 1989, Braak *et al.* 1991, Braak *et al.* 1994, Giannakopoulos *et al.* 2003, Braak *et al.* 2006), this unbalanced pathological loop involving PP1 and GSK3β may be a characteristic novel mechanism in the development and progression of AD. Additionally, identification of this molecular mechanism may lead to development of clinical biomarker tests using phosphorylation levels or enzyme activity, or development of novel pharmacological therapies targeting this signaling pathway.

Collectively, the current results support the hypothesis that, beyond stabilizing microtubules, tau can regulate PP1 activity, and post-translational modifications of tau that occur in disease (such as the AT8 phosphorylation site) can modulate this function (Sharma *et al.* 2007, Souter *et al.* 2010, Kanaan *et al.* 2013). Importantly, this is the only study to perform detailed investigation into the interaction between tau and PP1, including utilizing each PP1 isoform and tau modifications observed in tauopathies. Tau specifically interacts with PP1α and γ, and this interaction depends on the MTBR domain. Additionally, psAT8 tau increased its interaction and activity with PP1γ, and deletion of PAD reduced this interaction. Future studies are needed to further explore the role of this signaling pathway in other modified or mutant forms of tau that occur in tauopathies, such as FTDP-17 tau mutations (e.g. P301L), phosphorylation at tyrosine 18, and a comparison of the six tau isoforms (3R vs 4R). However, the novel evidence provided in this study suggests tau's function is multifaceted and complex, including, but not limited to, stabilizing microtubules to modulating cell signaling cascades in a highly specific manner. This specific level of detail is necessary to elucidate new molecular mechanisms of neurodegeneration and provide precise targets for pharmacological interventions, such as targeting the MTBRs of tau to compete with and prevent an interaction with PP1.

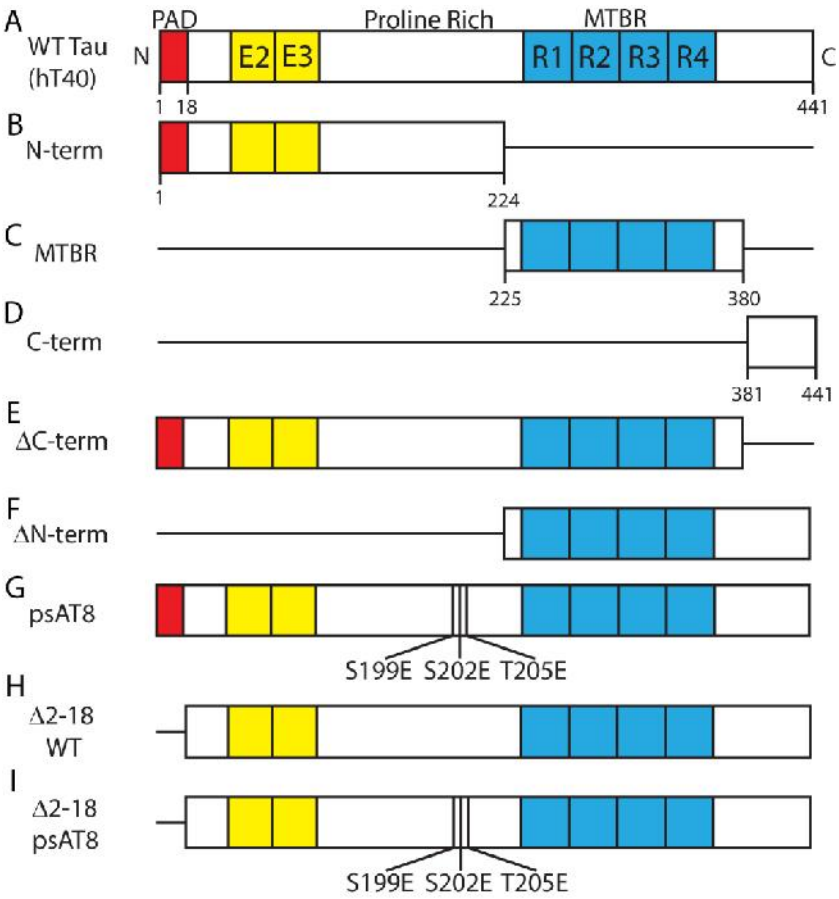

Figure 3.1 Schematic of tau constructs used in this study. (A) Full-length wild-type hT40 (WT Tau) containing the PAD region at amino acids 2-18 (red box), exons 2 and 3 in the N-terminus (E2 and E3), the proline rich region, and four microtubule binding repeat regions (MTBRs, R1-R4, blue boxes). (B) N-terminus domain (N-term) of WT tau corresponding to amino acids 1-224. (C) MTBR domain of WT tau corresponding to amino acids 225-380. (D) C-terminus domain (C-term) of WT tau corresponding to amino acids 381-441. (E) The N-term and MTBR domains, lacking the C-term domain corresponds to amino acids 1-380 (ΔC-term). (F) The MTBR and C-term domains, lacking the N-term domain corresponds to amino acids 225-441 (ΔN-term). (G) WT tau was pseudophosphorylated by mutating S199, S202, and T205 into glutamic acid (psAT8) to mimic the AT8 phosphoepitope. (H) WT tau with the PAD region removed (Δ2-18 WT). (I) psAT8 tau with the PAD region removed (Δ2-18 psAT8). All tau

Figure 3.1 (cont'd)

constructs were tagged at the C-terminus with NanoLuciferase for use of the same constructs in the Halo pulldown assays and NanoBRET in-cell protein interaction assays.

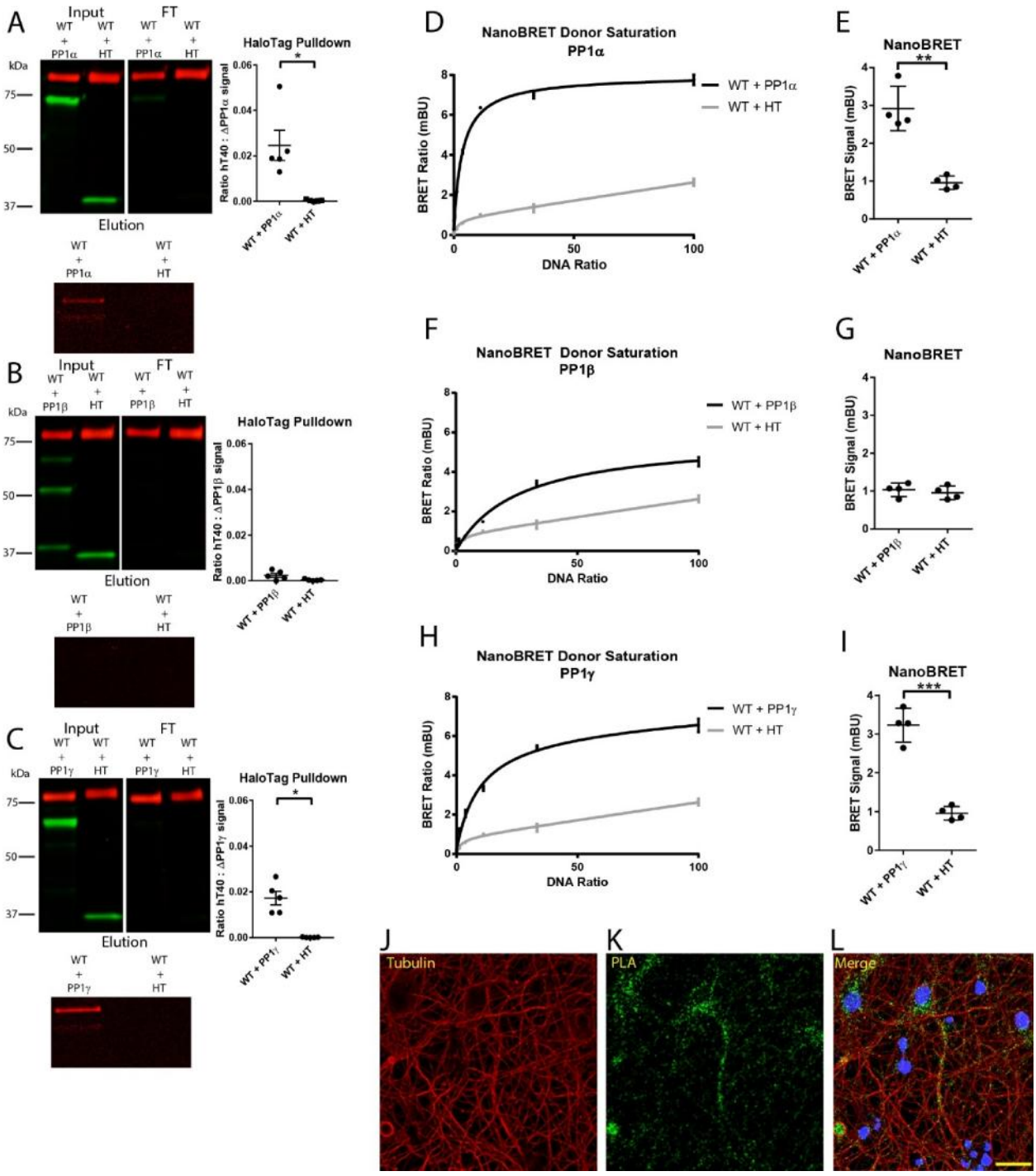

Figure 3.2 WT tau interacts with PP1α and PP1γ. (A-C) HEK 293T cells expressing WT tau (tagged with NLuc) and (A) PP1α, (B) PP1β, or (C) PP1γ (each tagged with HaloTag (HT) or HT only controls were used in pulldown assays. Western blots of starting lysate (Input) show similar expression of tau and PP1 constructs. Quantitation of tau signal in the elution sample

Figure 3.2 (cont'd)

shows significantly increased signal with (A) PP1α (**p* = 0.0217, paired t-test) and (C) γ (**p* = 0.0047), but not (B) PP1β (*p* = 0.1156) compared to the respective HaloTag only controls. Data are normalized to the pulldown efficiency (i.e. ratio of tau signal to the change in PP1 signal between the input and flow-through (FT) blots). All comparisons were done using a paired t-test. These experiments were repeated five independent times. (D-I) NanoBRET donor saturation assays and single ratio assays with PP1α (D-E), PP1β (F-G), and PP1γ (H-I). The hyperbolic curves with PP1α (D), β (F) and γ (H) indicate detection of a specific protein-protein interaction between tau and the PP1 isoforms. It is noteworthy that the curve is more linear with PP1β, which reflects much lower interaction of tau with this isoform. The more linear curves of the respective HaloTag only controls indicate a non-specific interaction. Single ratio NanoBRET assays (i.e. 30 PP1:1 Tau) show a significant increase in BRET signal with PP1α (E; ***p* = 0.0035) and γ (G; ****p* = 0.0006), but not PP1β (I; *p* = 0.3866) when compared to respective controls. All comparisons were done using a paired t-test. These experiments were repeated four independent times. (J-L) Rat primary hippocampal neurons were used to evaluate the relationship between endogenous tau and PP1 (green puncta). In the proximity ligation assay, the green puncta (K) indicate sites where endogenous Tau and PP1 are closely associated in the neurons. Cultures were counterstained for (J) β-tubulin (5H1, red) to visualize the cells. (L) Merging each color channel together indicates endogenous tau and PP1 associate throughout the neuron. DAPI was included to visualize nuclei (blue) Scale bar = 25 μm and applies to panels J-L. These experiments were repeated four independent times.

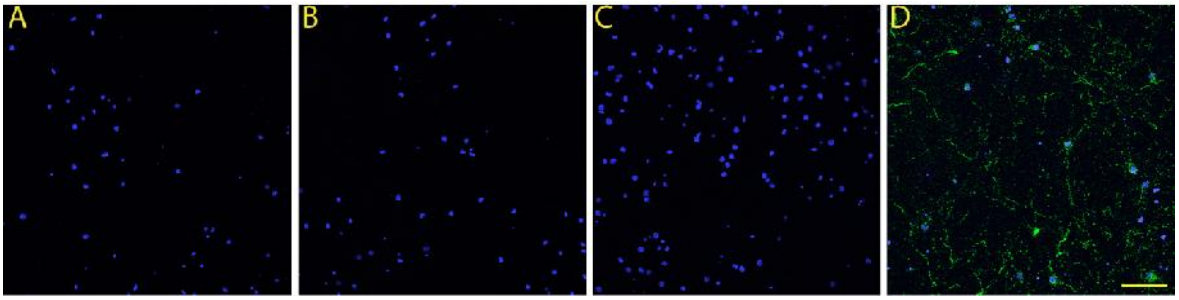

Figure 3.3 PLA antibody controls. (A) Omission of Tau7 and PP1 antibodies. (B) Omission of PP1 antibodies. (C) Omission of Tau7 antibody. (D) Positive PLA signal resulting from the inclusion of Tau7 and PP1 antibodies. Note that the lack of signal in the primary delete conditions confirms the specificity of the PLA signal. All cell counterstained with DAPI (nuclei). Scale bar = 25 μm.

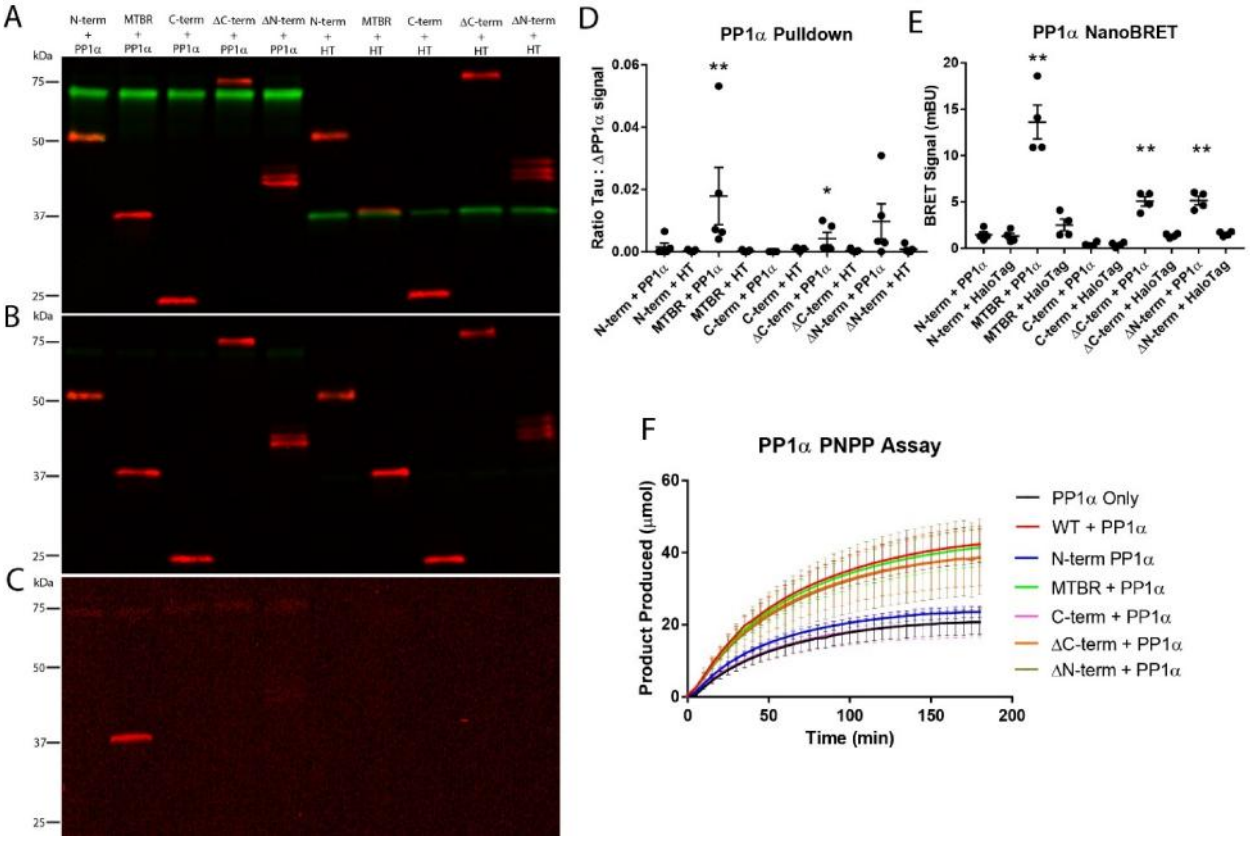

Figure 3.4 The MTBR domain of WT tau is necessary and sufficient for interaction with PP1α. (A-C) HEK 293T cells expressing each tau domain (tagged with NLuc) and PP1α (tagged with HaloTag (HT)) or HT only controls were used in pulldown assays. Western blots of input samples (A), flow-through samples (B), and elution samples (C) are shown with PP1 or HT in green and tau domains in red. (D) Quantification of tau signal in the elution sample shows significantly increased signal with the MTBR domain (**p = 0.0079) and ΔC-term domain (*p = 0.0317), but not the ΔN-term domain (*p = 0.0952) compared to the respective HT only controls. All comparisons between Tau+PP1α and HaloTag samples were done using a paired t-test. These experiments were repeated five independent times. (E) HEK 293T cells expressing each tau domain (tagged with NLuc) and PP1α (tagged with HT) or HT only controls were used in the NanoBRET assay. Significant differences in BRET signal were obtained with the MTBR domain (**p = 0.0026), ΔC-term domain (**p = 0.0039), and the ΔN-term domains (**p = 0.0038) when compared to their respective HaloTag only controls. Note quantitative comparisons between

Figure 3.4 (cont'd)

different tau proteins are not appropriate for the NanoBRET assay. All comparisons were done using a paired t-test. These experiments were repeated four independent times. (D) Recombinant tau and PP1α proteins were used to analyze phosphatase activity in the PNPP assay. Significant increases in the amount of product produced by PP1α were obtained for WT, MTBR, ΔC-term and ΔN-term domains (Table 3.1). No significant differences were observed in the reaction rate across tau constructs (Table 3.1). These experiments were repeated four independent times.

Table 3.1 PP1α activity kinetics with different tau domain constructs

PP1 Isoform	Tau Protein	V_{max} (Mean ± SD)	$t_{1/2}$ (Mean ± SD)
PP1α	No Tau	24.6 ± 8.1	72.4 ± 3.1
	WT Tau	51.3 ± 7.1*	76.2 ± 4.1
	N-term	37.4 ± 17.1	63.7 ± 5.7
	MTBR	48.7 ± 23.6*	75.3 ± 8.0
	C-term	22.7 ± 11.4	64.9 ± 1.7
	ΔC-term	52.8 ± 12.3*	71.5 ± 2.3
	ΔN-term	52.4 ± 16.0*	78.8 ± 2.3

Data were fit using Michaelis-Menten nonlinear curve to obtain the predicted maximum product (V_{max}) and reaction rate ($t_{½}$). Mean values represent data from four independent experiments ± standard deviations (SD). No significant differences were observed in the amount of product produced or reaction rates with a one-way ANOVA with Holm-Sidak *post hoc* test. No significant differences were observed in the amount of product produced or reaction rates with a one-way ANOVA with Dunnett's *post hoc* test. *$p \leq 0.05$ compared to No Tau as measured with a repeated measures one-way ANOVA with Dunnett's *post hoc* test.

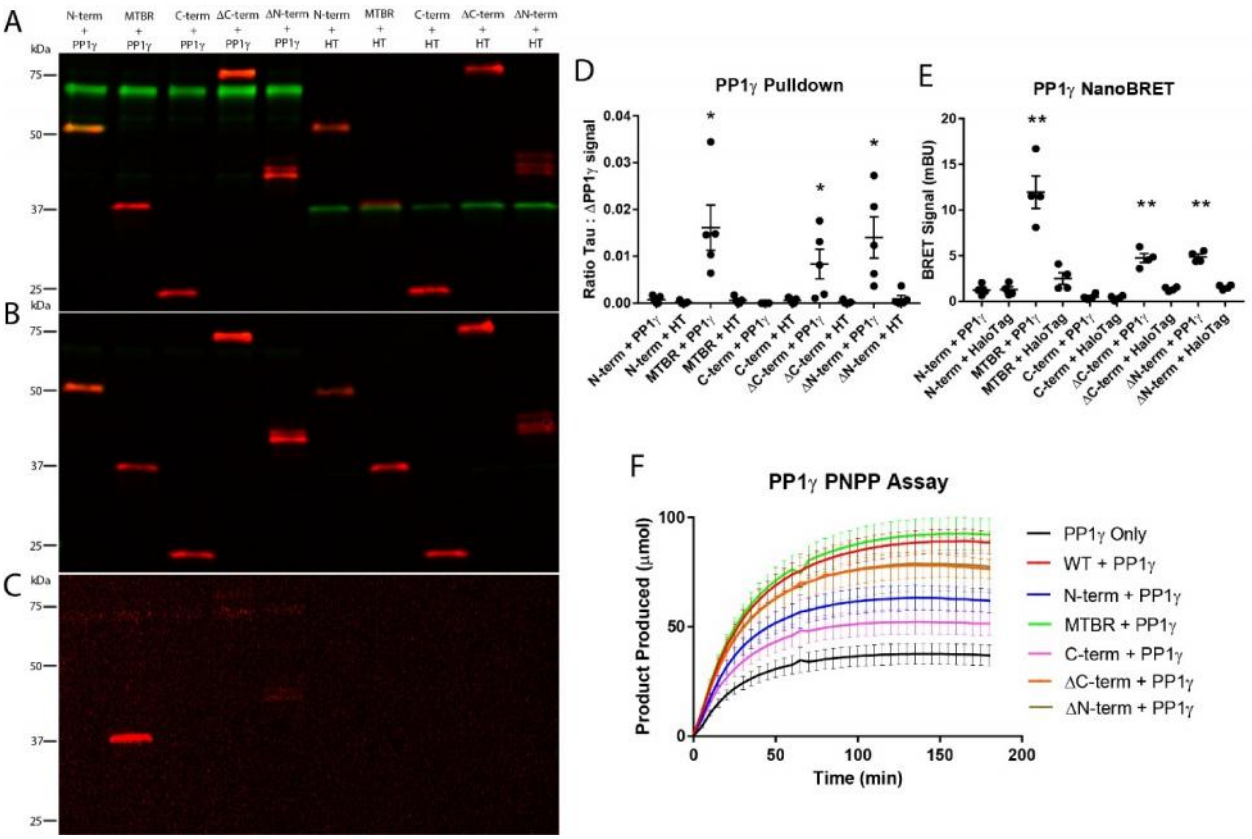

Figure 3.5 The MTBR domain of WT tau is necessary and sufficient for interaction with PP1γ. (A-C) HEK 293T cells expressing each tau domain (tagged with NLuc) and PP1γ (tagged with HaloTag (HT)) or HT only controls were used in pulldown assays. Western blots of input samples (A), flow-through samples (B), and elution samples (C) are shown with PP1 or HT in green and tau domains in red. (D) Quantification of tau signal in the elution sample shows significantly increased signal with the MTBR domain (**p* = 0.0125), ΔC-term domain (**p* = 0.0339), and ΔN-term domain (**p* = 0.0191) compared to the respective HT only controls. All comparisons were done using a paired t-test. This experiment was repeated five independent times. (E) NanoBRET single ratio assays were performed by co-expressing NLuc-tagged tau domains and HT-tagged PP1γ in HEK 293 cells. Significantly increased BRET signal was obtained with the MTBR domain (***p* = 0.0050), ΔC-term domain (***p* = 0.0086), and the ΔN-term domain (***p* = 0.0018) compared to the respective HT only controls. All comparisons were done using a paired t-test. (D) Recombinant tau and PP1γ proteins were

Figure 3.5 (cont'd)

used to analyze phosphatase activity in the PNPP assay. All tau constructs except the C-term domain significantly increased phosphatase activity of PP1γ when compared to the control not containing tau (Table 3.2). No significant differences were observed in the reaction rate across tau constructs (Table 3.2). These experiments were repeated four independent times.

Table 3.2 PP1γ activity kinetics with different tau domain proteins.

PP1 Isoform	Tau Protein	V_{max} (Mean ± SD)	$t_{1/2}$ (Mean ± SD)
PP1γ	No Tau	44.6 ± 5.7	24.7 ± 0.8
	WT Tau	107.9 ± 6.2*	30.0 ± 1.3
	N-term	74.8 ± 6.5*@	24.6 ± 1.2
	MTBR	112.2 ± 8.7*$	30.3 ± 1.5
	C-term	61.5 ± 6.5@#	23.4 ± 1.3
	ΔC-term	92.7 ± 2.7*%	25.4 ± 1.5
	ΔN-term	94.3 ± 7.2*%^	26.8 ± 1.2

Data were fit using Michaelis-Menten nonlinear curve to obtain the predicted maximum product (V_{max}) and reaction rate ($t_{½}$). Mean values represent data from four independent experiments ± standard deviations (SD). *$p \leq 0.05$ compared to No Tau control, @$p \leq 0.05$ compared to WT tau, $$p \leq 0.05$ compared to N-term domain, #$p \leq 0.05$ compared to MTBR domain, %$p \leq 0.05$ compared to C-term domain, and ^$p \leq 0.05$ compared to ΔC-term domain as measured with a one-way ANOVA with a Holm-Sidak *post hoc* test.

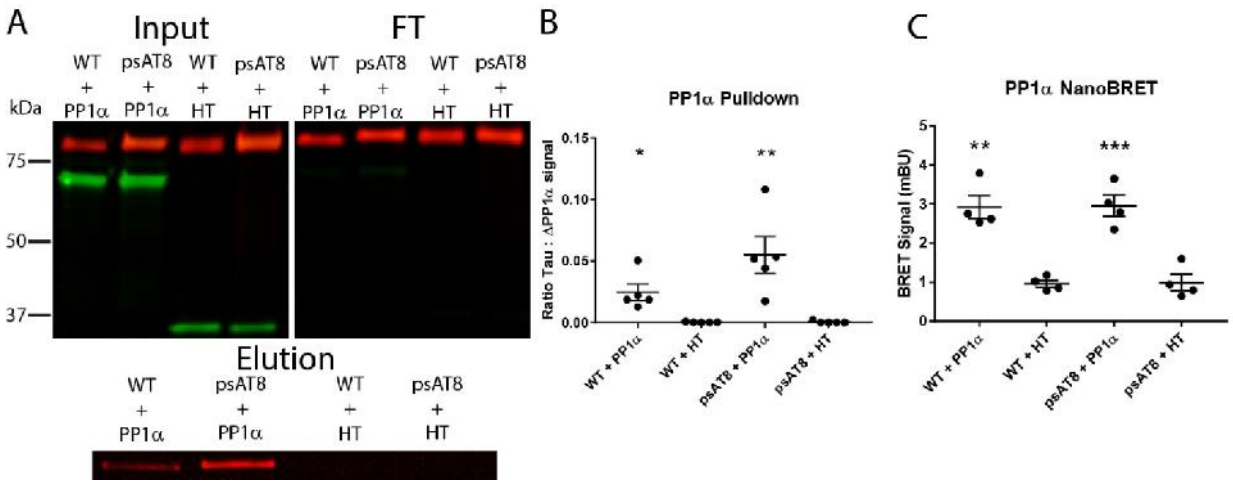

Figure 3.6 psAT8 did not significantly increase the interaction with PP1α. (A) HEK 293T cells expressing each tau construct (tagged with NLuc) and PP1α (tagged with HaloTag (HT)) or HT only controls were used in pulldown assays. Western blots of starting lysate (Input) show similar expression of tau and PP1 constructs. (B) Quantification of tau signal in the elution sample did not show a significant different in signal when tau is pseudophosphorylated at AT8 compared to WT (p = 0.1266, paired t-test). Both WT (*p = 0.0217, paired t-test) and psAT8 (**p = 0.0213, paired t-test) constructs significantly interact with PP1α relative to HT only controls. These experiments were repeated five independent times. (C) HEK 293T cells expressing each tau construct (tagged with NLuc) and PP1α (tagged with HT) or HT only controls were used in the NanoBRET assay. Significant differences in BRET signal were obtained with WT (**p = 0.0035, paired t-test) and psAT8 tau (***p = 0.0004, paired t-test) compared to the respective HT controls. Note quantitative comparisons between different tau proteins are not appropriate for the NanoBRET assay. All comparisons were done using a paired t-test. These experiments were repeated four independent times.

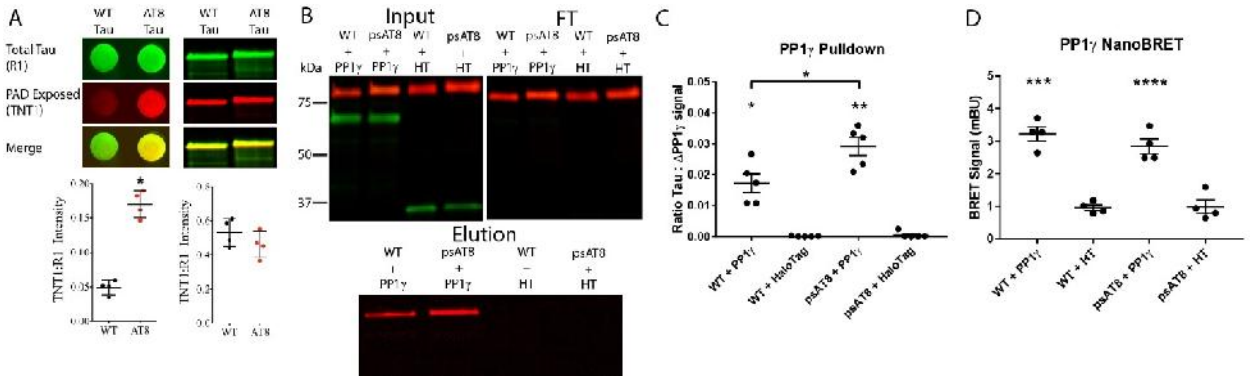

Figure 3.7 psAT8 Exposes PAD and Increases the Interaction with PP1¥. (A) Recombinant human tau (WT tau) and psAT8 tau proteins were blotted using non-denaturing dot blots and denaturing Western blots for TNT1 (a marker of PAD exposure in non-denaturing assays) and R1 (a pan-tau rabbit polyclonal antibody). Quantitation of blots indicate a significant increase in PAD exposure, as indicated by TNT1 reactivity, with psAT8 tau compared to WT tau (*p≤0.05, unpaired t-test,). Data represent mean of normalized signal (TNT1 to R1 ratio) ±SD from four independent samples. A lack of significant differences in the denaturing Western blot confirms that the TNT1 signal in the dot blots were due to conformational differences in the display of PAD. (B) HEK 293T cells expressing each tau construct (tagged with NLuc) and PP1γ (tagged with HaloTag (HT)) or HT only controls were used in pulldown assays. Western blots of starting lysate (Input) show similar expression of tau and PP1 constructs. (C) Quantification of tau signal in the elution sample shows significantly increased signal when tau is pseudophosphorylated at AT8 compared to WT (*p = 0.0141). Both WT (*p = 0.0141) and psAT8 (**p = 0.0048) constructs significantly interact with PP1γ relative to HT only controls. These experiments were repeated five independent times and data are mean ±SD (repeated measures one-way ANOVA with Holm-Sidak *post hoc* test used for comparisons). (D) HEK 293T cells expressing each tau domain (tagged with NLuc) and PP1γ (tagged with HT) or HT only controls were used in the NanoBRET assay. Significant differences in BRET signal were obtained with WT (***p = 0.0006) and psAT8 tau (****p < 0.0001) compared to the respective HT controls. Note quantitative comparisons between different tau proteins are not appropriate for the NanoBRET assay. All

Figure 3.7 (cont'd)

comparisons were done using a paired t-test. These experiments were repeated four independent times.

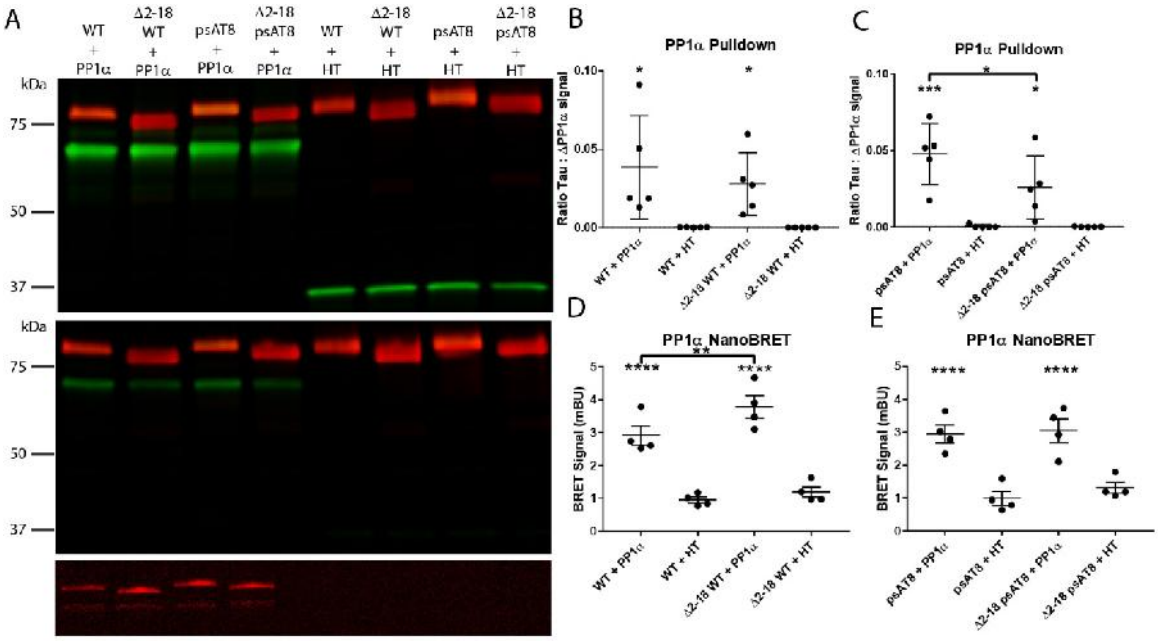

Figure 3.8 Removing the PAD decreases the interaction between psAT8 tau and PP1α. (A) HEK 293T cells expressing WT tau or psAT8 tau (tagged with NLuc) and PP1α (tagged with HaloTag) or HT only controls were used in pulldown assays. Western blots of starting lysate (Input, top blot) show similar expression of tau and PP1α constructs. (B) Quantification of WT tau signal in the elution samples showed no difference when PAD was deleted from WT tau (p = 0.5545). These experiments were repeated five independent times. (C) Deletion of PAD in psAT8 showed a significant decrease in the interaction with PP1α when compared to the full-length psAT8 tau protein (*p = 0.0262). (D) HEK 293T cells expressing each tau construct (tagged with NLuc) and PP1α (tagged with HT) or HT only controls were used in the NanoBRET assay. Significant differences in BRET signal were obtained with WT tau (****p < 0.0001) and Δ2-18 WT tau (****p < 0.0001) compared to the respective HT controls. Note quantitative comparisons between different tau proteins are not appropriate for the NanoBRET assay. (E) Significant differences in BRET signal were obtained with psAT8 (****p < 0.0001) and Δ2-18 psAT8 tau (****p < 0.0001) compared to the respective HT controls. All comparisons were done using a paired t-test. These experiments were repeated four independent times.

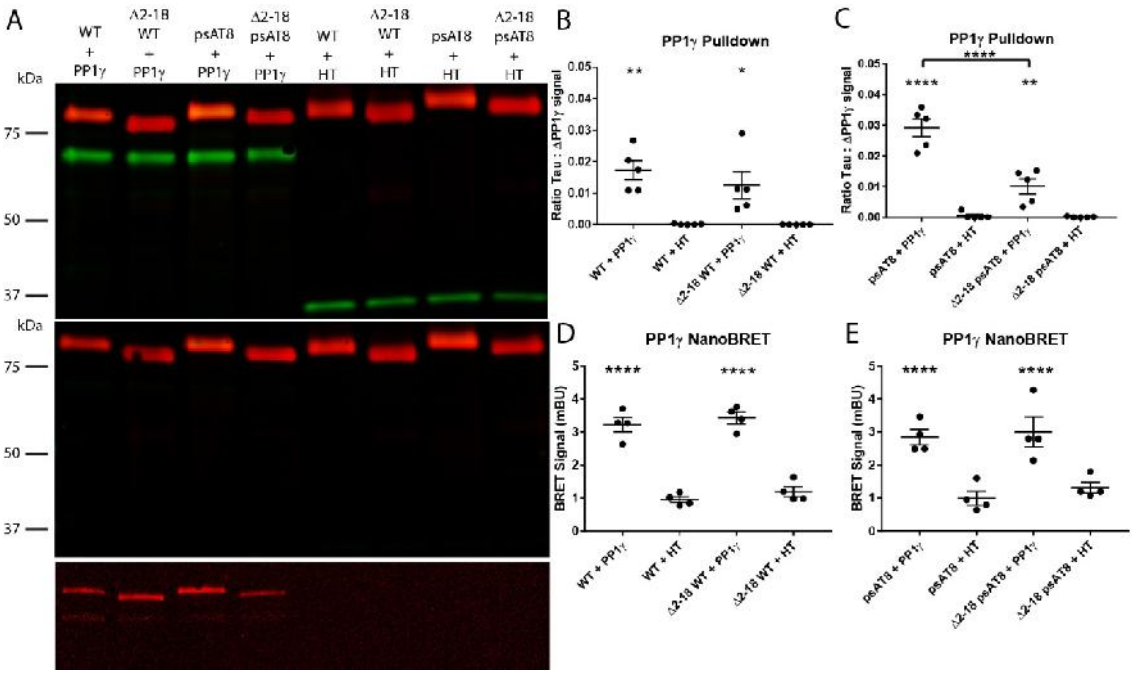

Figure 3.9 Removing the PAD decreases interaction between psAT8 tau and PP1γ. (A) HEK 293T cells expressing WT or psAT8 tau (tagged with NLuc) and PP1γ (tagged with HaloTag) or HT only controls were used in pulldown assays. Western blots of starting lysate (Input, top blot) show similar expression of tau and PP1γ constructs. (B) Quantification of pulldown elution samples indicate that both WT (***p* = 0.0017) and Δ2-18 WT tau (**p* = 0.0130) showed a significantly increased interaction with PP1γ when compared to their respective HaloTag only controls. Deletion of PAD from WT tau (Δ2-18 WT Tau) did not significantly affect the interaction with PP1γ (*p* = 0.3481). (C) Quantification of pulldown elution samples indicate that both psAT8 (*****p* < 0.0001) and Δ2-18 WT tau (*p* = 0.0042) showed a significantly increased interaction with PP1γ when compared to their respective HaloTag only controls. Deletion of PAD in psAT8 tau (Δ2-18 AT8) significantly decreased the interaction with PP1γ (*****p* < 0.0001). These experiments were repeated five independent times and data are mean ± SD compared using the repeated measures one-way ANOVA with Holm-Sidak *post hoc* test used for comparisons. (D) HEK 293T cells expressing each tau construct (tagged with NLuc) and PP1γ (tagged with HT) or HT only controls were used in the NanoBRET assay. Significant

Figure 3.9 (cont'd)

differences in BRET signals were obtained with WT (****$p < 0.0001$) and Δ2-18 WT tau (****$p < 0.0001$) compared to the respective HT controls (F) Significant differences in BRET signal were obtained with psAT8 (****$p < 0.0001$) and Δ2-18 psAT8 tau (****$p < 0.0001$) compared to the respective HT controls. Note quantitative comparisons between different tau proteins are not appropriate for the NanoBRET assay. All comparisons were done using a paired t-test. These experiments were repeated four independent times.

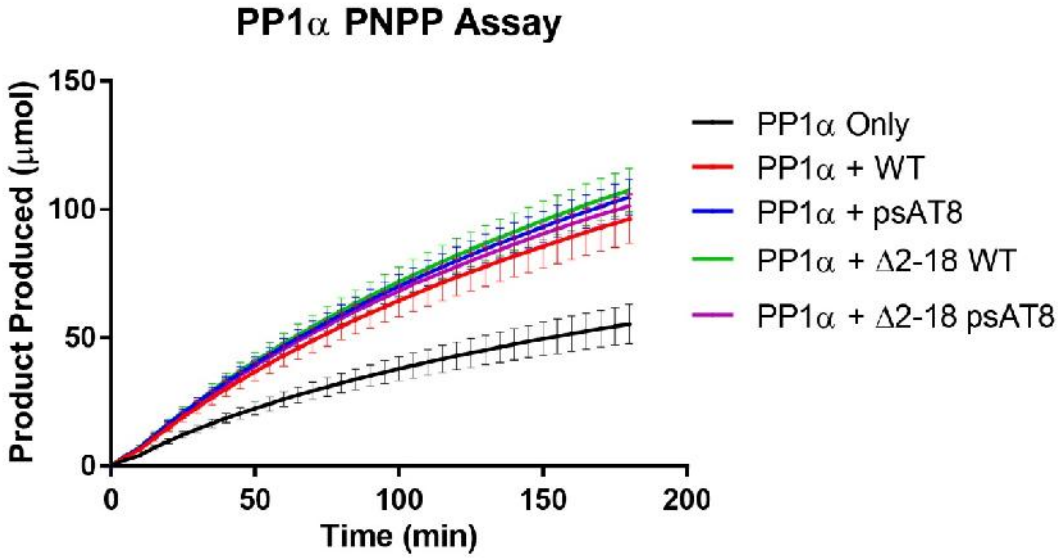

Figure 3.10 Tau increases PP1α phosphatase activity in the PNPP assay. WT and psAT8 tau significantly increased PP1γ phosphatase activity relative to the PP1α alone. Deleting the PAD region from WT tau did not significantly change PP1α activity relative to full-length WT tau. Deleting the PAD region from psAT8 did not significantly change PP1γ phosphatase activity relative to full-length psAT8. The calculated V_{max} and $t_{1/2}$ values for each PP1α and PP1γ condition are displayed in Table 3.3.

Table 3.3 PP1α activity kinetics with different tau constructs.

PP1 Isoform	Tau Protein	V_{max} (Mean ± SD)	$t_{1/2}$ (Mean ± SD)
PP1α	No Tau	129.8 ± 52.3	233.7 ± 46.8
	WT Tau	259.3 ± 52.0****	303.7 ± 14.2*
	psAT8	285.4 ± 34.7****	309.4 ± 7.4*
	Δ2-18 WT Tau	295.6 ± 39.9****	314.8 ± 18.6
	Δ2-18 psAT8	272.7 ± 26.9****	303.8 ± 47.1

Data were fit using Michaelis-Menten nonlinear curve to obtain the predicted maximum product (V_{max}) and reaction rate ($t_{½}$). Mean values represent data from four independent experiments ± standard deviations (SD). *$p < 0.05$ compared to No Tau. ****$p < 0.0001$ compared to No Tau. One-way ANOVA with Holm-Sidak *post hoc* test.

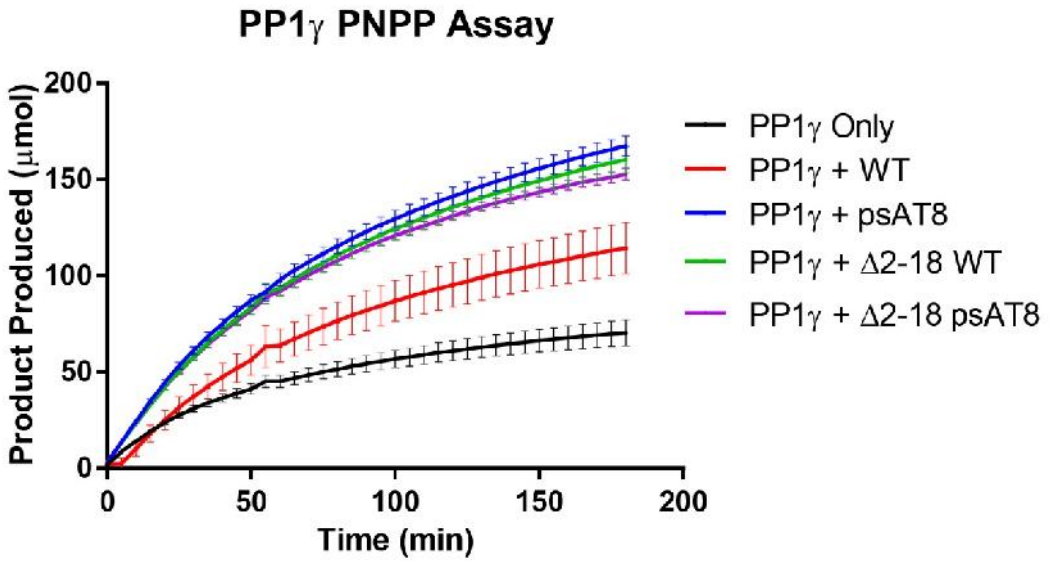

Figure 3.11 Tau increases PP1γ phosphatase activity in the PNPP assay. WT tau significantly increased PP1γ phosphatase activity relative to PP1γ by itself, and psAT8 further increased PP1γ activity relative to WT tau. Deleting the PAD region from WT tau significantly increased phosphatase activity relative to full-length WT tau. Deleting the PAD region from psAT8 tau did not change PP1γ phosphatase activity relative to full-length psAT8 protein. The calculated enzyme kinetic measurements (i.e. V_{max} and $t_{1/2}$) for PP1γ alone and with each tau protein are displayed in Table 3.4. Data represent mean ± SD from four independent experiments.

Table 3.4 PP1γ activity kinetics with different tau constructs.

PP1 Isoform	Tau Protein	V_{max} (Mean ± SD)	$t_{1/2}$ (Mean ± SD)
PP1γ	No Tau	94.3 ± 23.4	63 ± 13.11
	WT Tau	196.3 ± 30.01$^{\#}$	131.1 ± 22.52$^{\#}$
	AT8	256.4 ± 15.54$^{\#,*}$	97.1 ± 0.835$^{\#*}$
	Δ2-18 WT Tau	247.0 ± 21.01$^{\#,*}$	98.3 ± 2.727$^{\#*}$
	Δ2-18 AT8	229.6 ± 13.02$^{\#}$	90.3 ± 10.7$^{\#*}$

Data were fit to the Michaelis-Menten nonlinear curve to obtain the predicted maximum product (V_{max}) and reaction rate ($t_{½}$). Mean values represent data from four independent experiments ± standard deviations (SD). $^{\#}p \leq 0.05$ compared to No Tau. *p ≤ 0.05 compared to WT tau in one-way ANOVA with Holm-Sidak *post hoc* test.

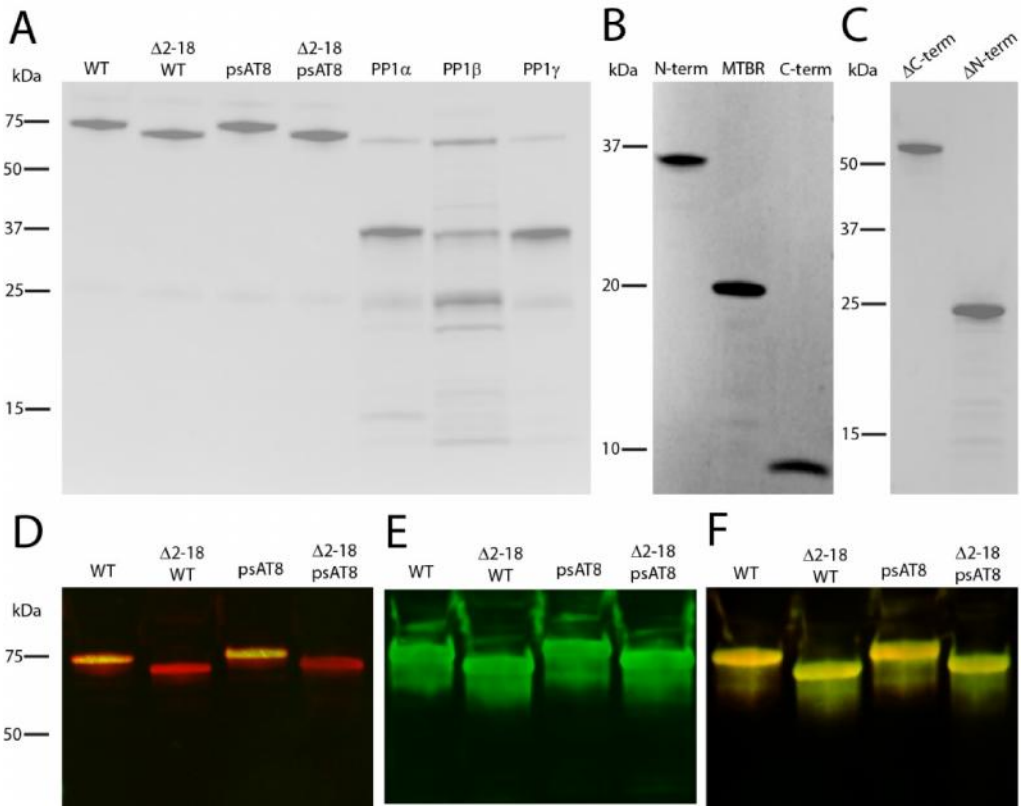

Figure 3.12 Characterization of recombinant proteins. (A) Recombinant tau and PP1 proteins were separated by SDS-PAGE and stained with Coomassie Brilliant Blue. Note the consistent loading of tau proteins and reduction in molecular weight of the Δ2-18 proteins. The catalytic subunit of PP1 is ~37 kDa. Other bands present are likely breakdown products (more are typically produced by N-terminal His-tagged recombinant proteins) and may include some co-purified scaffolding partners present in bacteria during expression. (B) Tau domain constructs separated by SDS-PAGE and stained with Coomassie. Note the molecular weights reflect the size of each domain construct. (C) Tau terminus domains separated by SDS-PAGE and visualized with Coomassie indicate the correct molecular weight for each protein. (D) Western blot of recombinant tau proteins probed with R1 (red) and TNT1 (green). PAD was successfully deleted from the Δ2-18 constructs due to the lack of TNT1 reactivity. (E and F) Western blot of recombinant tau proteins probed with Tau7 (E, green; an antibody against the extreme C-terminus of tau) or probed with R1 (F, red; a pan-tau polyclonal with epitopes

Figure 3.12 (cont'd)

throughout the protein) and Tau5 (F, green; a mid-region tau antibody) confirm proteins contain the correct amino acid sequence and are intact.

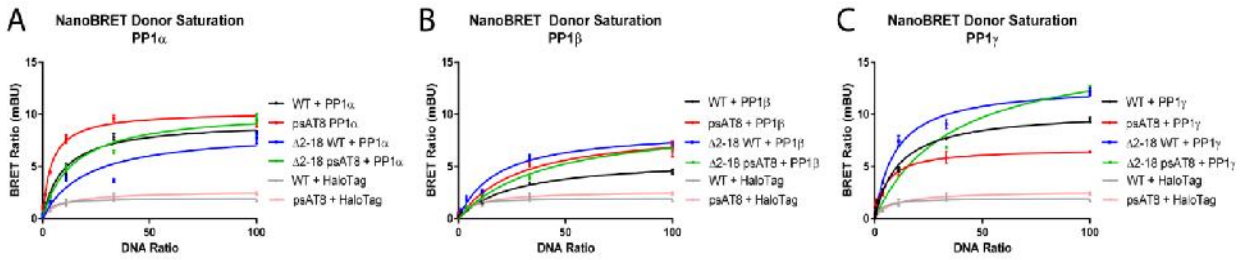

Figure 3.13 NanoBRET donor saturation assays with PP1α, PP1β, and PP1y. The hyperbolic curves with PP1α (A), β (B) and γ (C) indicate detection of a specific protein-protein interaction between tau and the PP1 isoforms. It is noteworthy that the curve is more linear with PP1β, which reflects much lower interaction of tau with this isoform. The more linear curves of the respective HaloTag only controls are indicative of a non-specific interaction.

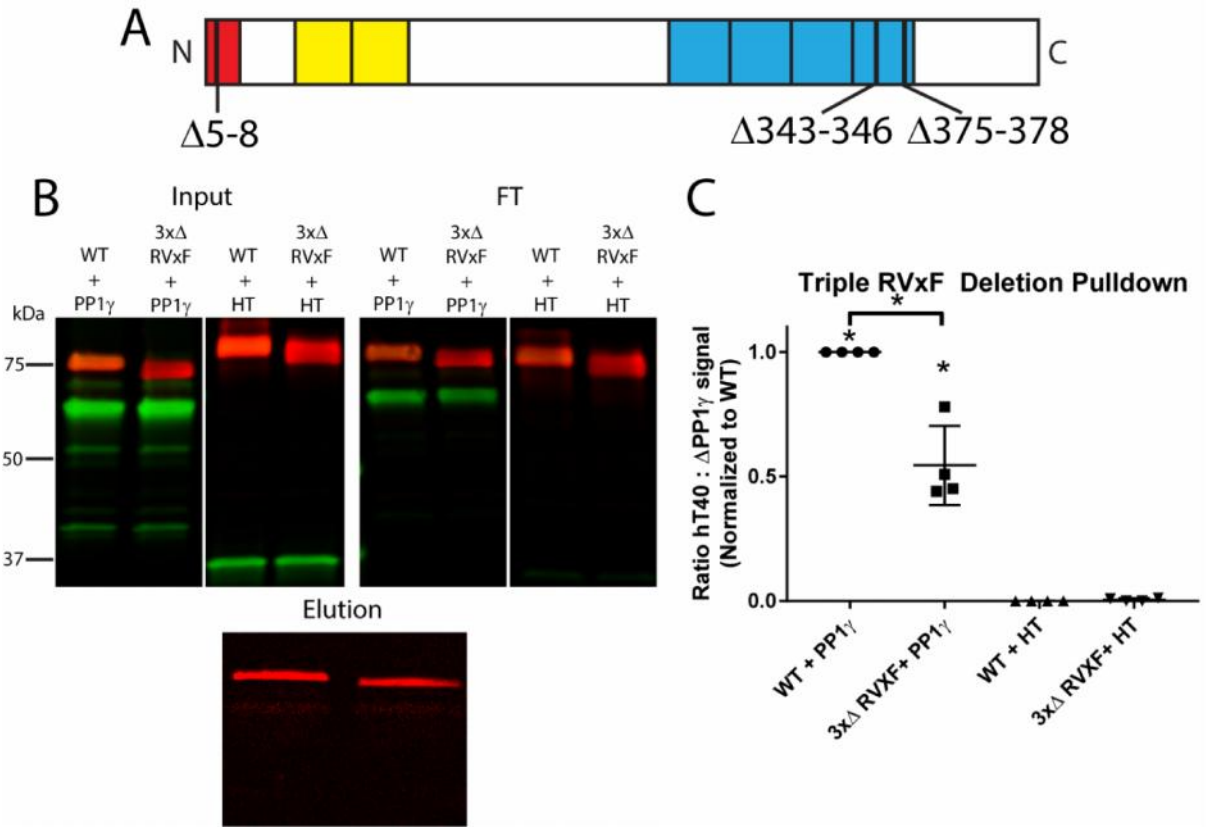

Figure 3.14 Deletion of the three RVxF motifs (3xΔ RVxF) in tau reduces the interaction with PP1¥. (A) Schematic of the 3xΔ RVxF tau protein showing deletion of the three RVxF motifs at amino acids 5-8, 343-346, and 375-378. (B). HEK 293T cells expressing WT tau or 3xΔ RVxF tau (tagged with NLuc) and PP1γ (tagged with HaloTag (HT)) or HT only controls were used in pulldown assays. Western blots of input samples (Input), flow-through samples (FT), and elution samples (bottom blot) are shown with PP1 or HT in green and tau domains in red. (C) Quantification of tau signal in the elution sample shows significantly reduced signal with the 3xΔ RVxF domain (*$p \leq 0.05$) compared to WT tau, and both WT and 3xΔ RVxF are significantly greater than their respective HT only controls (symbol $p \leq 0.05$. All comparisons were done using a paired t-test. This experiment was repeated four independent times.

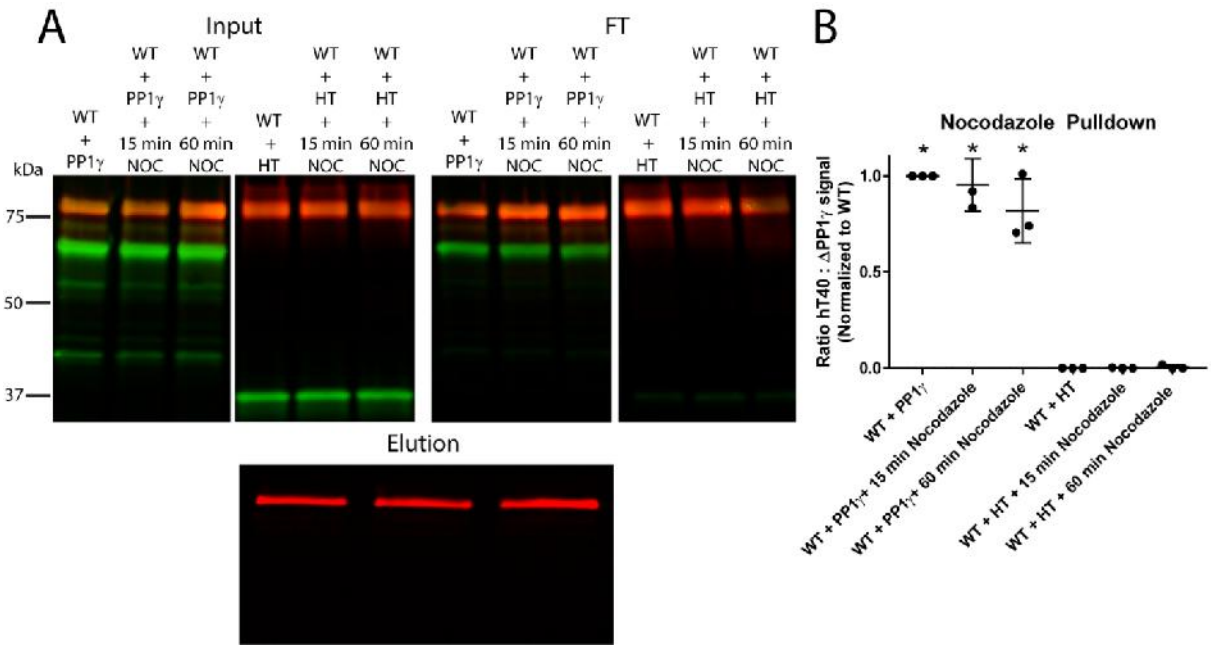

Figure 3.15 Nocodazole treatment of HEK 293 cells to disrupt microtubules did not significant affect interaction between WT tau and PP1y. (A). HEK 293T cells expressing WT tau (tagged with NLuc) and PP1γ (tagged with HaloTag (HT)) or HT only controls were exposed to nocodazole for either 15 minutes (to disrupt labile domains of microtubules) or 60 minutes (to disrupt more stable domains of microtubules) and then used in pulldown assays. Western blots of input samples (Input), flow-through samples (FT), and elution samples (bottom blot) are shown with PP1 or HT in green and tau domains in red. (B) Quantification of tau signal in the elution sample shows no significant difference in pulldown signal with either nocodazole treatment ($p > 0.05$) compared to WT tau, and as expected all tau containing samples were significantly different from their respective HT only controls ($*p \leq 0.05$). All comparisons were done using a one-way ANOVA with Holm-Sidak *post hoc* test. This experiment was repeated three independent times.

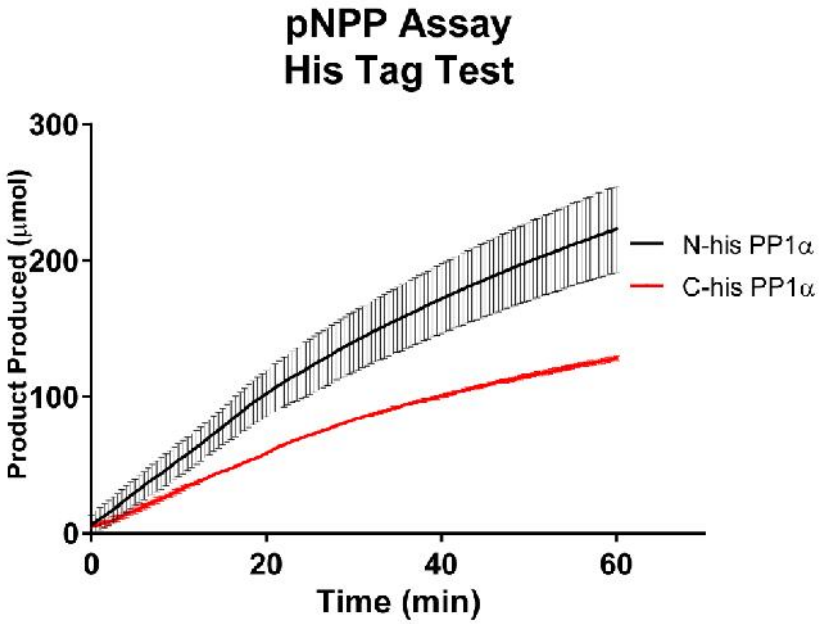

Figure 3.16 PP1α protein possessing a histidine tag on the N-terminus is more active than when the tag is present on the C-terminus. The His-tag located on the N-terminus resulted in about a doubling of activity in the PNPP assay. Data represent mean ± SD from two independent experiments.

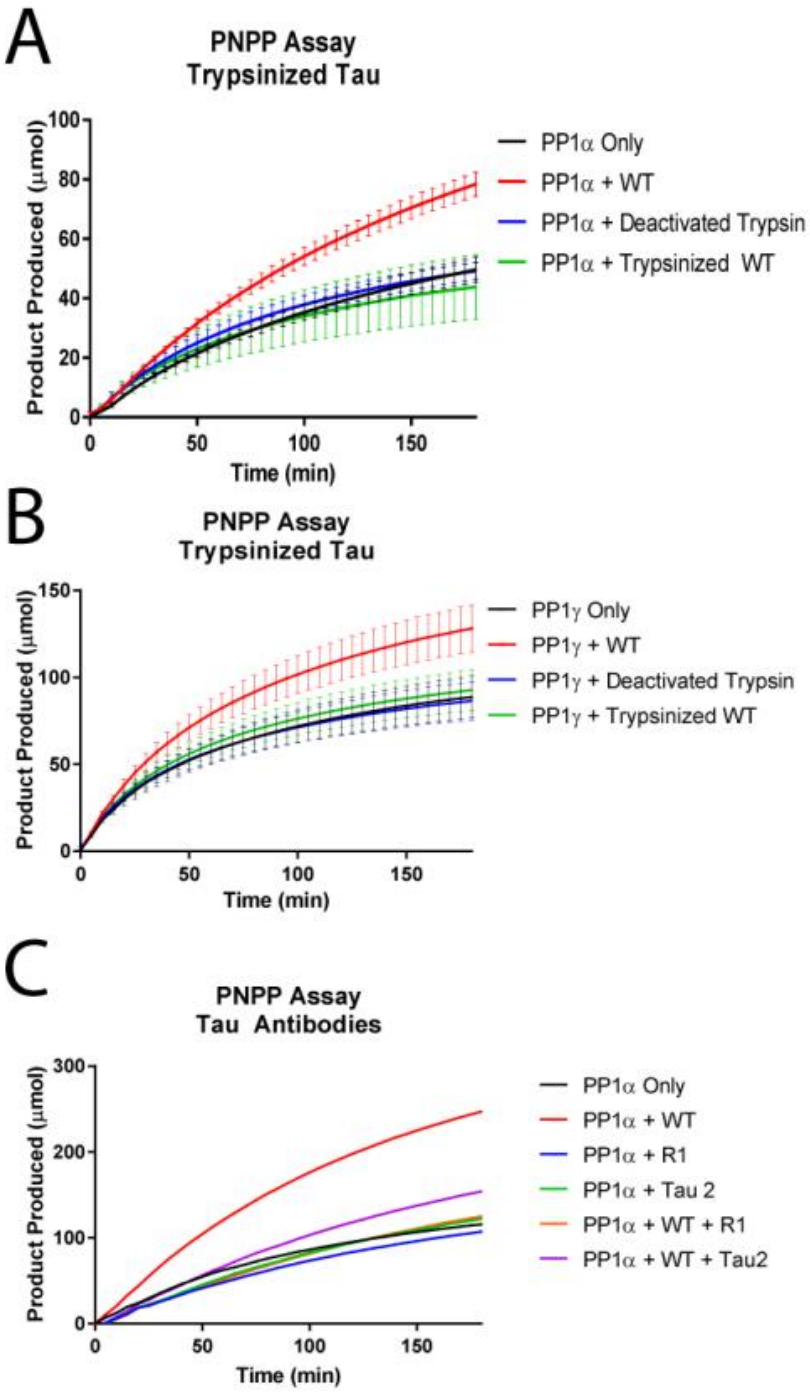

Figure 3.17 Digestion of tau with trypsin or incubation with tau antibodies prevents activation of PP1. (A) WT tau significantly increased PP1α phosphatase activity relative to PP1α alone. Digesting WT tau with trypsin, then deactivating trypsin at high temperatures prior to addition to PP1α prevented this increase in activity. (B) WT tau significantly increased PP1γ

Figure 3.17 (cont'd)

phosphatase activity relative to PP1γ alone. Digesting WT tau with trypsin, then deactivating trypsin at high temperatures prior to addition to PP1γ prevented this increase in activity. These data indicate that the protein within our recombinant tau preps are specifically responsible for the increase in phosphatase activity. Data represent mean ± SD from four independent experiments. (C) WT tau significantly increased PP1α phosphatase activity relative to PP1α by itself. Pre-incubating WT tau with R1 (a polyclonal tau antibody with epitopes throughout the protein) or Tau2 (a tau antibody with an epitope at amino acids 104-121) prevented an increase in PP1α activity. Additionally, the antibodies by themselves did not increase PP1α activity, indicating the increase in PP1 phosphatase activity in the presence of WT tau is specifically a result of tau and that addition of any protein in these assays does not increase PP1 activity. Data represent the mean from one run.

CHAPTER 4

Overall Discussion

Discussion

The overall goal of this dissertation was to address two critical gaps in our knowledge using two approaches including post-mortem human tissue samples to identify key aspects of early tau deposition and reductionistic *in vitro* protein biochemical studies to elucidate the details of a potential molecular mechanism of tau toxicity. First, a long-held hypothesis on the progressive deposition of tau pathology in AD is that pathological tau accumulates first in axons of neurons and then progresses back into the cell bodies to form neurofibrillary tangles, however, studies have not directly analyzed this relationship in human tissue. Here, we provide evidence that strongly supports this scheme of progressive tau deposition within discrete intrahippocampal pathways in human tissue. Second, prior work identified a novel mechanism of tau toxicity where pathogenic forms of tau aberrantly activate a signaling pathway that was PP1-dependent and led to disruption of axonal function, however, the connection between tau and PP1 was not well defined in previous studies. Additionally, we still do not understand the precise mechanisms that pathological forms of tau engage to cause neuronal dysfunction and degeneration in disease. Here, we described findings that implicate a relatively novel, specific molecular mechanism that pathological tau uses to impair axonal function, i.e. the tau-PP1 pathway.

The focus on tau's role in AD pathogenesis has expanded significantly over the past decade leading to important findings expanding our knowledgebase and understanding of tau. However, much remains to be discovered regarding the role of tau in AD and other tauopathies. Our work challenges the entrenched dogma that tau primarily functions to simply stabilize microtubules. Instead, we provide a number of findings related to the mechanism above (tau-PP1 pathway) that suggest tau's functional repertoire includes regulation of signaling pathways. Collectively, the work presented in this dissertation adds a great deal of key information to the

field and deepens our understanding of tau's role in AD pathogenesis. Below, I will discuss each of these key issues and the data we provide to address them in greater detail.

Due to the inability of current treatments and therapies to modify AD progression, and at best only mildly alleviate symptoms, investigating potential early pathological mechanisms adds critical value and knowledge in combating this disease. In this dissertation, I investigated one such previously proposed mechanism of neuronal dysfunction where loss of synapses, axonal dystrophy, and subsequent degeneration of neurons observed in AD may result from impaired anterograde axon transport of cargoes to the terminus. In the current model, dysfunction in axon transport is caused by phosphorylation of kinesin light chains (a component of the anterograde transport motor protein complex) by GSK3β. Kinesin light chains bind cargoes to be transported toward the positive ends of microtubules, and phosphorylation of the light chain dissociates the cargo from the motor protein, therefore preventing sufficient transport of materials to their destinations. GSK3β, known to phosphorylate kinesin, is regulated via phosphorylation at serine 9; dephosphorylation at serine 9 activates GSK3β. In AD brains, GSK3β activity increases, implying increased activity of serine/threonine phosphatases that act upon GSK3β. PP1 dephosphorylates GSK3β, therefore increased PP1 activation may contribute to this imbalance of active GSK3β. Additionally, the extreme N-terminus of tau is necessary and sufficient to inhibit anterograde axon transport through a PP1-dependent pathway and was thus termed the PAD.

AT8 Phosphorylation and PAD Exposure in the Human Hippocampus

AT8 phosphorylation of tau is an early and prominent immunohistological event in the hippocampal formation (i.e.the EC and perforant pathway) in human cases without cognitive impairments or a neurological disease (Braak *et al.* 1994). We expand on these findings by showing that this observation extends beyond the EC into the hippocampus, and that severity of AT8-positive tau deposition occurs prior to clinical presentation with mild cognitive decline.

Additionally, PAD exposed tau, as visualized with the TNT2 antibody, is observed throughout the hippocampus, albeit in lower abundance compared to AT8 tau. Taken together, this supports the hypothesis that tau pathology and subsequent deposition as neuropil threads and NFTs occurs early before symptom onset. However, the results presented here are the first to systematically evaluate whether tau pathology occurs in axon enriched strata of the hippocampal formation before the corresponding cell bodies.

We chose the mossy fiber and Schaffer collateral pathways as our sites of analyses due to the extensive pathology already observed in both neuronal compartments of other pathways (e.g. the perforant path), preventing any conclusions to be made of the timing of tau pathology. With both the AT8 and TNT2 markers, we found axonal tau pathology occurred without any corresponding somatodendritic pathology, as well as a strong positive correlation between pathology in the axon and pathology in the cell bodies. This supports the hypothesis that tau pathology occurs first in the axonal compartment. Additionally, these observations provide evidence for the feasibility of the proposed PP1/GSK3β signaling cascade as a cause of axon transport deficits and axon degeneration because the upstream triggers, AT8 phosphorylation and PAD exposure, occur in axons within regions that atrophy in AD before cognitive impairments (Nestor *et al.* 2004, Kanaan *et al.* 2011).

We observed no significant differences or correlations between the pathological tau markers and clinical exam scores, including MMSE, CERAD, and diagnosis, suggesting these differences occur after the presence of pathological tau. These results fit with previous findings suggesting NFTs contribute to neuron loss and cognitive decline, especially in CA1 (Giannakopoulos *et al.* 2003). Most of the pathology observed in our cases appeared in the form of neuropil threads in the absence of NFTs, further supporting the early nature of these pathological tau modifications. Additionally, the finding that AT8 phosphorylation and PAD-exposed tau are observed in neuropil threads before NFTs aligns with previous findings

describing maturation of NFTs in AD (Binder *et al.* 2005, Guillozet-Bongaarts *et al.* 2005, Mondragon-Rodriguez *et al.* 2008).

Tau phosphorylation precedes NFT formation, which may rely on a conformational change of tau to facilitate the formation of stable aggregated species. Also, different combinations of phosphorylation events can change tau's conformations in different ways. For example, AT8 phosphorylation results in the dissociation of the N-terminus of tau from the paperclip conformation; however, the combination of AT8 phosphorylation and PHF1 phosphorylation at the same time results in a tighter compaction of the paperclip (Guillozet-Bongaarts *et al.* 2005, Jeganathan *et al.* 2008).

The general absence of Aβ pathologies is not surprising, given that amyloid staging was shown to begin in neocortical areas (Thal *et al.* 2002). In our cohort of human tissue, we show extensive AT8- and TNT2-positive tau pathology without any observable Aβ plaques in most of cases, which ranged from Braak stage I-III (Braak *et al.* 1994). These findings do not support the amyloid hypothesis of AD which states that Aβ accumulation and plaque formation triggers tau pathology and subsequent formation of NFTs (Hardy *et al.* 1992, Selkoe 2000). One limitation to our experimental design is we did not evaluate circulating Aβ as the potential force behind the formation of tau pathology. However, the presence of robust Aβ pathology early and throughout the progression of disease in neocortical areas and clear lack of pathological tau deposition in these areas early in disease argues against other conceivable mechanisms of Aβ-induced tau pathology formation (e.g. activation of immune responses, circulating Aβ, etc). This is particularly true since cortical neurons are susceptible to pathological tau deposition as is seen later in AD and as the primary location of tau pathology in a number of non-AD tauopathies. Nonetheless, future studies specifically aimed at examining whether alternative Aβ-dependent mechanisms are driving tau pathology are warranted.

Indeed, Aβ activates several kinases that can phosphorylate tau, and sites phosphorylated by these kinases can result in increased PAD exposure and potentially lead to activation of the PP1-GSK3β cascade (Kanaan *et al.* 2013). Additionally, several animal models used in investigating Aβ toxicity require the presence of tau (Roberson *et al.* 2007). Investigating soluble and circulating Aβ species and the extent of AT8- and TNT2-positive tau pathology in humans before cognitive decline, ideally with imaging studies is still living patients, will address these limitations and concerns. Collectively, the available data appears to suggest that instead of Aβ causing tau pathology, AD may result from these pathologies developing independently in the prodromal and early clinical stages and only later in disease do they ultimately converge and potentially interact to exacerbate dysfunction and degeneration.

Tau-PP1 Interactions and Effects on Phosphatase Activity

The tau field has faced difficulty to identify a specific molecular mechanism or sets of molecular mechanisms that tau directly engages to cause cell dysfunction and toxicity. Several proposed models of toxicity are suggested and include a loss-of-function mechanism of tau where microtubules become destabilized, resulting in axon dysfunction (Lee *et al.* 2011) Moreover, the functional or dysfunctional implications of post-translational modifications of tau were not well-defined, leaving the field in a state where great tools existed to track pathological modifications of tau, but with no clear definition of what those PTMs did to tau to cause tau-mediated toxicity. Historically, the primary dogma on tau-based mechanisms of disease was PTMs of tau, including phosphorylation, caused tau to dissociate from microtubules resulting in two potentially pathological events: microtubule destabilization and an increase in free tau that could self-associate into aggregates (Alonso *et al.* 1996).

A turning point came approximately a decade ago when a specific molecular mechanism of tau toxicity was identified. Utilizing the squid axoplasm model of axon transport, infusion of a physiologically relevant concentration of tau aggregates inhibit fast anterograde axonal

transport, whereas tau monomers did not (LaPointe *et al.* 2009). Subsequent follow-up studies found that psAT8 tau also inhibited axonal transport similar to the tau aggregates (Kanaan *et al.* 2011). Importantly, a link between these pathological tau modifications and axon transport deficits arose with the discovery that amino acids 2-18 of tau alone was necessary and sufficient to recapitulate the observed reduction in axonal transport. Additionally, inhibiting PP1 or GSK3β preventing this transport deficit (LaPointe *et al.* 2009, Kanaan *et al.* 2011). Thus, amino acids 2-18 were termed the phosphatase activating domain (PAD) and was proposed to initiate the PP1-GSK3β signaling cascade thought to be responsible for this reduction in transport (Kanaan *et al.* 2011, Kanaan *et al.* 2012). Collectively, this work provided a definable, discrete and direct pathway by which pathological forms of tau could actively cause cell dysfunction and toxicity.

Previous studies defined a PP1-GSK3-kinesin light chain-cargo dissociation pathway (Morfini *et al.* 2002, Morfini *et al.* 2004, Morfini *et al.* 2009), and findings with tau-induced toxicity implicated PP1 in this pathway because PP1-specific inhibitors prevented tau-mediated transport impairments (LaPointe *et al.* 2009, Kanaan *et al.* 2011). Despite these advances, questions of how tau engaged PP1 were not fully addressed in prior studies. This gap in our knowledge led to the work described in this dissertation and was specifically investigated in chapter 3. A single previous study showed that tau interacts with PP1 when isolating microtubules from brain can target PP1 to microtubules (Liao *et al.* 1998). Our results expand on this finding by establishing which PP1 isoforms interact with tau, which domain of tau is required for this interaction, how AT8 phosphorylation and PAD modulate this interaction, and the subsequent effect on PP1 phosphatase activity.

First, we show that tau directly interacts with PP1α and γ, but the interaction with PP1β was much lower or not detectable through affinity pulldown assays and intracellular BRET assays. Importantly, tau and PP1 associate in rat primary hippocampal neurons as shown through the proximity ligation assay, demonstrating these interactions likely occur under physiological conditions in neurons. This difference in interaction with PP1 isoform may relate to

the enrichment of PP1α and γ1 in dendritic spines and presynaptic terminals, and their proposed role in post-synaptic signaling or synapse maintenance, whereas PP1β is enriched in the cell body (Ouimet *et al.* 1995, Strack *et al.* 1999).

Previous results suggested that the functional deficits in transport caused by tau required PP1 activation and were dependent on PAD. Our results suggest the region of tau with the strongest impact on the physical interaction between tau and PP1, as indicated by pulldown or BRET assays, is the MTBR. However, PAD did not significantly modulate PP1 activity as expected in the *in vitro* pNPP assays used here. It is reasonable to propose that PAD may act as a modulator of the interaction and/or activation of PP1 downstream of initially forming a relatively stable interaction with PP1 that is driven by the MTBRs. Moreover, fundamental differences between the *in vitro* biochemical PP1 activity assays used here and functional assay in the squid axoplasm using endogenous PP1 may account for the disconnection in these findings related to the role of PAD in PP1 activation. For example, we did not rule out the possibility of tau and PP1 interacting in a complex with other proteins, and this may occur in the squid axoplasm but not the *in vitro* biochemical assays. Nonetheless, our data implicate a strong role for the MTBRs in binding PP1.

The important role of the MTBR in PP1 binding has implications that fit with the observed effects of pathological tau modifications on PP1 binding. Specifically, soluble tau proteins can normally adopt a folded paperclip conformation where the termini interact with the MTBRs, but upon phosphorylated at the AT8 epitope, the N-terminus is extended potentially making the MTBRs more available for PP1 binding. After PP1 binds to the MTBRs, the N-terminus interacts with PP1 through one of the binding groves or other PP1 surface motifs to help anchor the proteins together. This proposed model is supported by our results showing an increased interaction between PP1γ and psAT8 tau, and that the interaction between PP1γ and psAT8 is decreased when PAD is removed.

Next, we show that tau activates PP1 phosphatase activity, and that AT8 phosphorylation further increases activity. PP1 interacting proteins are essential for directing PP1 localization and substrate specificity (Bollen *et al.* 2010). Since we show an increased interaction between AT8 tau and PP1γ, the increase in activity fits with the function of PP1 interacting partners. If AT8 phosphorylation results in a more stable interaction with PP1, then an extended increase in phosphatase activity could subsequently activate more GSK3β and exacerbate our pathological signaling cascade. Interestingly, PAD deletion, which was shown to decrease the interaction between PP1γ and AT8 tau, did not decrease PP1γ activity relative to full length AT8 tau. If PAD causes a more stable interaction, it is surprising the removal of PAD did not decrease activity. However, if the result of PAD deletion is a more transient interaction, the rate of PAD-deleted tau binding and unbinding with PP1 due to a loss of a potential stabilizing binding motif may be quick enough to not lose any effect on activity, as it may possibly establish an equilibrium with other nearby tau molecules ready to bind PP1. Taken together, our results support the hypothesis that the tau-PP1-GSK3β signaling cascade is a realistic possibility in the progression of AD pathology and provides further evidence that tau can act as a regulator of PP1 signaling instead of simply binding to PP1 solely as a substrate.

Proposed Mechanism of Tau-Induced Degeneration

Taken together, our results align with and support the previous findings and hypotheses that pathological forms of tau first appear in axons and that these forms of tau promote neuronal dysfunction by a PP1-dependent mechanism. By coupling our data with those previously published, I propose a mechanism of tau-mediated toxicity that occurs following specific pathological modifications that begin in the axons and impair axonal functions (Figure 4.1). It was previously unknown whether AT8 phosphorylation affected tau-PP1 interactions and PP1 activity; I expanded our knowledge on this mechanism by identifying the isoforms of PP1 that interact with tau, the role of the PAD region, effects on phosphatase activity, and linked these

modifications to human cases. Additionally, this interaction does indeed result in an increase in PP1 phosphatase activity as shown in the PNPP assay. These novel results provide the first evidence of tau interacting with PP1 in an isoform specific manner, providing numerous possibilities to investigate specific amino acid differences across the isoforms, the location of tau binding to the surface of PP1, and the development of specific competitive inhibitors to prevent this potential pathological mechanism.

AT8 phosphorylation opens the paperclip conformation of tau by the extending the N-terminus and increases the exposure of the MTBRs. The increased availability of the MTBRs allows for a more unobstructed interaction with PP1, resulting in activation of PP1 phosphatase activity and localization to axonal microtubules. Here, active PP1 dephosphorylates GSK3β at serine 9, which subsequently causes GSK3β to phosphorylate kinesin light chains. Interestingly, GSK3β can also phosphorylate tau at the AT8 epitope, possibly inducing a detrimental feed-forward loop mechanism resulting in a large increase of AT8 phosphorylated tau over tau. This phosphorylation causes axon cargoes being transported to dissociate from kinesin motor proteins, starving other compartments of the neuron of necessary cellular components. The synapse becomes dystrophic and degenerates, which causes the axon to degenerate as well. Finally, the neuron degenerates as it no longer has a downstream connection with its target cells. I propose that AT8 phosphorylation and PAD exposure contribute over time to an imbalance in the regulation of kinases and phosphatases in the axonal compartment of neurons, triggering the pathological and neurodegenerative signaling cascade described above. Future studies are required to further support this proposed signaling cascade, and several testable components remain to be investigated. It would be interesting to reduce GSK3 activity with pharmacological approaches such as dimethyl fumarate (DMF) under the conditions tested above in rodent or primary neuron models in an attempt to reduce kinesin light chain phosphorylation as well as prevent the proposed detrimental feed-forward loop of tau phosphorylation proposed above. A recent study investigated whether DMF could reduce P301L

tau-induced neurodegeneration in a mouse model and found DMF reduced GSK3β activity and reduced degradation of the transcription factor NRF2, resulting in reduced kinase activity, tau phosphorylation, and helped correct intraneuronal calcium imbalances (Cuadrado *et al.* 2018). The authors proposed repurposing DMF to treat tauopathies, as it targets multiple pathways (e.g. neuroinflammation and GSK3β signaling). Utilizing DMF in conjunction with our tau and PP1 treatments may provide insight into other contributing physiological factors involved in our proposed model of degeneration.

Future Directions

Here, I used a host of post-mortem human tissue studies, *in vitro* biochemical assays and in-cell (non-neuronal and neuronal) experiments to explore the connections between PP1, AT8 tau, PAD-exposed tau and toxicity. The most critical next step is to translate these findings into *in vivo* model systems such as transgenic mice expressing pathological forms of tau under physiological conditions, such as the rTg4510 or rTgTauEC transgenic models, rather than artificially overexpressing pathological tau proteins far in excess of what normally is produced in cells. Additionally, since PP1γ is normally enriched in synapses and dendritic spines, the discrete subcellular localization of the tau-PP1 complex to axonal microtubules should be analyzed to support the proposed pathological signaling cascade.

Manipulating PP1 is also in important and interesting approach to testing the proposed model of degeneration. The exact nature of which interacting motifs on the surface of PP1 are involved in the interaction with tau is still unknown. Therefore, modifying the PP1 enzyme to prevent binding at the RVxF motif, the three surface grooves, or any other combination of the numerous surface binding sites will provide insight into exactly how tau is influencing PP1 localization and substrate specificity. Additionally, results from that study could provide a potential druggable target, such as a competitive inhibitor or gene therapy approach introducing a dominant negative interactor with PP1 to decrease the interaction between tau and PP1 and

deplete the pool of activated phosphatase enzyme. While it's important to know which forms of tau promote its interaction with PP1, it could be equally important to understand the complex structural biology of PP1 in neurodegeneration.

Another avenue of research to expand on our previous findings that AT8 phosphorylation and PAD exposure are early modifications linked to the proposed PP1-dependent pathway of toxicity is using primary neuron cultures to study the effects of tau on axonal transport and/or other axonal/cellular functions. Additionally, knocking down expression of individual PP1 isoforms with RNA-interference using shRNAs could help to identify whether tau-mediated effects are PP1 dependent and which isoform is responsible. AT8 tau inhibits fast anterograde axonal transport in squid axoplasm through a PP1-dependent mechanism (LaPointe *et al.* 2009, Kanaan *et al.* 2011). Thus, investigating tau's ability to impair axonal transport in a mammalian system is a critical next step. Rodent primary neuron cultures offer a useful system to investigate transport, and neurons can be cultured for weeks and induced to stably express endogenous proteins by introducing plasmids coding for proteins of interest, such as various forms of tau. However, care must be taken to ensure the proper amount of time between protein expression and imaging of transport, reduce toxicity, and ensure the long-term expression of the protein of interest.

If psAT8 expression in rodent primary neurons inhibits axonal transport, this would align with the previous findings that pathological forms of tau inhibit anterograde axonal transport in the squid axoplasm model (Kanaan *et al.* 2011). Interestingly, knocking down PP1γ may rescue any detrimental effect by restoring transport velocity, decreasing the number of pauses, and decreasing pause duration of psAT8 expressing neurons. Results from knocking down PP1γ would provide further evidence supporting our proposed pathological signaling cascade by removing the step that activates GSK3β. The deficit in transport previously observed with AT8 tau could therefore prevent the synapses from receiving vital material from the cell body and becomes dystrophic. The dystrophic synapse and axon degenerates followed by the cell body

and neuron. The rescue in these transport outcomes observed by knocking down PP1γ indicates PP1γ activation is a central event in this cascade, fitting with the previously proposed model (Morfini *et al.* 2009, Kanaan *et al.* 2011, Kanaan *et al.* 2013). Another component of an intraneuronal signaling pathway to investigate in the context of this mechanism is calcium homeostasis. Tau can associate with membranes of the endoplasmic reticulum and mitochondria, each possessing large stores of calcium ions. Disruption of the function of calcium transporters or ion channel receptors can lead to altered activation of calcium-dependent proteins, such as calpain and EFhd2, or reduction in the response of ryanodine receptors, leading to increased protease degradation of proteins and impaired intracellular signaling (Adamec *et al.* 2002, Goussakov *et al.* 2010, Kneynsberg *et al.* 2017). Additionally, the N-terminus of tau was shown to bind synaptic vesicles and reduce their motility, as well as inhibiting vesicles from docking with the presynaptic terminal and reducing neurotransmission in both fly and rat neurons (Zhou *et al.* 2017). These results show that tau could possibly possess numerous functions beyond stabilizing microtubules and intersects with several intracellular pathways to promote pathology.

In conclusion, the current studies provide additional evidence and support for the previously proposed signaling cascade of degeneration by showing the upstream pathological modifications are normally present in humans before cognitive decline, these pathological modifications increase the interaction with tau and PP1α and γ specifically, and results in increased phosphatase activity. These findings provide previously unknown insight into the nuances of tau and PP1 biology. For example, the observation that tau interacts with PP1α and γ, but not β, provides for an interesting avenue of research into the divergent amino acid sequences between PP1 isoforms and how they influence PP1 structure and function. It would be interesting to determine precisely where tau binds with PP1 and develop a small molecule or synthetic peptide to block this interaction by artificially masking PP1α and γ to appear more like the β isoform. While investigating GSK3 activity was beyond the scope of this dissertation, it

remains a critical question in how the increases in phosphatase activity observed can actually dephosphorylate, and subsequently increase the activity of, GSK3 to power the proposed pathological mechanism. Furthermore, analyzing any potential increases in endogenous AT8 phosphorylation in primary neuron cultures or animal models will elucidate whether GSK3 activation results in a feed-forward AT8 phosphorylation loop and imbalance of Tau-PP1 signaling. This furthers our understanding of the etiology of AD and may lead to the developing of new therapies and interventions for treating or preventing the disease, such as using DMF to target GSK3β, correct disruptions in calcium homeostasis, and treat neuroinflammation or small molecular competitive inhibitors targeting the MTBRs of tau to prevent its interaction with PP1.

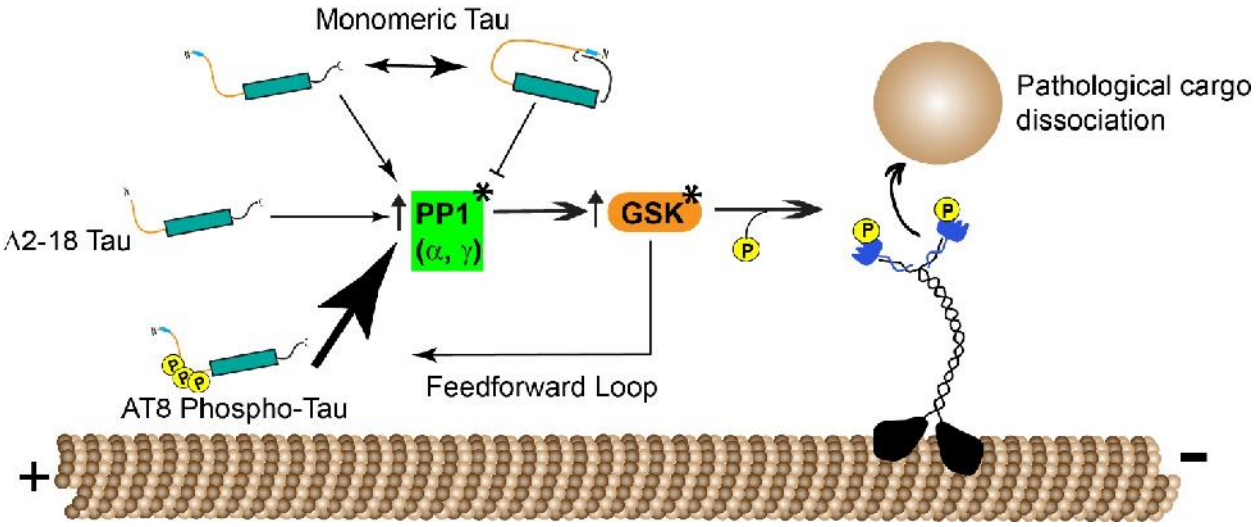

Figure 4.1 Proposed model of AT8 tau phosphorylation and subsequent pathological cargo dissociation through a PP1/GSK signaling cascade. Monomeric WT tau, Δ2-18 tau, and AT8-phosphorylated tau all interact with PP1α and γ, however, AT8 phosphorylation increases this interaction (as illustrated with a larger arrow) and deletion of amino acids 2-18 decreases, but does not completely abolish, this interaction (as illustrated by a smaller arrow). This results in increased PP1 activity, which dephosphorylates GSK3 and promotes kinase activity. GSK3 can phosphorylate kinesin light chains to promote dissociation of cargoes but can also phosphorylate tau at the AT8 epitope. This would result in a detrimental feedforward AT8 phosphorylation loop, increasing the signaling of this PP1/GSK3 cascade and promoting a pathological phenotype in affected neurons.

LITERATURE CITED

LITERATURE CITED

(1991). "Molecular classification of Alzheimer's disease." Lancet **337**(8753): 1342-1343.

Adamec, E., P. Mohan, J. P. Vonsattel and R. A. Nixon (2002). "Calpain activation in neurodegenerative diseases: confocal immunofluorescence study with antibodies specifically recognizing the active form of calpain 2." Acta Neuropathol **104**(1): 92-104.

Adey, W. R. and M. Meyer (1952). "Hippocampal and hypothalamic connexions of the temporal lobe in the monkey." Brain **75**(3): 358-384.

Albrecht, S., N. Bogdanovic, B. Ghetti, B. Winblad and A. C. LeBlanc (2009). "Caspase-6 activation in familial alzheimer disease brains carrying amyloid precursor protein or presenilin i or presenilin II mutations." J Neuropathol Exp Neurol **68**(12): 1282-1293.

Alonso, A. C., I. Grundke-Iqbal and K. Iqbal (1996). "Alzheimer's disease hyperphosphorylated tau sequesters normal tau into tangles of filaments and disassembles microtubules." Nat Med **2**(7): 783-787.

Alzheimer's, A. (2018). "2018 Alzheimer's disease facts and figures." Alzheimers & Dementia **14**(3): 367-425.

Amaral, D. G. and M. P. Witter (1989). "The three-dimensional organization of the hippocampal formation: a review of anatomical data." Neuroscience **31**(3): 571-591.

Andersen, P., R. Morris, D. Amaral, T. Bliss and J. O'Keefe (2006). The hippocampus book, Oxford University Press, USA.

Andorfer, C., Y. Kress, M. Espinoza, R. de Silva, K. L. Tucker, Y. A. Barde, K. Duff and P. Davies (2003). "Hyperphosphorylation and aggregation of tau in mice expressing normal human tau isoforms." J Neurochem **86**(3): 582-590.

Andreadis, A., W. M. Brown and K. S. Kosik (1992). "Structure and novel exons of the human tau gene." Biochemistry **31**(43): 10626-10633.

Arendt, T., M. Holzer, R. Fruth, M. K. Bruckner and U. Gartner (1995). "Paired helical filament-like phosphorylation of tau, deposition of beta/A4-amyloid and memory impairment in rat induced by chronic inhibition of phosphatase 1 and 2A." Neuroscience **69**(3): 691-698.

Arendt, T., M. Holzer, R. Fruth, M. K. Bruckner and U. Gartner (1998). "Phosphorylation of tau, Abeta-formation, and apoptosis after in vivo inhibition of PP-1 and PP-2A." Neurobiol Aging **19**(1): 3-13.

Arnaud, L. T., N. Myeku and M. E. Figueiredo-Pereira (2009). "Proteasome-caspase-cathepsin sequence leading to tau pathology induced by prostaglandin J2 in neuronal cells." J Neurochem **110**(1): 328-342.

Arriagada, P. V., J. H. Growdon, E. T. Hedley-Whyte and B. T. Hyman (1992). "Neurofibrillary tangles but not senile plaques parallel duration and severity of Alzheimer's disease." Neurology **42**(3 Pt 1): 631-639.

Bancher, C., H. Braak, P. Fischer and K. A. Jellinger (1993). "Neuropathological staging of Alzheimer lesions and intellectual status in Alzheimer's and Parkinson's disease patients." Neurosci Lett **162**(1-2): 179-182.

Bancher, C., C. Brunner, H. Lassmann, H. Budka, K. Jellinger, G. Wiche, F. Seitelberger, I. Grundke-Iqbal, K. Iqbal and H. M. Wisniewski (1989). "Accumulation of abnormally phosphorylated tau precedes the formation of neurofibrillary tangles in Alzheimer's disease." Brain Res **477**(1-2): 90-99.

Basurto-Islas, G., J. Luna-Munoz, A. L. Guillozet-Bongaarts, L. I. Binder, R. Mena and F. Garcia-Sierra (2008). "Accumulation of aspartic acid421- and glutamic acid391-cleaved tau in neurofibrillary tangles correlates with progression in Alzheimer disease." J Neuropathol Exp Neurol **67**(5): 470-483.

Beach, T. G., C. H. Adler, L. I. Sue, G. Serrano, H. A. Shill, D. G. Walker, L. Lue, A. E. Roher, B. N. Dugger, C. Maarouf, A. C. Birdsill, A. Intorcia, M. Saxon-Labelle, J. Pullen, A. Scroggins, J. Filon, S. Scott, B. Hoffman, A. Garcia, J. N. Caviness, J. G. Hentz, E. Driver-Dunckley, S. A. Jacobson, K. J. Davis, C. M. Belden, K. E. Long, M. Malek-Ahmadi, J. J. Powell, L. D. Gale, L. R. Nicholson, R. J. Caselli, B. K. Woodruff, S. Z. Rapscak, G. L. Ahern, J. Shi, A. D. Burke, E. M. Reiman and M. N. Sabbagh (2015). "Arizona Study of Aging and Neurodegenerative Disorders and Brain and Body Donation Program." Neuropathology **35**(4): 354-389.

Bell, K. F. and A. Claudio Cuello (2006). "Altered synaptic function in Alzheimer's disease." Eur J Pharmacol **545**(1): 11-21.

Benilova, I., E. Karran and B. De Strooper (2012). "The toxic Abeta oligomer and Alzheimer's disease: an emperor in need of clothes." Nat Neurosci **15**(3): 349-357.

Berry, R. W., A. P. Sweet, F. A. Clark, S. Lagalwar, B. R. Lapin, T. Wang, S. Topgi, A. L. Guillozet-Bongaarts, E. J. Cochran, E. H. Bigio and L. I. Binder (2004). "Tau epitope display in progressive supranuclear palsy and corticobasal degeneration." J Neurocytol **33**(3): 287-295.

Bertram, L., C. M. Lill and R. E. Tanzi (2010). "The genetics of Alzheimer disease: back to the future." Neuron **68**(2): 270-281.

Biernat, J., E. M. Mandelkow, C. Schroter, B. Lichtenberg-Kraag, B. Steiner, B. Berling, H. Meyer, M. Mercken, A. Vandermeeren, M. Goedert and et al. (1992). "The switch of tau protein to an Alzheimer-like state includes the phosphorylation of two serine-proline motifs upstream of the microtubule binding region." EMBO J **11**(4): 1593-1597.

Binder, L. I., A. Frankfurter and L. I. Rebhun (1985). "The distribution of tau in the mammalian central nervous system." J Cell Biol **101**(4): 1371-1378.

Binder, L. I., A. Frankfurter and L. I. Rebhun (1986). "Differential localization of MAP-2 and tau in mammalian neurons in situ." Ann N Y Acad Sci **466**: 145-166.

Binder, L. I., A. L. Guillozet-Bongaarts, F. Garcia-Sierra and R. W. Berry (2005). "Tau, tangles, and Alzheimer's disease." Biochim Biophys Acta **1739**(2-3): 216-223.

Bodner, R. A., D. E. Housman and A. G. Kazantsev (2006). "New directions for neurodegenerative disease therapy: using chemical compounds to boost the formation of mutant protein inclusions." Cell Cycle **5**(14): 1477-1480.

Bollen, M. (2001). "Combinatorial control of protein phosphatase-1." Trends Biochem Sci **26**(7): 426-431.

Bollen, M., W. Peti, M. J. Ragusa and M. Beullens (2010). "The extended PP1 toolkit: designed to create specificity." Trends Biochem Sci **35**(8): 450-458.

Bollen, M. and W. Stalmans (1992). "The structure, role, and regulation of type 1 protein phosphatases." Crit Rev Biochem Mol Biol **27**(3): 227-281.

Boluda, S., J. B. Toledo, D. J. Irwin, K. M. Raible, M. D. Byrne, E. B. Lee, V. M. Lee and J. Q. Trojanowski (2014). "A comparison of Abeta amyloid pathology staging systems and correlation with clinical diagnosis." Acta Neuropathol **128**(4): 543-550.

Bordelon, J. R., Y. Smith, A. C. Nairn, R. J. Colbran, P. Greengard and E. C. Muly (2005). "Differential localization of protein phosphatase-1alpha, beta and gamma1 isoforms in primate prefrontal cortex." Cereb Cortex **15**(12): 1928-1937.

Boschert, U., E. Merlo-Pich, G. Higgins, A. D. Roses and S. Catsicas (1999). "Apolipoprotein E expression by neurons surviving excitotoxic stress." Neurobiol Dis **6**(6): 508-514.

Boyce, M., K. F. Bryant, C. Jousse, K. Long, H. P. Harding, D. Scheuner, R. J. Kaufman, D. Ma, D. M. Coen, D. Ron and J. Yuan (2005). "A selective inhibitor of eIF2alpha dephosphorylation protects cells from ER stress." Science **307**(5711): 935-939.

Bozzali, M., A. Falini, M. Franceschi, M. Cercignani, M. Zuffi, G. Scotti, G. Comi and M. Filippi (2002). "White matter damage in Alzheimer's disease assessed in vivo using diffusion tensor magnetic resonance imaging." J Neurol Neurosurg Psychiatry **72**(6): 742-746.

Braak, E., H. Braak and E. M. Mandelkow (1994). "A sequence of cytoskeleton changes related to the formation of neurofibrillary tangles and neuropil threads." Acta Neuropathol **87**(6): 554-567.

Braak, H., I. Alafuzoff, T. Arzberger, H. Kretzschmar and K. Del Tredici (2006). "Staging of Alzheimer disease-associated neurofibrillary pathology using paraffin sections and immunocytochemistry." Acta Neuropathol **112**(4): 389-404.

Braak, H. and E. Braak (1991). "Neuropathological stageing of Alzheimer-related changes." Acta Neuropathol **82**(4): 239-259.

Braak, H. and E. Braak (1995). "Staging of Alzheimer's disease-related neurofibrillary changes." Neurobiol Aging **16**(3): 271-278; discussion 278-284.

Brady, R. M., R. P. Zinkowski and L. I. Binder (1995). "Presence of tau in isolated nuclei from human brain." Neurobiol Aging **16**(3): 479-486.

Braithwaite, S. P., J. B. Stock, P. J. Lombroso and A. C. Nairn (2012). "Protein phosphatases and Alzheimer's disease." Prog Mol Biol Transl Sci **106**: 343-379.

Breydo, L., J. W. Wu and V. N. Uversky (2012). "Alpha-synuclein misfolding and Parkinson's disease." Biochim Biophys Acta **1822**(2): 261-285.

Brookmeyer, R., E. Johnson, K. Ziegler-Graham and H. M. Arrighi (2007). "Forecasting the global burden of Alzheimer's disease." Alzheimers Dement **3**(3): 186-191.

Brouwers, N., K. Sleegers, S. Engelborghs, V. Bogaerts, S. Serneels, K. Kamali, E. Corsmit, E. De Leenheir, J. J. Martin, P. P. De Deyn, C. Van Broeckhoven and J. Theuns (2006). "Genetic risk and transcriptional variability of amyloid precursor protein in Alzheimer's disease." Brain **129**(Pt 11): 2984-2991.

Brush, M. H., D. C. Weiser and S. Shenolikar (2003). "Growth arrest and DNA damage-inducible protein GADD34 targets protein phosphatase 1 alpha to the endoplasmic reticulum and promotes dephosphorylation of the alpha subunit of eukaryotic translation initiation factor 2." Mol Cell Biol **23**(4): 1292-1303.

Bryant, J. C., R. S. Westphal and B. E. Wadzinski (1999). "Methylated C-terminal leucine residue of PP2A catalytic subunit is important for binding of regulatory Balpha subunit." Biochem J **339 (Pt 2)**: 241-246.

Bukar Maina, M., Y. K. Al-Hilaly and L. C. Serpell (2016). "Nuclear Tau and Its Potential Role in Alzheimer's Disease." Biomolecules **6**(1): 9.

Buxbaum, J. D., E. H. Koo and P. Greengard (1993). "Protein phosphorylation inhibits production of Alzheimer amyloid beta/A4 peptide." Proc Natl Acad Sci U S A **90**(19): 9195-9198.

Carmel, G., E. M. Mager, L. I. Binder and J. Kuret (1996). "The structural basis of monoclonal antibody Alz50's selectivity for Alzheimer's disease pathology." J Biol Chem **271**(51): 32789-32795.

Ceulemans, H. and M. Bollen (2004). "Functional diversity of protein phosphatase-1, a cellular economizer and reset button." Physiol Rev **84**(1): 1-39.

Cleveland, D. W., S. Y. Hwo and M. W. Kirschner (1977). "Physical and chemical properties of purified tau factor and the role of tau in microtubule assembly." J Mol Biol **116**(2): 227-247.

Cohen, P. T. (2002). "Protein phosphatase 1--targeted in many directions." J Cell Sci **115**(Pt 2): 241-256.

Combs, B., C. Hamel and N. M. Kanaan (2016). "Pathological conformations involving the amino terminus of tau occur early in Alzheimer's disease and are differentially detected by monoclonal antibodies." Neurobiol Dis **94**: 18-31.

Combs, B. and N. M. Kanaan (2017). "Exposure of the Amino Terminus of Tau Is a Pathological Event in Multiple Tauopathies." Am J Pathol **187**(6): 1222-1229.

Combs, B., C. T. Tiernan, C. Hamel and N. M. Kanaan (2017). "Production of recombinant tau oligomers in vitro." Methods Cell Biol **141**: 45-64.

Cook, C., Y. Carlomagno, T. F. Gendron, J. Dunmore, K. Scheffel, C. Stetler, M. Davis, D. Dickson, M. Jarpe, M. DeTure and L. Petrucelli (2014). "Acetylation of the KXGS motifs in tau is a critical determinant in modulation of tau aggregation and clearance." Hum Mol Genet **23**(1): 104-116.

Corder, E. H., A. M. Saunders, W. J. Strittmatter, D. E. Schmechel, P. C. Gaskell, G. W. Small, A. D. Roses, J. L. Haines and M. A. Pericak-Vance (1993). "Gene dose of apolipoprotein E type 4 allele and the risk of Alzheimer's disease in late onset families." Science **261**(5123): 921-923.

Cox, K., B. Combs, B. Abdelmesih, G. Morfini, S. T. Brady and N. M. Kanaan (2016). "Analysis of isoform-specific tau aggregates suggests a common toxic mechanism involving similar pathological conformations and axonal transport inhibition." Neurobiol Aging **47**: 113-126.

Cuadrado, A., S. Kugler and I. Lastres-Becker (2018). "Pharmacological targeting of GSK-3 and NRF2 provides neuroprotection in a preclinical model of tauopathy." Redox Biol **14**: 522-534.

da Cruz e Silva, E. F., C. A. Fox, C. C. Ouimet, E. Gustafson, S. J. Watson and P. Greengard (1995). "Differential expression of protein phosphatase 1 isoforms in mammalian brain." J Neurosci **15**(5 Pt 1): 3375-3389.

Dahm, R. (2006). "Alzheimer's discovery." Curr Biol **16**(21): R906-910.

Dajani, R., E. Fraser, S. M. Roe, N. Young, V. Good, T. C. Dale and L. H. Pearl (2001). "Crystal structure of glycogen synthase kinase 3 beta: structural basis for phosphate-primed substrate specificity and autoinhibition." Cell **105**(6): 721-732.

Dancheck, B., A. C. Nairn and W. Peti (2008). "Detailed structural characterization of unbound protein phosphatase 1 inhibitors." Biochemistry **47**(47): 12346-12356.

de Calignon, A., M. Polydoro, M. Suarez-Calvet, C. William, D. H. Adamowicz, K. J. Kopeikina, R. Pitstick, N. Sahara, K. H. Ashe, G. A. Carlson, T. L. Spires-Jones and B. T. Hyman (2012). "Propagation of tau pathology in a model of early Alzheimer's disease." Neuron **73**(4): 685-697.

De Strooper, B., P. Saftig, K. Craessaerts, H. Vanderstichele, G. Guhde, W. Annaert, K. Von Figura and F. Van Leuven (1998). "Deficiency of presenilin-1 inhibits the normal cleavage of amyloid precursor protein." Nature **391**(6665): 387-390.

DeKosky, S. T. and S. W. Scheff (1990). "Synapse loss in frontal cortex biopsies in Alzheimer's disease: correlation with cognitive severity." Ann Neurol **27**(5): 457-464.

Deng, Y., B. Li, Y. Liu, K. Iqbal, I. Grundke-Iqbal and C. X. Gong (2009). "Dysregulation of insulin signaling, glucose transporters, O-GlcNAcylation, and phosphorylation of tau and neurofilaments in the brain: Implication for Alzheimer's disease." Am J Pathol **175**(5): 2089-2098.

Dixit, R., J. L. Ross, Y. E. Goldman and E. L. Holzbaur (2008). "Differential regulation of dynein and kinesin motor proteins by tau." Science **319**(5866): 1086-1089.

Dorval, V. and P. E. Fraser (2006). "Small ubiquitin-like modifier (SUMO) modification of natively unfolded proteins tau and alpha-synuclein." J Biol Chem **281**(15): 9919-9924.

Drechsel, D. N., A. A. Hyman, M. H. Cobb and M. W. Kirschner (1992). "Modulation of the dynamic instability of tubulin assembly by the microtubule-associated protein tau." Mol Biol Cell **3**(10): 1141-1154.

Egloff, M. P., D. F. Johnson, G. Moorhead, P. T. Cohen, P. Cohen and D. Barford (1997). "Structural basis for the recognition of regulatory subunits by the catalytic subunit of protein phosphatase 1." EMBO J **16**(8): 1876-1887.

Fardilha, M., S. L. Esteves, L. Korrodi-Gregorio, O. A. da Cruz e Silva and F. F. da Cruz e Silva (2010). "The physiological relevance of protein phosphatase 1 and its interacting proteins to health and disease." Curr Med Chem **17**(33): 3996-4017.

Fasulo, L., G. Ugolini, M. Visintin, A. Bradbury, C. Brancolini, V. Verzillo, M. Novak and A. Cattaneo (2000). "The neuronal microtubule-associated protein tau is a substrate for caspase-3 and an effector of apoptosis." J Neurochem **75**(2): 624-633.

Fellous, A., J. Francon, A. M. Lennon and J. Nunez (1977). "Microtubule assembly in vitro. Purification of assembly-promoting factors." Eur J Biochem **78**(1): 167-174.

Fitzpatrick, A. W. P., B. Falcon, S. He, A. G. Murzin, G. Murshudov, H. J. Garringer, R. A. Crowther, B. Ghetti, M. Goedert and S. H. W. Scheres (2017). "Cryo-EM structures of tau filaments from Alzheimer's disease." Nature **547**(7662): 185-190.

Flores-Delgado, G., C. W. Liu, R. Sposto and N. Berndt (2007). "A limited screen for protein interactions reveals new roles for protein phosphatase 1 in cell cycle control and apoptosis." J Proteome Res **6**(3): 1165-1175.

Florian, S. and T. J. Mitchison (2016). "Anti-Microtubule Drugs." Methods Mol Biol **1413**: 403-421.

Furukawa, K., Y. Wang, P. J. Yao, W. Fu, M. P. Mattson, Y. Itoyama, H. Onodera, I. D'Souza, P. H. Poorkaj, T. D. Bird and G. D. Schellenberg (2003). "Alteration in calcium channel properties is responsible for the neurotoxic action of a familial frontotemporal dementia tau mutation." J Neurochem **87**(2): 427-436.

Gamblin, T. C., F. Chen, A. Zambrano, A. Abraha, S. Lagalwar, A. L. Guillozet, M. Lu, Y. Fu, F. Garcia-Sierra, N. LaPointe, R. Miller, R. W. Berry, L. I. Binder and V. L. Cryns (2003). "Caspase cleavage of tau: linking amyloid and neurofibrillary tangles in Alzheimer's disease." Proc Natl Acad Sci U S A **100**(17): 10032-10037.

Ghoshal, N., F. Garcia-Sierra, Y. Fu, L. A. Beckett, E. J. Mufson, J. Kuret, R. W. Berry and L. I. Binder (2001). "Tau-66: evidence for a novel tau conformation in Alzheimer's disease." J Neurochem **77**(5): 1372-1385.

Ghoshal, N., F. Garcia-Sierra, J. Wuu, S. Leurgans, D. A. Bennett, R. W. Berry and L. I. Binder (2002). "Tau conformational changes correspond to impairments of episodic memory in mild cognitive impairment and Alzheimer's disease." Exp Neurol **177**(2): 475-493.

Giannakopoulos, P., F. R. Herrmann, T. Bussiere, C. Bouras, E. Kovari, D. P. Perl, J. H. Morrison, G. Gold and P. R. Hof (2003). "Tangle and neuron numbers, but not amyloid load, predict cognitive status in Alzheimer's disease." Neurology **60**(9): 1495-1500.

Gibbons, J. A., L. Kozubowski, K. Tatchell and S. Shenolikar (2007). "Expression of human protein phosphatase-1 in Saccharomyces cerevisiae highlights the role of phosphatase isoforms in regulating eukaryotic functions." J Biol Chem **282**(30): 21838-21847.

Glenner, G. G. and C. W. Wong (1984). "Alzheimer's disease: initial report of the purification and characterization of a novel cerebrovascular amyloid protein." Biochem Biophys Res Commun **120**(3): 885-890.

Glickman, M. H. and A. Ciechanover (2002). "The ubiquitin-proteasome proteolytic pathway: destruction for the sake of construction." Physiol Rev **82**(2): 373-428.

Goate, A., M. C. Chartier-Harlin, M. Mullan, J. Brown, F. Crawford, L. Fidani, L. Giuffra, A. Haynes, N. Irving, L. James and et al. (1991). "Segregation of a missense mutation in the amyloid precursor protein gene with familial Alzheimer's disease." Nature **349**(6311): 704-706.

Goedert, M., R. Jakes and E. Vanmechelen (1995). "Monoclonal antibody AT8 recognises tau protein phosphorylated at both serine 202 and threonine 205." Neurosci Lett **189**(3): 167-169.

Goedert, M., M. G. Spillantini, N. J. Cairns and R. A. Crowther (1992). "Tau proteins of Alzheimer paired helical filaments: abnormal phosphorylation of all six brain isoforms." Neuron **8**(1): 159-168.

Goedert, M., M. G. Spillantini, R. Jakes, D. Rutherford and R. A. Crowther (1989). "Multiple isoforms of human microtubule-associated protein tau: sequences and localization in neurofibrillary tangles of Alzheimer's disease." Neuron **3**(4): 519-526.

Goedert, M., M. G. Spillantini, M. C. Potier, J. Ulrich and R. A. Crowther (1989). "Cloning and sequencing of the cDNA encoding an isoform of microtubule-associated protein tau containing four tandem repeats: differential expression of tau protein mRNAs in human brain." Embo j **8**(2): 393-399.

Goldberg, J., H. B. Huang, Y. G. Kwon, P. Greengard, A. C. Nairn and J. Kuriyan (1995). "Three-dimensional structure of the catalytic subunit of protein serine/threonine phosphatase-1." Nature **376**(6543): 745-753.

Gomez-Isla, T., J. L. Price, D. W. McKeel, Jr., J. C. Morris, J. H. Growdon and B. T. Hyman (1996). "Profound loss of layer II entorhinal cortex neurons occurs in very mild Alzheimer's disease." J Neurosci **16**(14): 4491-4500.

Gomez de Barreda, E., M. Perez, P. Gomez Ramos, J. de Cristobal, P. Martin-Maestro, A. Moran, H. N. Dawson, M. P. Vitek, J. J. Lucas, F. Hernandez and J. Avila (2010). "Tau-knockout mice show reduced GSK3-induced hippocampal degeneration and learning deficits." Neurobiol Dis **37**(3): 622-629.

Gong, C. X., F. Liu, I. Grundke-Iqbal and K. Iqbal (2006). "Impaired brain glucose metabolism leads to Alzheimer neurofibrillary degeneration through a decrease in tau O-GlcNAcylation." J Alzheimers Dis **9**(1): 1-12.

Gong, C. X., T. J. Singh, I. Grundke-Iqbal and K. Iqbal (1993). "Phosphoprotein phosphatase activities in Alzheimer disease brain." J Neurochem **61**(3): 921-927.

Gotz, J., A. Probst, E. Ehler, B. Hemmings and W. Kues (1998). "Delayed embryonic lethality in mice lacking protein phosphatase 2A catalytic subunit Calpha." Proc Natl Acad Sci U S A **95**(21): 12370-12375.

Goussakov, I., M. B. Miller and G. E. Stutzmann (2010). "NMDA-mediated Ca(2+) influx drives aberrant ryanodine receptor activation in dendrites of young Alzheimer's disease mice." J Neurosci **30**(36): 12128-12137.

Grabinski, T. and N. M. Kanaan (2016). "Novel Non-phosphorylated Serine 9/21 GSK3beta/alpha Antibodies: Expanding the Tools for Studying GSK3 Regulation." Front Mol Neurosci **9**: 123.

Greenberg, S. G., P. Davies, J. D. Schein and L. I. Binder (1992). "Hydrofluoric acid-treated tau PHF proteins display the same biochemical properties as normal tau." J Biol Chem **267**(1): 564-569.

Grundke-Iqbal, I., K. Iqbal, M. Quinlan, Y. C. Tung, M. S. Zaidi and H. M. Wisniewski (1986). "Microtubule-associated protein tau. A component of Alzheimer paired helical filaments." J Biol Chem **261**(13): 6084-6089.

Grundke-Iqbal, I., K. Iqbal, Y. C. Tung, M. Quinlan, H. M. Wisniewski and L. I. Binder (1986). "Abnormal phosphorylation of the microtubule-associated protein tau (tau) in Alzheimer cytoskeletal pathology." Proc Natl Acad Sci U S A **83**(13): 4913-4917.

Guillozet-Bongaarts, A. L., F. Garcia-Sierra, M. R. Reynolds, P. M. Horowitz, Y. Fu, T. Wang, M. E. Cahill, E. H. Bigio, R. W. Berry and L. I. Binder (2005). "Tau truncation during neurofibrillary tangle evolution in Alzheimer's disease." Neurobiol Aging **26**(7): 1015-1022.

Guo, H., S. Albrecht, M. Bourdeau, T. Petzke, C. Bergeron and A. C. LeBlanc (2004). "Active caspase-6 and caspase-6-cleaved tau in neuropil threads, neuritic plaques, and neurofibrillary tangles of Alzheimer's disease." Am J Pathol **165**(2): 523-531.

Han, J. D., N. Bertin, T. Hao, D. S. Goldberg, G. F. Berriz, L. V. Zhang, D. Dupuy, A. J. Walhout, M. E. Cusick, F. P. Roth and M. Vidal (2004). "Evidence for dynamically organized modularity in the yeast protein-protein interaction network." Nature **430**(6995): 88-93.

Hanger, D. P., B. H. Anderton and W. Noble (2009). "Tau phosphorylation: the therapeutic challenge for neurodegenerative disease." Trends Mol Med **15**(3): 112-119.

Hardy, J. and D. J. Selkoe (2002). "The amyloid hypothesis of Alzheimer's disease: progress and problems on the road to therapeutics." Science **297**(5580): 353-356.

Hardy, J. A. and G. A. Higgins (1992). "Alzheimer's disease: the amyloid cascade hypothesis." Science **256**(5054): 184-185.

Harper, J. D. and P. T. Lansbury, Jr. (1997). "Models of amyloid seeding in Alzheimer's disease and scrapie: mechanistic truths and physiological consequences of the time-dependent solubility of amyloid proteins." Annu Rev Biochem **66**: 385-407.

Hebert, L. E., P. A. Scherr, J. L. Bienias, D. A. Bennett and D. A. Evans (2003). "Alzheimer disease in the US population: prevalence estimates using the 2000 census." Arch Neurol **60**(8): 1119-1122.

Hebert, L. E., J. Weuve, P. A. Scherr and D. A. Evans (2013). "Alzheimer disease in the United States (2010-2050) estimated using the 2010 census." Neurology **80**(19): 1778-1783.

Hendrickx, A., M. Beullens, H. Ceulemans, T. Den Abt, A. Van Eynde, E. Nicolaescu, B. Lesage and M. Bollen (2009). "Docking motif-guided mapping of the interactome of protein phosphatase-1." Chem Biol **16**(4): 365-371.

Hendriks, L., C. M. van Duijn, P. Cras, M. Cruts, W. Van Hul, F. van Harskamp, A. Warren, M. G. McInnis, S. E. Antonarakis, J. J. Martin and et al. (1992). "Presenile dementia and cerebral haemorrhage linked to a mutation at codon 692 of the beta-amyloid precursor protein gene." Nat Genet **1**(3): 218-221.

Heroes, E., B. Lesage, J. Gornemann, M. Beullens, L. Van Meervelt and M. Bollen (2013). "The PP1 binding code: a molecular-lego strategy that governs specificity." Febs j **280**(2): 584-595.

Hirokawa, N., Y. Shiomura and S. Okabe (1988). "Tau proteins: the molecular structure and mode of binding on microtubules." J Cell Biol **107**(4): 1449-1459.

Hoffman, A., G. Taleski and E. Sontag (2017). "The protein serine/threonine phosphatases PP2A, PP1 and calcineurin: A triple threat in the regulation of the neuronal cytoskeleton." Mol Cell Neurosci **84**: 119-131.

Holmes, B. B. and M. I. Diamond (2014). "Prion-like properties of Tau protein: the importance of extracellular Tau as a therapeutic target." J Biol Chem **289**(29): 19855-19861.

Holmes, C., D. Boche, D. Wilkinson, G. Yadegarfar, V. Hopkins, A. Bayer, R. W. Jones, R. Bullock, S. Love, J. W. Neal, E. Zotova and J. A. Nicoll (2008). "Long-term effects of Abeta42 immunisation in Alzheimer's disease: follow-up of a randomised, placebo-controlled phase I trial." Lancet **372**(9634): 216-223.

Hong, M., V. Zhukareva, V. Vogelsberg-Ragaglia, Z. Wszolek, L. Reed, B. I. Miller, D. H. Geschwind, T. D. Bird, D. McKeel, A. Goate, J. C. Morris, K. C. Wilhelmsen, G. D. Schellenberg, J. Q. Trojanowski and V. M. Lee (1998). "Mutation-specific functional impairments in distinct tau isoforms of hereditary FTDP-17." Science **282**(5395): 1914-1917.

Hooper, C., R. Killick and S. Lovestone (2008). "The GSK3 hypothesis of Alzheimer's disease." J Neurochem **104**(6): 1433-1439.

Horowitz, P. M., N. LaPointe, A. L. Guillozet-Bongaarts, R. W. Berry and L. I. Binder (2006). "N-terminal fragments of tau inhibit full-length tau polymerization in vitro." Biochemistry **45**(42): 12859-12866.

Horowitz, P. M., K. R. Patterson, A. L. Guillozet-Bongaarts, M. R. Reynolds, C. A. Carroll, S. T. Weintraub, D. A. Bennett, V. L. Cryns, R. W. Berry and L. I. Binder (2004). "Early N-terminal changes and caspase-6 cleavage of tau in Alzheimer's disease." J Neurosci **24**(36): 7895-7902.

Hsieh, H., J. Boehm, C. Sato, T. Iwatsubo, T. Tomita, S. Sisodia and R. Malinow (2006). "AMPAR removal underlies Abeta-induced synaptic depression and dendritic spine loss." Neuron **52**(5): 831-843.

Huang, C. Y. and M. N. Rasband (2018). "Axon initial segments: structure, function, and disease." Ann N Y Acad Sci **1420**(1): 46-61.

Huang, J. and A. P. Auchus (2007). "Diffusion tensor imaging of normal appearing white matter and its correlation with cognitive functioning in mild cognitive impairment and Alzheimer's disease." Ann N Y Acad Sci **1097**: 259-264.

Huang, Y. and L. Mucke (2012). "Alzheimer Mechanisms and Therapeutic Strategies." Cell **148**(6): 1204-1222.

Hurley, T. D., J. Yang, L. Zhang, K. D. Goodwin, Q. Zou, M. Cortese, A. K. Dunker and A. A. DePaoli-Roach (2007). "Structural basis for regulation of protein phosphatase 1 by inhibitor-2." J Biol Chem **282**(39): 28874-28883.

Hutton, M., C. L. Lendon, P. Rizzu, M. Baker, S. Froelich, H. Houlden, S. Pickering-Brown, S. Chakraverty, A. Isaacs, A. Grover, J. Hackett, J. Adamson, S. Lincoln, D. Dickson, P. Davies, R. C. Petersen, M. Stevens, E. de Graaff, E. Wauters, J. van Baren, M. Hillebrand, M. Joosse, J. M. Kwon, P. Nowotny, L. K. Che, J. Norton, J. C. Morris, L. A. Reed, J. Trojanowski, H. Basun, L. Lannfelt, M. Neystat, S. Fahn, F. Dark, T. Tannenberg, P. R. Dodd, N. Hayward, J. B. Kwok, P. R. Schofield, A. Andreadis, J. Snowden, D. Craufurd, D. Neary, F. Owen, B. A. Oostra, J. Hardy, A. Goate, J. van Swieten, D. Mann, T. Lynch and P. Heutink (1998). "Association of missense and 5'-splice-site mutations in tau with the inherited dementia FTDP-17." Nature **393**(6686): 702-705.

Hyman, B. T., C. H. Phelps, T. G. Beach, E. H. Bigio, N. J. Cairns, M. C. Carrillo, D. W. Dickson, C. Duyckaerts, M. P. Frosch, E. Masliah, S. S. Mirra, P. T. Nelson, J. A. Schneider, D. R. Thal, B. Thies, J. Q. Trojanowski, H. V. Vinters and T. J. Montine (2012). "National Institute on Aging-Alzheimer's Association guidelines for the neuropathologic assessment of Alzheimer's disease." Alzheimers Dement **8**(1): 1-13.

Iqbal, K., A. C. Alonso, C. X. Gong, S. Khatoon, J. J. Pei, J. Z. Wang and I. Grundke-Iqbal (1998). "Mechanisms of neurofibrillary degeneration and the formation of neurofibrillary tangles." J Neural Transm Suppl **53**: 169-180.

Iqbal, K., C. Alonso Adel, S. Chen, M. O. Chohan, E. El-Akkad, C. X. Gong, S. Khatoon, B. Li, F. Liu, A. Rahman, H. Tanimukai and I. Grundke-Iqbal (2005). "Tau pathology in Alzheimer disease and other tauopathies." Biochim Biophys Acta **1739**(2-3): 198-210.

Iqbal, K. and I. Grundke-Iqbal (1991). "Ubiquitination and abnormal phosphorylation of paired helical filaments in Alzheimer's disease." Mol Neurobiol **5**(2-4): 399-410.

Irwin, D. J., T. J. Cohen, M. Grossman, S. E. Arnold, E. McCarty-Wood, V. M. Van Deerlin, V. M. Lee and J. Q. Trojanowski (2013). "Acetylated tau neuropathology in sporadic and hereditary tauopathies." Am J Pathol **183**(2): 344-351.

Ittner, L. M., Y. D. Ke, F. Delerue, M. Bi, A. Gladbach, J. van Eersel, H. Wolfing, B. C. Chieng, M. J. Christie, I. A. Napier, A. Eckert, M. Staufenbiel, E. Hardeman and J. Gotz (2010). "Dendritic function of tau mediates amyloid-beta toxicity in Alzheimer's disease mouse models." Cell **142**(3): 387-397.

Ittner, L. M., Y. D. Ke and J. Gotz (2009). "Phosphorylated Tau interacts with c-Jun N-terminal kinase-interacting protein 1 (JIP1) in Alzheimer disease." J Biol Chem **284**(31): 20909-20916.

Jarrett, J. T. and P. T. Lansbury, Jr. (1993). "Seeding "one-dimensional crystallization" of amyloid: a pathogenic mechanism in Alzheimer's disease and scrapie?" Cell **73**(6): 1055-1058.

Jeganathan, S., A. Hascher, S. Chinnathambi, J. Biernat, E. M. Mandelkow and E. Mandelkow (2008). "Proline-directed pseudo-phosphorylation at AT8 and PHF1 epitopes induces a compaction of the paperclip folding of Tau and generates a pathological (MC-1) conformation." J Biol Chem **283**(46): 32066-32076.

Jeganathan, S., M. von Bergen, H. Brutlach, H. J. Steinhoff and E. Mandelkow (2006). "Global hairpin folding of tau in solution." Biochemistry **45**(7): 2283-2293.

Ji, Z. S., R. D. Miranda, Y. M. Newhouse, K. H. Weisgraber, Y. Huang and R. W. Mahley (2002). "Apolipoprotein E4 potentiates amyloid beta peptide-induced lysosomal leakage and apoptosis in neuronal cells." J Biol Chem **277**(24): 21821-21828.

Kadavath, H., R. V. Hofele, J. Biernat, S. Kumar, K. Tepper, H. Urlaub, E. Mandelkow and M. Zweckstetter (2015). "Tau stabilizes microtubules by binding at the interface between tubulin heterodimers." Proc Natl Acad Sci U S A **112**(24): 7501-7506.

Kanaan, N. M., K. Cox, V. E. Alvarez, T. D. Stein, S. Poncil and A. C. McKee (2016). "Characterization of Early Pathological Tau Conformations and Phosphorylation in Chronic Traumatic Encephalopathy." J Neuropathol Exp Neurol **75**(1): 19-34.

Kanaan, N. M., G. Morfini, G. Pigino, N. E. LaPointe, A. Andreadis, Y. Song, E. Leitman, L. I. Binder and S. T. Brady (2012). "Phosphorylation in the amino terminus of tau prevents inhibition of anterograde axonal transport." Neurobiol Aging **33**(4): 826.e815-830.

Kanaan, N. M., G. A. Morfini, N. E. LaPointe, G. F. Pigino, K. R. Patterson, Y. Song, A. Andreadis, Y. Fu, S. T. Brady and L. I. Binder (2011). "Pathogenic forms of tau inhibit kinesin-dependent axonal transport through a mechanism involving activation of axonal phosphotransferases." J Neurosci **31**(27): 9858-9868.

Kanaan, N. M., G. F. Pigino, S. T. Brady, O. Lazarov, L. I. Binder and G. A. Morfini (2013). "Axonal degeneration in Alzheimer's disease: when signaling abnormalities meet the axonal transport system." Exp Neurol **246**: 44-53.

Kanemaru, K., K. Takio, R. Miura, K. Titani and Y. Ihara (1992). "Fetal-type phosphorylation of the tau in paired helical filaments." J Neurochem **58**(5): 1667-1675.

Kayed, R. and C. A. Lasagna-Reeves (2013). "Molecular mechanisms of amyloid oligomers toxicity." J Alzheimers Dis **33 Suppl 1**: S67-78.

Kidd, M. (1963). "Paired helical filaments in electron microscopy of Alzheimer's disease." Nature **197**: 192-193.

Kimberly, W. T., M. J. LaVoie, B. L. Ostaszewski, W. Ye, M. S. Wolfe and D. J. Selkoe (2003). "Gamma-secretase is a membrane protein complex comprised of presenilin, nicastrin, Aph-1, and Pen-2." Proc Natl Acad Sci U S A **100**(11): 6382-6387.

Kimura, T., T. Ono, J. Takamatsu, H. Yamamoto, K. Ikegami, A. Kondo, M. Hasegawa, Y. Ihara, E. Miyamoto and T. Miyakawa (1996). "Sequential changes of tau-site-specific phosphorylation during development of paired helical filaments." Dementia **7**(4): 177-181.

Kitagawa, Y., K. Sasaki, H. Shima, M. Shibuya, T. Sugimura and M. Nagao (1990). "Protein phosphatases possibly involved in rat spermatogenesis." Biochem Biophys Res Commun **171**(1): 230-235.

Kneynsberg, A., B. Combs, K. Christensen, G. Morfini and N. M. Kanaan (2017). "Axonal Degeneration in Tauopathies: Disease Relevance and Underlying Mechanisms." Front Neurosci **11**: 572.

Kopke, E., Y. C. Tung, S. Shaikh, A. C. Alonso, K. Iqbal and I. Grundke-Iqbal (1993). "Microtubule-associated protein tau. Abnormal phosphorylation of a non-paired helical filament pool in Alzheimer disease." J Biol Chem **268**(32): 24374-24384.

Korrodi-Gregorio, L., S. L. Esteves and M. Fardilha (2014). "Protein phosphatase 1 catalytic isoforms: specificity toward interacting proteins." Transl Res **164**(5): 366-391.

Kosik, K. S., C. L. Joachim and D. J. Selkoe (1986). "Microtubule-associated protein tau (tau) is a major antigenic component of paired helical filaments in Alzheimer disease." Proc Natl Acad Sci U S A **83**(11): 4044-4048.

Kovacs, G. G. (2015). "Invited review: Neuropathology of tauopathies: principles and practice." Neuropathol Appl Neurobiol **41**(1): 3-23.

Kowall, N. W., M. F. Beal, J. Busciglio, L. K. Duffy and B. A. Yankner (1991). "An in vivo model for the neurodegenerative effects of beta amyloid and protection by substance P." Proc Natl Acad Sci U S A **88**(16): 7247-7251.

Kowall, N. W. and K. S. Kosik (1987). "Axonal disruption and aberrant localization of tau protein characterize the neuropil pathology of Alzheimer's disease." Ann Neurol **22**(5): 639-643.

Kuhla, B., C. Haase, K. Flach, H. J. Luth, T. Arendt and G. Munch (2007). "Effect of pseudophosphorylation and cross-linking by lipid peroxidation and advanced glycation

end product precursors on tau aggregation and filament formation." J Biol Chem **282**(10): 6984-6991.

Lai, F. and R. S. Williams (1989). "A prospective study of Alzheimer disease in Down syndrome." Arch Neurol **46**(8): 849-853.

LaPointe, N. E., G. Morfini, G. Pigino, I. N. Gaisina, A. P. Kozikowski, L. I. Binder and S. T. Brady (2009). "The amino terminus of tau inhibits kinesin-dependent axonal transport: implications for filament toxicity." J Neurosci Res **87**(2): 440-451.

Lee, E. Y., S. R. Silberman, M. K. Ganapathi, S. Petrovic and H. Paris (1980). "The phosphoprotein phosphatases: properties of the enzymes involved in the regulation of glycogen metabolism." Adv Cyclic Nucleotide Res **13**: 95-131.

Lee, G., N. Cowan and M. Kirschner (1988). "The primary structure and heterogeneity of tau protein from mouse brain." Science **239**(4837): 285-288.

Lee, V. M., K. R. Brunden, M. Hutton and J. Q. Trojanowski (2011). "Developing therapeutic approaches to tau, selected kinases, and related neuronal protein targets." Cold Spring Harb Perspect Med **1**(1): a006437.

Leroy, K., Z. Yilmaz and J. P. Brion (2007). "Increased level of active GSK-3beta in Alzheimer's disease and accumulation in argyrophilic grains and in neurones at different stages of neurofibrillary degeneration." Neuropathol Appl Neurobiol **33**(1): 43-55.

Levy-Lahad, E., W. Wasco, P. Poorkaj, D. M. Romano, J. Oshima, W. H. Pettingell, C. E. Yu, P. D. Jondro, S. D. Schmidt, K. Wang and et al. (1995). "Candidate gene for the chromosome 1 familial Alzheimer's disease locus." Science **269**(5226): 973-977.

Li, S., S. Hong, N. E. Shepardson, D. M. Walsh, G. M. Shankar and D. Selkoe (2009). "Soluble oligomers of amyloid Beta protein facilitate hippocampal long-term depression by disrupting neuronal glutamate uptake." Neuron **62**(6): 788-801.

Li, X., Y. Kumar, H. Zempel, E. M. Mandelkow, J. Biernat and E. Mandelkow (2011). "Novel diffusion barrier for axonal retention of Tau in neurons and its failure in neurodegeneration." Embo j **30**(23): 4825-4837.

Liao, H., Y. Li, D. L. Brautigan and G. G. Gundersen (1998). "Protein phosphatase 1 is targeted to microtubules by the microtubule-associated protein Tau." J Biol Chem **273**(34): 21901-21908.

Lindwall, G. and R. D. Cole (1984). "Phosphorylation affects the ability of tau protein to promote microtubule assembly." J Biol Chem **259**(8): 5301-5305.

Liu, C. and J. Gotz (2013). "Profiling murine tau with 0N, 1N and 2N isoform-specific antibodies in brain and peripheral organs reveals distinct subcellular localization, with the 1N isoform being enriched in the nucleus." PLoS One **8**(12): e84849.

Liu, F., I. Grundke-Iqbal, K. Iqbal and C. X. Gong (2005). "Contributions of protein phosphatases PP1, PP2A, PP2B and PP5 to the regulation of tau phosphorylation." Eur J Neurosci **22**(8): 1942-1950.

Liu, F., K. Iqbal, I. Grundke-Iqbal, G. W. Hart and C. X. Gong (2004). "O-GlcNAcylation regulates phosphorylation of tau: a mechanism involved in Alzheimer's disease." Proc Natl Acad Sci U S A **101**(29): 10804-10809.

Liu, F., J. Shi, H. Tanimukai, J. Gu, J. Gu, I. Grundke-Iqbal, K. Iqbal and C. X. Gong (2009). "Reduced O-GlcNAcylation links lower brain glucose metabolism and tau pathology in Alzheimer's disease." Brain **132**(Pt 7): 1820-1832.

Liu, F., T. Zaidi, K. Iqbal, I. Grundke-Iqbal and C. X. Gong (2002). "Aberrant glycosylation modulates phosphorylation of tau by protein kinase A and dephosphorylation of tau by protein phosphatase 2A and 5." Neuroscience **115**(3): 829-837.

Liu, Y., F. Liu, I. Grundke-Iqbal, K. Iqbal and C. X. Gong (2009). "Brain glucose transporters, O-GlcNAcylation and phosphorylation of tau in diabetes and Alzheimer's disease." J Neurochem **111**(1): 242-249.

Liu, Y. H., W. Wei, J. Yin, G. P. Liu, Q. Wang, F. Y. Cao and J. Z. Wang (2009). "Proteasome inhibition increases tau accumulation independent of phosphorylation." Neurobiol Aging **30**(12): 1949-1961.

Loomis, P. A., T. H. Howard, R. P. Castleberry and L. I. Binder (1990). "Identification of nuclear tau isoforms in human neuroblastoma cells." Proc Natl Acad Sci U S A **87**(21): 8422-8426.

LoPresti, P., S. Szuchet, S. C. Papasozomenos, R. P. Zinkowski and L. I. Binder (1995). "Functional implications for the microtubule-associated protein tau: localization in oligodendrocytes." Proc Natl Acad Sci U S A **92**(22): 10369-10373.

Lu, J., T. Li, R. He, P. F. Bartlett and J. Gotz (2014). "Visualizing the microtubule-associated protein tau in the nucleus." Sci China Life Sci **57**(4): 422-431.

Luo, H. B., Y. Y. Xia, X. J. Shu, Z. C. Liu, Y. Feng, X. H. Liu, G. Yu, G. Yin, Y. S. Xiong, K. Zeng, J. Jiang, K. Ye, X. C. Wang and J. Z. Wang (2014). "SUMOylation at K340 inhibits tau degradation through deregulating its phosphorylation and ubiquitination." Proc Natl Acad Sci U S A **111**(46): 16586-16591.

Machleidt, T., C. C. Woodroofe, M. K. Schwinn, J. Mendez, M. B. Robers, K. Zimmerman, P. Otto, D. L. Daniels, T. A. Kirkland and K. V. Wood (2015). "NanoBRET--A Novel BRET Platform for the Analysis of Protein-Protein Interactions." ACS Chem Biol **10**(8): 1797-1804.

Mahley, R. W. (1988). "Apolipoprotein E: cholesterol transport protein with expanding role in cell biology." Science **240**(4852): 622-630.

Mandell, J. W. and G. A. Banker (1995). "The microtubule cytoskeleton and the development of neuronal polarity." Neurobiol Aging **16**(3): 229-237; discussion 238.

Manders, E. M. M., F. J. Verbeek and J. A. Aten (1993). "Measurement of co-localization of objects in dual-colour confocal images." Journal of Microscopy **169**(3): 375-382.

Marciniak, S. J. and D. Ron (2006). "Endoplasmic reticulum stress signaling in disease." Physiol Rev **86**(4): 1133-1149.

Markesbery, W. R., F. A. Schmitt, R. J. Kryscio, D. G. Davis, C. D. Smith and D. R. Wekstein (2006). "Neuropathologic substrate of mild cognitive impairment." Arch Neurol **63**(1): 38-46.

Martin, L., X. Latypova and F. Terro (2011). "Post-translational modifications of tau protein: implications for Alzheimer's disease." Neurochem Int **58**(4): 458-471.

Martin, L., X. Latypova, C. M. Wilson, A. Magnaudeix, M. L. Perrin, C. Yardin and F. Terro (2013). "Tau protein kinases: involvement in Alzheimer's disease." Ageing Res Rev **12**(1): 289-309.

Masliah, E., L. Hansen, T. Albright, M. Mallory and R. D. Terry (1991). "Immunoelectron microscopic study of synaptic pathology in Alzheimer's disease." Acta Neuropathol **81**(4): 428-433.

Masters, C. L., G. Simms, N. A. Weinman, G. Multhaup, B. L. McDonald and K. Beyreuther (1985). "Amyloid plaque core protein in Alzheimer disease and Down syndrome." Proc Natl Acad Sci U S A **82**(12): 4245-4249.

Maurer, K., S. Volk and H. Gerbaldo (1997). "Auguste D and Alzheimer's disease." Lancet **349**(9064): 1546-1549.

McAvoy, T. and A. C. Nairn (2010). "Serine/Threonine Protein Phosphatase Assays." Curr Protoc Mol Biol **CHAPTER**: Unit18 18.

Meiselbach, H., H. Sticht and R. Enz (2006). "Structural analysis of the protein phosphatase 1 docking motif: molecular description of binding specificities identifies interacting proteins." Chem Biol **13**(1): 49-59.

Min, S. W., X. Chen, T. E. Tracy, Y. Li, Y. Zhou, C. Wang, K. Shirakawa, S. S. Minami, E. Defensor, S. A. Mok, P. D. Sohn, B. Schilling, X. Cong, L. Ellerby, B. W. Gibson, J. Johnson, N. Krogan, M. Shamloo, J. Gestwicki, E. Masliah, E. Verdin and L. Gan (2015). "Critical role of acetylation in tau-mediated neurodegeneration and cognitive deficits." Nat Med **21**(10): 1154-1162.

Min, S. W., S. H. Cho, Y. Zhou, S. Schroeder, V. Haroutunian, W. W. Seeley, E. J. Huang, Y. Shen, E. Masliah, C. Mukherjee, D. Meyers, P. A. Cole, M. Ott and L. Gan (2010). "Acetylation of tau inhibits its degradation and contributes to tauopathy." Neuron **67**(6): 953-966.

Mondragon-Rodriguez, S., G. Basurto-Islas, I. Santa-Maria, R. Mena, L. I. Binder, J. Avila, M. A. Smith, G. Perry and F. Garcia-Sierra (2008). "Cleavage and conformational changes of tau protein follow phosphorylation during Alzheimer's disease." Int J Exp Pathol **89**(2): 81-90.

Moorhead, G., R. W. MacKintosh, N. Morrice, T. Gallagher and C. MacKintosh (1994). "Purification of type 1 protein (serine/threonine) phosphatases by microcystin-Sepharose affinity chromatography." FEBS Lett **356**(1): 46-50.

Moorhead, G. B., T. A. Haystead and C. MacKintosh (2007). "Synthesis and use of the protein phosphatase affinity matrices microcystin-sepharose and microcystin-biotin-sepharose." Methods Mol Biol **365**: 39-45.

Morfini, G., G. Pigino, N. Mizuno, M. Kikkawa and S. T. Brady (2007). "Tau binding to microtubules does not directly affect microtubule-based vesicle motility." J Neurosci Res **85**(12): 2620-2630.

Morfini, G., G. Szebenyi, H. Brown, H. C. Pant, G. Pigino, S. DeBoer, U. Beffert and S. T. Brady (2004). "A novel CDK5-dependent pathway for regulating GSK3 activity and kinesin-driven motility in neurons." EMBO J **23**(11): 2235-2245.

Morfini, G., G. Szebenyi, R. Elluru, N. Ratner and S. T. Brady (2002). "Glycogen synthase kinase 3 phosphorylates kinesin light chains and negatively regulates kinesin-based motility." EMBO J **21**(3): 281-293.

Morfini, G. A., M. Burns, L. I. Binder, N. M. Kanaan, N. LaPointe, D. A. Bosco, R. H. Brown, Jr., H. Brown, A. Tiwari, L. Hayward, J. Edgar, K. A. Nave, J. Garberrn, Y. Atagi, Y. Song, G. Pigino and S. T. Brady (2009). "Axonal transport defects in neurodegenerative diseases." J Neurosci **29**(41): 12776-12786.

Morgan, D., D. M. Diamond, P. E. Gottschall, K. E. Ugen, C. Dickey, J. Hardy, K. Duff, P. Jantzen, G. DiCarlo, D. Wilcock, K. Connor, J. Hatcher, C. Hope, M. Gordon and G. W. Arendash (2000). "A beta peptide vaccination prevents memory loss in an animal model of Alzheimer's disease." Nature **408**(6815): 982-985.

Morris, M., S. Maeda, K. Vossel and L. Mucke (2011). "The many faces of tau." Neuron **70**(3): 410-426.

Morrow, J. A., D. M. Hatters, B. Lu, P. Hochtl, K. A. Oberg, B. Rupp and K. H. Weisgraber (2002). "Apolipoprotein E4 forms a molten globule. A potential basis for its association with disease." J Biol Chem **277**(52): 50380-50385.

Morsch, R., W. Simon and P. D. Coleman (1999). "Neurons may live for decades with neurofibrillary tangles." J Neuropathol Exp Neurol **58**(2): 188-197.

Mufson, E. J., M. D. Ikonomovic, S. E. Counts, S. E. Perez, M. Malek-Ahmadi, S. W. Scheff and S. D. Ginsberg (2016). "Molecular and cellular pathophysiology of preclinical Alzheimer's disease." Behav Brain Res **311**: 54-69.

Mufson, E. J., M. Malek-Ahmadi, S. E. Perez and K. Chen (2016). "Braak staging, plaque pathology, and APOE status in elderly persons without cognitive impairment." Neurobiol Aging **37**: 147-153.

Mukrasch, M. D., S. Bibow, J. Korukottu, S. Jeganathan, J. Biernat, C. Griesinger, E. Mandelkow and M. Zweckstetter (2009). "Structural polymorphism of 441-residue tau at single residue resolution." PLoS Biol **7**(2): e34.

Mukrasch, M. D., J. Biernat, M. von Bergen, C. Griesinger, E. Mandelkow and M. Zweckstetter (2005). "Sites of tau important for aggregation populate {beta}-structure and bind to microtubules and polyanions." J Biol Chem **280**(26): 24978-24986.

Mullan, M., F. Crawford, K. Axelman, H. Houlden, L. Lilius, B. Winblad and L. Lannfelt (1992). "A pathogenic mutation for probable Alzheimer's disease in the APP gene at the N-terminus of beta-amyloid." Nat Genet **1**(5): 345-347.

Murphy, M. P. and H. LeVine, 3rd (2010). "Alzheimer's disease and the amyloid-beta peptide." J Alzheimers Dis **19**(1): 311-323.

Murrell, J., M. Farlow, B. Ghetti and M. D. Benson (1991). "A mutation in the amyloid precursor protein associated with hereditary Alzheimer's disease." Science **254**(5028): 97-99.

Nacharaju, P., L. Ko and S. H. Yen (1997). "Characterization of in vitro glycation sites of tau." J Neurochem **69**(4): 1709-1719.

Necula, M. and J. Kuret (2004). "Pseudophosphorylation and glycation of tau protein enhance but do not trigger fibrillization in vitro." J Biol Chem **279**(48): 49694-49703.

Nestor, P. J., P. Scheltens and J. R. Hodges (2004). "Advances in the early detection of Alzheimer's disease." Nat Med **10 Suppl**: S34-41.

Neve, R. L., P. Harris, K. S. Kosik, D. M. Kurnit and T. A. Donlon (1986). "Identification of cDNA clones for the human microtubule-associated protein tau and chromosomal localization of the genes for tau and microtubule-associated protein 2." Brain Res **387**(3): 271-280.

Novak, M., J. Kabat and C. M. Wischik (1993). "Molecular characterization of the minimal protease resistant tau unit of the Alzheimer's disease paired helical filament." Embo j **12**(1): 365-370.

O'Connor, T., K. R. Sadleir, E. Maus, R. A. Velliquette, J. Zhao, S. L. Cole, W. A. Eimer, B. Hitt, L. A. Bembinster, S. Lammich, S. F. Lichtenthaler, S. S. Hebert, B. De Strooper, C. Haass, D. A. Bennett and R. Vassar (2008). "Phosphorylation of the translation initiation factor eIF2alpha increases BACE1 levels and promotes amyloidogenesis." Neuron **60**(6): 988-1009.

Olsen, J. V., M. Vermeulen, A. Santamaria, C. Kumar, M. L. Miller, L. J. Jensen, F. Gnad, J. Cox, T. S. Jensen, E. A. Nigg, S. Brunak and M. Mann (2010). "Quantitative phosphoproteomics reveals widespread full phosphorylation site occupancy during mitosis." Sci Signal **3**(104): ra3.

Ouimet, C. C., E. F. da Cruz e Silva and P. Greengard (1995). "The alpha and gamma 1 isoforms of protein phosphatase 1 are highly and specifically concentrated in dendritic spines." Proc Natl Acad Sci U S A **92**(8): 3396-3400.

Palop, J. J. and L. Mucke (2010). "Amyloid-beta-induced neuronal dysfunction in Alzheimer's disease: from synapses toward neural networks." Nat Neurosci **13**(7): 812-818.

Park, S. Y. and A. Ferreira (2005). "The generation of a 17 kDa neurotoxic fragment: an alternative mechanism by which tau mediates beta-amyloid-induced neurodegeneration." J Neurosci **25**(22): 5365-5375.

Patterson, K. I., T. Brummer, P. M. O'Brien and R. J. Daly (2009). "Dual-specificity phosphatases: critical regulators with diverse cellular targets." Biochem J **418**(3): 475-489.

Pei, J. J., T. Tanaka, Y. C. Tung, E. Braak, K. Iqbal and I. Grundke-Iqbal (1997). "Distribution, levels, and activity of glycogen synthase kinase-3 in the Alzheimer disease brain." J Neuropathol Exp Neurol **56**(1): 70-78.

Pelech, S. L. (1995). "Networking with proline-directed protein kinases implicated in tau phosphorylation." Neurobiol Aging **16**(3): 247-256; discussion 257-261.

Petersen, R. C. (2003). "Mild cognitive impairment clinical trials." Nat Rev Drug Discov **2**(8): 646-653.

Petersen, R. C., R. Doody, A. Kurz, R. C. Mohs, J. C. Morris, P. V. Rabins, K. Ritchie, M. Rossor, L. Thal and B. Winblad (2001). "Current concepts in mild cognitive impairment." Arch Neurol **58**(12): 1985-1992.

Peti, W., A. C. Nairn and R. Page (2013). "Structural basis for protein phosphatase 1 regulation and specificity." FEBS J **280**(2): 596-611.

Pettegrew, J. W., K. Panchalingam, R. L. Hamilton and R. J. McClure (2001). "Brain membrane phospholipid alterations in Alzheimer's disease." Neurochem Res **26**(7): 771-782.

Pinheiro, A. S., J. A. Marsh, J. D. Forman-Kay and W. Peti (2011). "Structural signature of the MYPT1-PP1 interaction." J Am Chem Soc **133**(1): 73-80.

Pooler, A. M., A. Usardi, C. J. Evans, K. L. Philpott, W. Noble and D. P. Hanger (2012). "Dynamic association of tau with neuronal membranes is regulated by phosphorylation." Neurobiol Aging **33**(2): 431.e427-438.

Pountney, D. L., Y. Huang, R. J. Burns, E. Haan, P. D. Thompson, P. C. Blumbergs and W. P. Gai (2003). "SUMO-1 marks the nuclear inclusions in familial neuronal intranuclear inclusion disease." Exp Neurol **184**(1): 436-446.

Raff, M. C., A. V. Whitmore and J. T. Finn (2002). "Axonal self-destruction and neurodegeneration." Science **296**(5569): 868-871.

Ragusa, M. J., B. Dancheck, D. A. Critton, A. C. Nairn, R. Page and W. Peti (2010). "Spinophilin directs protein phosphatase 1 specificity by blocking substrate binding sites." Nat Struct Mol Biol **17**(4): 459-464.

Rahman, A., I. Grundke-Iqbal and K. Iqbal (2005). "Phosphothreonine-212 of Alzheimer abnormally hyperphosphorylated tau is a preferred substrate of protein phosphatase-1." Neurochem Res **30**(2): 277-287.

Rapoport, M., H. N. Dawson, L. I. Binder, M. P. Vitek and A. Ferreira (2002). "Tau is essential to beta -amyloid-induced neurotoxicity." Proc Natl Acad Sci U S A **99**(9): 6364-6369.

Rissman, R. A., W. W. Poon, M. Blurton-Jones, S. Oddo, R. Torp, M. P. Vitek, F. M. LaFerla, T. T. Rohn and C. W. Cotman (2004). "Caspase-cleavage of tau is an early event in Alzheimer disease tangle pathology." J Clin Invest **114**(1): 121-130.

Roberson, E. D., K. Scearce-Levie, J. J. Palop, F. Yan, I. H. Cheng, T. Wu, H. Gerstein, G. Q. Yu and L. Mucke (2007). "Reducing endogenous tau ameliorates amyloid beta-induced deficits in an Alzheimer's disease mouse model." Science **316**(5825): 750-754.

Rogaev, E. I., R. Sherrington, E. A. Rogaeva, G. Levesque, M. Ikeda, Y. Liang, H. Chi, C. Lin, K. Holman, T. Tsuda and et al. (1995). "Familial Alzheimer's disease in kindreds with missense mutations in a gene on chromosome 1 related to the Alzheimer's disease type 3 gene." Nature **376**(6543): 775-778.

Rosenberg, K. J., J. L. Ross, H. E. Feinstein, S. C. Feinstein and J. Israelachvili (2008). "Complementary dimerization of microtubule-associated tau protein: Implications for microtubule bundling and tau-mediated pathogenesis." Proc Natl Acad Sci U S A **105**(21): 7445-7450.

Rovelet-Lecrux, A., D. Hannequin, G. Raux, N. Le Meur, A. Laquerriere, A. Vital, C. Dumanchin, S. Feuillette, A. Brice, M. Vercelletto, F. Dubas, T. Frebourg and D. Campion (2006). "APP locus duplication causes autosomal dominant early-onset Alzheimer disease with cerebral amyloid angiopathy." Nat Genet **38**(1): 24-26.

Salloway, S., R. Sperling, N. C. Fox, K. Blennow, W. Klunk, M. Raskind, M. Sabbagh, L. S. Honig, A. P. Porsteinsson, S. Ferris, M. Reichert, N. Ketter, B. Nejadnik, V. Guenzler, M. Miloslavsky, D. Wang, Y. Lu, J. Lull, I. C. Tudor, E. Liu, M. Grundman, E. Yuen, R. Black and H. R. Brashear (2014). "Two phase 3 trials of bapineuzumab in mild-to-moderate Alzheimer's disease." N Engl J Med **370**(4): 322-333.

Schenk, D., R. Barbour, W. Dunn, G. Gordon, H. Grajeda, T. Guido, K. Hu, J. Huang, K. Johnson-Wood, K. Khan, D. Kholodenko, M. Lee, Z. Liao, I. Lieberburg, R. Motter, L. Mutter, F. Soriano, G. Shopp, N. Vasquez, C. Vandevert, S. Walker, M. Wogulis, T. Yednock, D. Games and P. Seubert (1999). "Immunization with amyloid-beta attenuates Alzheimer-disease-like pathology in the PDAPP mouse." Nature **400**(6740): 173-177.

Schweers, O., E. Schonbrunn-Hanebeck, A. Marx and E. Mandelkow (1994). "Structural studies of tau protein and Alzheimer paired helical filaments show no evidence for beta-structure." J Biol Chem **269**(39): 24290-24297.

Selenica, M. L., M. Brownlow, J. P. Jimenez, D. C. Lee, G. Pena, C. A. Dickey, M. N. Gordon and D. Morgan (2013). "Amyloid oligomers exacerbate tau pathology in a mouse model of tauopathy." Neurodegener Dis **11**(4): 165-181.

Selkoe, D. J. (1991). "The molecular pathology of Alzheimer's disease." Neuron **6**(4): 487-498.

Selkoe, D. J. (2000). "Toward a comprehensive theory for Alzheimer's disease. Hypothesis: Alzheimer's disease is caused by the cerebral accumulation and cytotoxicity of amyloid beta-protein." Ann N Y Acad Sci **924**: 17-25.

Sents, W., E. Ivanova, C. Lambrecht, D. Haesen and V. Janssens (2013). "The biogenesis of active protein phosphatase 2A holoenzymes: a tightly regulated process creating phosphatase specificity." Febs j **280**(2): 644-661.

Shankar, G. M., B. L. Bloodgood, M. Townsend, D. M. Walsh, D. J. Selkoe and B. L. Sabatini (2007). "Natural oligomers of the Alzheimer amyloid-beta protein induce reversible synapse loss by modulating an NMDA-type glutamate receptor-dependent signaling pathway." J Neurosci **27**(11): 2866-2875.

Sharma, V. M., J. M. Litersky, K. Bhaskar and G. Lee (2007). "Tau impacts on growth-factor-stimulated actin remodeling." J Cell Sci **120**(Pt 5): 748-757.

Shaw, P. C., A. F. Davies, K. F. Lau, M. Garcia-Barcelo, M. M. Waye, S. Lovestone, C. C. Miller and B. H. Anderton (1998). "Isolation and chromosomal mapping of human glycogen synthase kinase-3 alpha and -3 beta encoding genes." Genome **41**(5): 720-727.

Sherrington, R., E. I. Rogaev, Y. Liang, E. A. Rogaeva, G. Levesque, M. Ikeda, H. Chi, C. Lin, G. Li, K. Holman, T. Tsuda, L. Mar, J. F. Foncin, A. C. Bruni, M. P. Montesi, S. Sorbi, I. Rainero, L. Pinessi, L. Nee, I. Chumakov, D. Pollen, A. Brookes, P. Sanseau, R. J. Polinsky, W. Wasco, H. A. Da Silva, J. L. Haines, M. A. Perkicak-Vance, R. E. Tanzi, A. D. Roses, P. E. Fraser, J. M. Rommens and P. H. St George-Hyslop (1995). "Cloning of a gene bearing missense mutations in early-onset familial Alzheimer's disease." Nature **375**(6534): 754-760.

Shi, Y. (2009). "Serine/threonine phosphatases: mechanism through structure." Cell **139**(3): 468-484.

Shi, Y., K. Yamada, S. A. Liddelow, S. T. Smith, L. Zhao, W. Luo, R. M. Tsai, S. Spina, L. T. Grinberg, J. C. Rojas, G. Gallardo, K. Wang, J. Roh, G. Robinson, M. B. Finn, H. Jiang, P. M. Sullivan, C. Baufeld, M. W. Wood, C. Sutphen, L. McCue, C. Xiong, J. L. Del-Aguila, J. C. Morris, C. Cruchaga, A. M. Fagan, B. L. Miller, A. L. Boxer, W. W. Seeley, O. Butovsky, B. A. Barres, S. M. Paul and D. M. Holtzman (2017). "ApoE4 markedly exacerbates tau-mediated neurodegeneration in a mouse model of tauopathy." Nature **549**(7673): 523-527.

Shima, H., T. Haneji, Y. Hatano, I. Kasugai, T. Sugimura and M. Nagao (1993). "Protein phosphatase 1 gamma 2 is associated with nuclei of meiotic cells in rat testis." Biochem Biophys Res Commun **194**(2): 930-937.

Silva, T., J. Reis, J. Teixeira and F. Borges (2014). "Alzheimer's disease, enzyme targets and drug discovery struggles: From natural products to drug prototypes." Ageing Res Rev.

Sontag, E., C. Hladik, L. Montgomery, A. Luangpirom, I. Mudrak, E. Ogris and C. L. White, 3rd (2004). "Downregulation of protein phosphatase 2A carboxyl methylation and methyltransferase may contribute to Alzheimer disease pathogenesis." J Neuropathol Exp Neurol **63**(10): 1080-1091.

Sontag, E., A. Luangpirom, C. Hladik, I. Mudrak, E. Ogris, S. Speciale and C. L. White, 3rd (2004). "Altered expression levels of the protein phosphatase 2A ABalphaC enzyme are associated with Alzheimer disease pathology." J Neuropathol Exp Neurol **63**(4): 287-301.

Sontag, E., V. Nunbhakdi-Craig, G. Lee, G. S. Bloom and M. C. Mumby (1996). "Regulation of the phosphorylation state and microtubule-binding activity of Tau by protein phosphatase 2A." Neuron **17**(6): 1201-1207.

Sontag, E., V. Nunbhakdi-Craig, G. Lee, R. Brandt, C. Kamibayashi, J. Kuret, C. L. White, 3rd, M. C. Mumby and G. S. Bloom (1999). "Molecular interactions among protein phosphatase 2A, tau, and microtubules. Implications for the regulation of tau phosphorylation and the development of tauopathies." J Biol Chem **274**(36): 25490-25498.

Soto, C. (2003). "Unfolding the role of protein misfolding in neurodegenerative diseases." Nat Rev Neurosci **4**(1): 49-60.

Soto, C. and L. D. Estrada (2008). "Protein misfolding and neurodegeneration." Arch Neurol **65**(2): 184-189.

Souter, S. and G. Lee (2010). "Tubulin-independent tau in Alzheimer's disease and cancer: implications for disease pathogenesis and treatment." Curr Alzheimer Res **7**(8): 697-707.

Spillantini, M. G. and M. Goedert (2013). "Tau pathology and neurodegeneration." Lancet Neurol **12**(6): 609-622.

St George-Hyslop, P., J. Haines, E. Rogaev, M. Mortilla, G. Vaula, M. Pericak-Vance, J. F. Foncin, M. Montesi, A. Bruni, S. Sorbi, I. Rainero, L. Pinessi, D. Pollen, R. Polinsky, L. Nee, J. Kennedy, F. Macciardi, E. Rogaeva, Y. Liang, N. Alexandrova, W. Lukiw, K. Schlumpf, R. Tanzi, T. Tsuda, L. Farrer, J. M. Cantu, R. Duara, L. Amaducci, L. Bergamini, J. Gusella, A. Roses, D. Crapper McLachlan and et al. (1992). "Genetic evidence for a novel familial Alzheimer's disease locus on chromosome 14." Nat Genet **2**(4): 330-334.

Stambolic, V. and J. R. Woodgett (1994). "Mitogen inactivation of glycogen synthase kinase-3 beta in intact cells via serine 9 phosphorylation." Biochem J **303 (Pt 3)**: 701-704.

Stern, J. L., D. V. Lessard, G. J. Hoeprich, G. A. Morfini and C. L. Berger (2017). "Phosphoregulation of Tau modulates inhibition of kinesin-1 motility." Mol Biol Cell **28**(8): 1079-1087.

Stoub, T. R., L. deToledo-Morrell, G. T. Stebbins, S. Leurgans, D. A. Bennett and R. C. Shah (2006). "Hippocampal disconnection contributes to memory dysfunction in individuals at risk for Alzheimer's disease." Proc Natl Acad Sci U S A **103**(26): 10041-10045.

Strack, S., S. Kini, F. F. Ebner, B. E. Wadzinski and R. J. Colbran (1999). "Differential cellular and subcellular localization of protein phosphatase 1 isoforms in brain." J Comp Neurol **413**(3): 373-384.

Su, J. H., G. Deng and C. W. Cotman (1997). "Transneuronal degeneration in the spread of Alzheimer's disease pathology: immunohistochemical evidence for the transmission of tau hyperphosphorylation." Neurobiol Dis **4**(5): 365-375.

Suzuki, N., T. T. Cheung, X. D. Cai, A. Odaka, L. Otvos, Jr., C. Eckman, T. E. Golde and S. G. Younkin (1994). "An increased percentage of long amyloid beta protein secreted by familial amyloid beta protein precursor (beta APP717) mutants." Science **264**(5163): 1336-1340.

Takahashi, K., M. Ishida, H. Komano and H. Takahashi (2008). "SUMO-1 immunoreactivity co-localizes with phospho-Tau in APP transgenic mice but not in mutant Tau transgenic mice." Neurosci Lett **441**(1): 90-93.

Takashima, A., K. Noguchi, G. Michel, M. Mercken, M. Hoshi, K. Ishiguro and K. Imahori (1996). "Exposure of rat hippocampal neurons to amyloid beta peptide (25-35) induces the inactivation of phosphatidyl inositol-3 kinase and the activation of tau protein kinase I/glycogen synthase kinase-3 beta." Neurosci Lett **203**(1): 33-36.

Taleski, G. and E. Sontag (2018). "Protein phosphatase 2A and tau: an orchestrated 'Pas de Deux'." FEBS Lett **592**(7): 1079-1095.

Terrak, M., F. Kerff, K. Langsetmo, T. Tao and R. Dominguez (2004). "Structural basis of protein phosphatase 1 regulation." Nature **429**(6993): 780-784.

Terry, R. D. (1994). "Neuropathological changes in Alzheimer disease." Prog Brain Res **101**: 383-390.

Terry, R. D., N. K. Gonatas and M. Weiss (1964). "Ultrastructural Studies in Alzheimer's Presenile Dementia." Am J Pathol **44**: 269-297.

Thal, D. R., U. Rub, M. Orantes and H. Braak (2002). "Phases of A beta-deposition in the human brain and its relevance for the development of AD." Neurology **58**(12): 1791-1800.

Thurston, V. C., P. Pena, R. Pestell and L. I. Binder (1997). "Nucleolar localization of the microtubule-associated protein tau in neuroblastomas using sense and anti-sense transfection strategies." Cell Motil Cytoskeleton **38**(1): 100-110.

Tiernan, C. T., B. Combs, K. Cox, G. Morfini, S. T. Brady, S. E. Counts and N. M. Kanaan (2016). "Pseudophosphorylation of tau at S422 enhances SDS-stable dimer formation and impairs both anterograde and retrograde fast axonal transport." Exp Neurol **283**(Pt A): 318-329.

Tiernan, C. T., S. D. Ginsberg, A. L. Guillozet-Bongaarts, S. M. Ward, B. He, N. M. Kanaan, E. J. Mufson, L. I. Binder and S. E. Counts (2016). "Protein homeostasis gene dysregulation in pretangle-bearing nucleus basalis neurons during the progression of Alzheimer's disease." Neurobiol Aging **42**: 80-90.

Uversky, V. N., J. Li and A. L. Fink (2001). "Evidence for a partially folded intermediate in alpha-synuclein fibril formation." J Biol Chem **276**(14): 10737-10744.

van Beuningen, S. F. B., L. Will, M. Harterink, A. Chazeau, E. Y. van Battum, C. P. Frias, M. A. M. Franker, E. A. Katrukha, R. Stucchi, K. Vocking, A. T. Antunes, L. Slenders, S. Doulkeridou, P. Sillevis Smitt, A. F. M. Altelaar, J. A. Post, A. Akhmanova, R. J. Pasterkamp, L. C. Kapitein, E. de Graaff and C. C. Hoogenraad (2015). "TRIM46 Controls Neuronal Polarity and Axon Specification by Driving the Formation of Parallel Microtubule Arrays." Neuron **88**(6): 1208-1226.

Vana, L., N. M. Kanaan, I. C. Ugwu, J. Wuu, E. J. Mufson and L. I. Binder (2011). "Progression of tau pathology in cholinergic Basal forebrain neurons in mild cognitive impairment and Alzheimer's disease." Am J Pathol **179**(5): 2533-2550.

Vossel, K. A., J. C. Xu, V. Fomenko, T. Miyamoto, E. Suberbielle, J. A. Knox, K. Ho, D. H. Kim, G. Q. Yu and L. Mucke (2015). "Tau reduction prevents Abeta-induced axonal transport deficits by blocking activation of GSK3beta." J Cell Biol **209**(3): 419-433.

Vossel, K. A., K. Zhang, J. Brodbeck, A. C. Daub, P. Sharma, S. Finkbeiner, B. Cui and L. Mucke (2010). "Tau reduction prevents Abeta-induced defects in axonal transport." Science **330**(6001): 198.

Wai, M. S., Y. Liang, C. Shi, E. Y. Cho, H. F. Kung and D. T. Yew (2009). "Co-localization of hyperphosphorylated tau and caspases in the brainstem of Alzheimer's disease patients." Biogerontology **10**(4): 457-469.

Wakula, P., M. Beullens, H. Ceulemans, W. Stalmans and M. Bollen (2003). "Degeneracy and function of the ubiquitous RVXF motif that mediates binding to protein phosphatase-1." J Biol Chem **278**(21): 18817-18823.

Wang, C., R. Najm, Q. Xu, D. E. Jeong, D. Walker, M. E. Balestra, S. Y. Yoon, H. Yuan, G. Li, Z. A. Miller, B. L. Miller, M. J. Malloy and Y. Huang (2018). "Gain of toxic apolipoprotein E4 effects in human iPSC-derived neurons is ameliorated by a small-molecule structure corrector." Nat Med **24**(5): 647-657.

Wang, J. Z., I. Grundke-Iqbal and K. Iqbal (1996). "Glycosylation of microtubule-associated protein tau: an abnormal posttranslational modification in Alzheimer's disease." Nat Med **2**(8): 871-875.

Wang, J. Z. and F. Liu (2008). "Microtubule-associated protein tau in development, degeneration and protection of neurons." Prog Neurobiol **85**(2): 148-175.

Wang, Q. M., C. J. Fiol, A. A. DePaoli-Roach and P. J. Roach (1994). "Glycogen synthase kinase-3 beta is a dual specificity kinase differentially regulated by tyrosine and serine/threonine phosphorylation." J Biol Chem **269**(20): 14566-14574.

Wang, Y., P. A. Loomis, R. P. Zinkowski and L. I. Binder (1993). "A novel tau transcript in cultured human neuroblastoma cells expressing nuclear tau." J Cell Biol **121**(2): 257-267.

Wang, Y. and E. Mandelkow (2016). "Tau in physiology and pathology." Nat Rev Neurosci **17**(1): 5-21.

Watanabe, A., W. K. Hong, N. Dohmae, K. Takio, M. Morishima-Kawashima and Y. Ihara (2004). "Molecular aging of tau: disulfide-independent aggregation and non-enzymatic degradation in vitro and in vivo." J Neurochem **90**(6): 1302-1311.

Watanabe, T., E. F. da Cruz e Silva, H. B. Huang, N. Starkova, Y. G. Kwon, A. Horiuchi, P. Greengard and A. C. Nairn (2003). "Preparation and characterization of recombinant protein phosphatase 1." Methods Enzymol **366**: 321-338.

Weingarten, M. D., A. H. Lockwood, S. Y. Hwo and M. W. Kirschner (1975). "A protein factor essential for microtubule assembly." Proc Natl Acad Sci U S A **72**(5): 1858-1862.

Wenk, J., H. I. Trompeter, K. G. Pettrich, P. T. Cohen, D. G. Campbell and G. Mieskes (1992). "Molecular cloning and primary structure of a protein phosphatase 2C isoform." FEBS Lett **297**(1-2): 135-138.

Wischik, C. M., M. Novak, H. C. Thogersen, P. C. Edwards, M. J. Runswick, R. Jakes, J. E. Walker, C. Milstein, M. Roth and A. Klug (1988). "Isolation of a fragment of tau derived

from the core of the paired helical filament of Alzheimer disease." Proc Natl Acad Sci U S A **85**(12): 4506-4510.

Wisniewski, K. E., H. M. Wisniewski and G. Y. Wen (1985). "Occurrence of neuropathological changes and dementia of Alzheimer's disease in Down's syndrome." Ann Neurol **17**(3): 278-282.

Wood, J. G., S. S. Mirra, N. J. Pollock and L. I. Binder (1986). "Neurofibrillary tangles of Alzheimer disease share antigenic determinants with the axonal microtubule-associated protein tau (tau)." Proc Natl Acad Sci U S A **83**(11): 4040-4043.

Xie, X. J., W. Huang, C. Z. Xue and Q. Wei (2009). "The nonconserved N-terminus of protein phosphatase 2B confers its properties to protein phosphatase 1." IUBMB Life **61**(2): 178-183.

Xu, Y., Y. Chen, P. Zhang, P. D. Jeffrey and Y. Shi (2008). "Structure of a protein phosphatase 2A holoenzyme: insights into B55-mediated Tau dephosphorylation." Mol Cell **31**(6): 873-885.

Yamaguchi, H., K. Ishiguro, T. Uchida, A. Takashima, C. A. Lemere and K. Imahori (1996). "Preferential labeling of Alzheimer neurofibrillary tangles with antisera for tau protein kinase (TPK) I/glycogen synthase kinase-3 beta and cyclin-dependent kinase 5, a component of TPK II." Acta Neuropathol **92**(3): 232-241.

Yan, S. D., X. Chen, A. M. Schmidt, J. Brett, G. Godman, Y. S. Zou, C. W. Scott, C. Caputo, T. Frappier, M. A. Smith and et al. (1994). "Glycated tau protein in Alzheimer disease: a mechanism for induction of oxidant stress." Proc Natl Acad Sci U S A **91**(16): 7787-7791.

Yan, S. D., S. F. Yan, X. Chen, J. Fu, M. Chen, P. Kuppusamy, M. A. Smith, G. Perry, G. C. Godman, P. Nawroth and et al. (1995). "Non-enzymatically glycated tau in Alzheimer's disease induces neuronal oxidant stress resulting in cytokine gene expression and release of amyloid beta-peptide." Nat Med **1**(7): 693-699.

Yang, L. B., K. Lindholm, R. Yan, M. Citron, W. Xia, X. L. Yang, T. Beach, L. Sue, P. Wong, D. Price, R. Li and Y. Shen (2003). "Elevated beta-secretase expression and enzymatic activity detected in sporadic Alzheimer disease." Nat Med **9**(1): 3-4.

Youmans, K. L., L. M. Tai, T. Kanekiyo, W. B. Stine, Jr., S. C. Michon, E. Nwabuisi-Heath, A. M. Manelli, Y. Fu, S. Riordan, W. A. Eimer, L. Binder, G. Bu, C. Yu, D. M. Hartley and M. J. LaDu (2012). "Intraneuronal Abeta detection in 5xFAD mice by a new Abeta-specific antibody." Mol Neurodegener **7**: 8.

Young, J. C., V. R. Agashe, K. Siegers and F. U. Hartl (2004). "Pathways of chaperone-mediated protein folding in the cytosol." Nat Rev Mol Cell Biol **5**(10): 781-791.

Yuzwa, S. A., A. H. Cheung, M. Okon, L. P. McIntosh and D. J. Vocadlo (2014). "O-GlcNAc modification of tau directly inhibits its aggregation without perturbing the conformational properties of tau monomers." J Mol Biol **426**(8): 1736-1752.

Zeke, A., M. Lukacs, W. A. Lim and A. Remenyi (2009). "Scaffolds: interaction platforms for cellular signalling circuits." Trends Cell Biol **19**(8): 364-374.

Zhang, F., C. J. Phiel, L. Spece, N. Gurvich and P. S. Klein (2003). "Inhibitory phosphorylation of glycogen synthase kinase-3 (GSK-3) in response to lithium. Evidence for autoregulation of GSK-3." J Biol Chem **278**(35): 33067-33077.

Zhang, Y. W., R. Thompson, H. Zhang and H. Xu (2011). "APP processing in Alzheimer's disease." Mol Brain **4**: 3.

Zhao, J., Y. Fu, M. Yasvoina, P. Shao, B. Hitt, T. O'Connor, S. Logan, E. Maus, M. Citron, R. Berry, L. Binder and R. Vassar (2007). "Beta-site amyloid precursor protein cleaving enzyme 1 levels become elevated in neurons around amyloid plaques: implications for Alzheimer's disease pathogenesis." J Neurosci **27**(14): 3639-3649.

Zhou, L., J. McInnes, K. Wierda, M. Holt, A. G. Herrmann, R. J. Jackson, Y. C. Wang, J. Swerts, J. Beyens, K. Miskiewicz, S. Vilain, I. Dewachter, D. Moechars, B. De Strooper, T. L. Spires-Jones, J. De Wit and P. Verstreken (2017). "Tau association with synaptic vesicles causes presynaptic dysfunction." Nat Commun **8**: 15295.

Zhou, L., B. L. Miller, C. H. McDaniel, L. Kelly, O. J. Kim and C. A. Miller (1998). "Frontotemporal dementia: neuropil spheroids and presynaptic terminal degeneration." Ann Neurol **44**(1): 99-109.

Zhou, X. W., J. A. Gustafsson, H. Tanila, C. Bjorkdahl, R. Liu, B. Winblad and J. J. Pei (2008). "Tau hyperphosphorylation correlates with reduced methylation of protein phosphatase 2A." Neurobiol Dis **31**(3): 386-394.

Zhu, J. B., C. C. Tan, L. Tan and J. T. Yu (2017). "State of Play in Alzheimer's Disease Genetics." J Alzheimers Dis **58**(3): 631-659.